Downloaded from specialpapers.gsapubs.org on September 29, 2015

The Geological Society of America
Special Paper 506
2014

Late Devonian–Mississippian(?) Zn-Pb(-Ag-Au-Ba-F) deposits and related aluminous alteration zones in the Nome Complex, Seward Peninsula, Alaska

John F. Slack
U.S. Geological Survey, National Center, MS 954, Reston, Virginia 20192, USA

Alison B. Till
U.S. Geological Survey, 4210 University Drive, Anchorage, Alaska 99508, USA

Harvey E. Belkin
U.S. Geological Survey, National Center, MS 956, Reston, Virginia 20192, USA

W.C. Pat Shanks, III
U.S. Geological Survey, Federal Center, MS 973, Denver, Colorado 80225, USA

ABSTRACT

Stratabound base-metal sulfide deposits and occurrences are present in metasedimentary rocks of the Neoproterozoic and Paleozoic Nome Complex on south-central Seward Peninsula, Alaska. Stratabound and locally stratiform deposits including Aurora Creek (Zn-Au-Ba-F), Wheeler North (Pb-Zn-Ag-Au-F), and Nelson (Zn-Pb-Cu-Ag), consist of lenses typically 0.5–2.0 m thick containing disseminated to semimassive sulfides. Host strata of the Aurora Creek and Wheeler North deposits are variably calcareous and graphitic siliciclastic metasedimentary rocks of Middle Devonian or younger age based on detrital zircon geochronology; the Nelson deposit is within Ordovician–Devonian marble (Till et al., this volume, Chapter 4). Deformed veins such as Quarry (Zn-Pb-Ag-Ba-F) and Galena (Pb-Zn-Ag-F) occur in a unit composed mainly of marble and schist; fossil and detrital zircon data indicate that this unit contains rocks of Ordovician, Silurian, and Devonian age. None of these Zn- and Pb-rich deposits or occurrences has spatially associated metavolcanic or intrusive rocks. All were deformed and metamorphosed to blueschist facies and then retrograded to greenschist facies during the Jurassic and Early Cretaceous Brookian orogeny. Disseminated Cu-rich deposits including Copper King (Cu-Bi-Sb-Pb-Ag-Au) and Wheeler South (Cu-Ag-Au) occur in silicified carbonate rocks and have textures that indicate a pre- to syn-metamorphic origin.

The Zn- and Pb-rich sulfide deposits and occurrences consist mainly of pyrite, sphalerite, and/or galena in a gangue of quartz and carbonate. Minor minerals include arsenopyrite, chalcopyrite, magnetite, pyrrhotite, tetrahedrite, barite, fluorite, and

Slack, J.F., Till, A.B., Belkin, H.E., and Shanks, W.C.P., III, 2014, Late Devonian–Mississippian(?) Zn-Pb(-Ag-Au-Ba-F) deposits and related aluminous alteration zones in the Nome Complex, Seward Peninsula, Alaska, *in* Dumoulin, J.A., and Till, A.B., eds., Reconstruction of a Late Proterozoic to Devonian Continental Margin Sequence, Northern Alaska, Its Paleogeographic Significance, and Contained Base-Metal Sulfide Deposits: Geological Society of America Special Paper 506, p. 173–212, doi:10.1130/2014.2506(06). For permission to copy, contact editing@geosociety.org. © 2014 The Geological Society of America. All rights reserved.

Downloaded from specialpapers.gsapubs.org on September 29, 2015

chlorite; gold and electrum are trace to minor constituents locally. Sphalerite is uniformly unzoned and commonly aligned in the dominant foliation. These textures, together with the presence of folded layers of barite at Aurora Creek and folded sulfide layers at Wheeler North, indicate that mineralization in the stratabound deposits predated deformation and metamorphism. Electron microprobe (EMP) analyses of the carbonate gangue show three major compositions comprising siderite, ankerite, and lesser dolomite. The Cu-rich deposits differ in containing chalcopyrite and bornite in a quartzose matrix.

Altered wall rocks surrounding the Zn- and Pb-rich deposits and occurrences have aluminous assemblages composed of muscovite + chloritoid + siderite + chlorite + quartz ± tourmaline ± ilmenite ± apatite ± monazite. Muscovite within these assemblages and in sulfide-rich samples is phengitic and locally enriched in barium; chloritoid at Aurora Creek is enriched in zinc. Minor minerals including pyrite, sphalerite, galena, chalcopyrite, barite, and hyalophane occur as fine-grained disseminations. These altered rocks vary from small lenses a few meters thick to large zones tens of meters in thickness that extend along strike, discontinuously, for 4 km or more. Whole-rock geochemical analyses of the altered rocks from deposit-proximal and deposit-distal settings reveal generally lower SiO_2/Al_2O_3 ratios and higher $Fe_2O_3^T/MgO$ ratios compared to those of unaltered clastic metasedimentary rocks of the Nome Complex and of average shale or graywacke. The deposit-proximal samples are also characterized by anomalously high Zn, Pb, Hg, and Sb, relative to the unaltered metasediments. These data, together with mass change calculations, suggest that the aluminous rocks formed as replacements of permeable graywacke in semi-conformable alteration zones, beneath the seafloor contemporaneously with Zn- and/or Pb-rich sulfide mineralization.

Exposures of all three stratabound Zn-Pb deposits show evidence of deformation and recrystallization that occurred in a largely brittle deformational regime. This evidence includes small faults and veins that cut foliation and localized zones of breccia. Sulfide minerals, fluorite, quartz, chlorite, and carbonate minerals crystallized within these structures, which probably formed during Cretaceous deformation of the Nome Complex.

Previous studies of the Zn-Pb(-Ag-Au-Ba-F) deposits and occurrences have invoked models of epigenetic veins, volcanogenic massive sulfides (VMS), or carbonate-replacement deposits (CRD). In contrast, our field and laboratory data (including sulfur isotopes; Shanks et al., this volume) suggest that these Zn- and/or Pb-rich deposits represent different levels of sediment-hosted, seafloor-hydrothermal systems, with stratabound and locally stratiform deposits such as Aurora Creek and Wheeler North having formed on the seafloor and/or in the shallow subsurface like many sedimentary-exhalative (SEDEX) deposits worldwide. The deformed veins such as Quarry and Galena are interpreted to have formed deep in the subsurface, possibly as feeders to overlying SEDEX deposits such as Aurora Creek. Formation of all of the Zn- and Pb-rich deposits and occurrences took place during episodic rifting of the continental margin between the Ordovician and Mississippian(?). Regional relationships are consistent with at least some of the deposits having formed in Late Devonian–Mississippian(?) time.

INTRODUCTION

Deciphering the origin of small, minimally explored mineral deposits is often challenging due to the generally limited amount of information available on the geometry and style of the metal accumulations. Understanding such small deposits nevertheless is important, in resource assessments and mineral exploration programs, as a framework for evaluating the potential for larger deposits in the area. This study highlights the geology, mineralogy, and geochemistry of several types of stratabound Zn-Pb(-Ag-Au-Ba-F) deposits and occurrences within the Neoproterozoic to Mississippian(?) Nome Complex on south-central Seward Peninsula, northwestern Alaska. Results presented here establish the foundation for a new model involving both shallow

Downloaded from specialpapers.gsapubs.org on September 29, 2015

and deep facies of multiple sedimentary-exhalative (SEDEX) seafloor-hydrothermal systems, broadly coeval with deposition of enclosing Paleozoic sedimentary strata. This model, and related data, also provides insights into the Paleozoic history and evolution of the Nome Complex and the Arctic Alaska terrane.

REGIONAL METALLOGENY

Diverse types of metallic mineral deposits occur on Seward Peninsula (Fig. 1; Table 1). Prominent in the region are (1) granite-hosted Sn(±W-F) veins at Lost River, Kougarok, and other localities (Dobson, 1982; Hudson and Arth, 1983; Puchner, 1986); (2) granitoid-associated Fe-Cu-Au-Ag skarns, replacements, and veins near the Cretaceous Kugruk granite (Chutas and Robinson, 2010; TintinaGold Resources, Inc., 2010a); (3) orogenic Au-quartz veins at Big Hurrah, Bluff, Mount Distin, and Rock Creek (Read and Meinert, 1986; Ford, 1993; Apodoca, 1994; Ford and Snee, 1996; Otto et al., 2009; Pink and Rodgers, 2010); (4) stratabound Pb-Zn-Ag veins and replacements at Omilak, Omilak East, Foster, Independence, and Hannum (Levensaler and Anderson, 1944; Mulligan, 1962, 1965; Herreid, 1965, 1966b; Sainsbury, 1975; TintinaGold Resources, Inc., 2010b); and (5) sandstone-hosted U concentrations at Boulder Creek (Dickinson et al., 1987). The Rock Creek mine, which was in production only briefly during the fall of 2008, is now closed (NovaGold Resources Inc., 2012); the deposits at Big Hurrah, Bluff, Kugruk, Hannum/Harry's Creek, and Omilak were being explored as of 2010 (TintinaGold Resources, Inc., 2010a, 2010b; Millrock Resources, 2010; Full Metal Minerals Ltd., 2010).

THE NOME COMPLEX

The Nome Complex underlies much of central and eastern Seward Peninsula, an area covering ~240 × 200 km (Fig. 1). The complex is a metamorphic unit composed of Neoproterozoic and early to middle Paleozoic rocks thought to have formed in continental margin and slope environments (Till et al., this volume, Chapter 1). Together, these rocks underwent penetrative

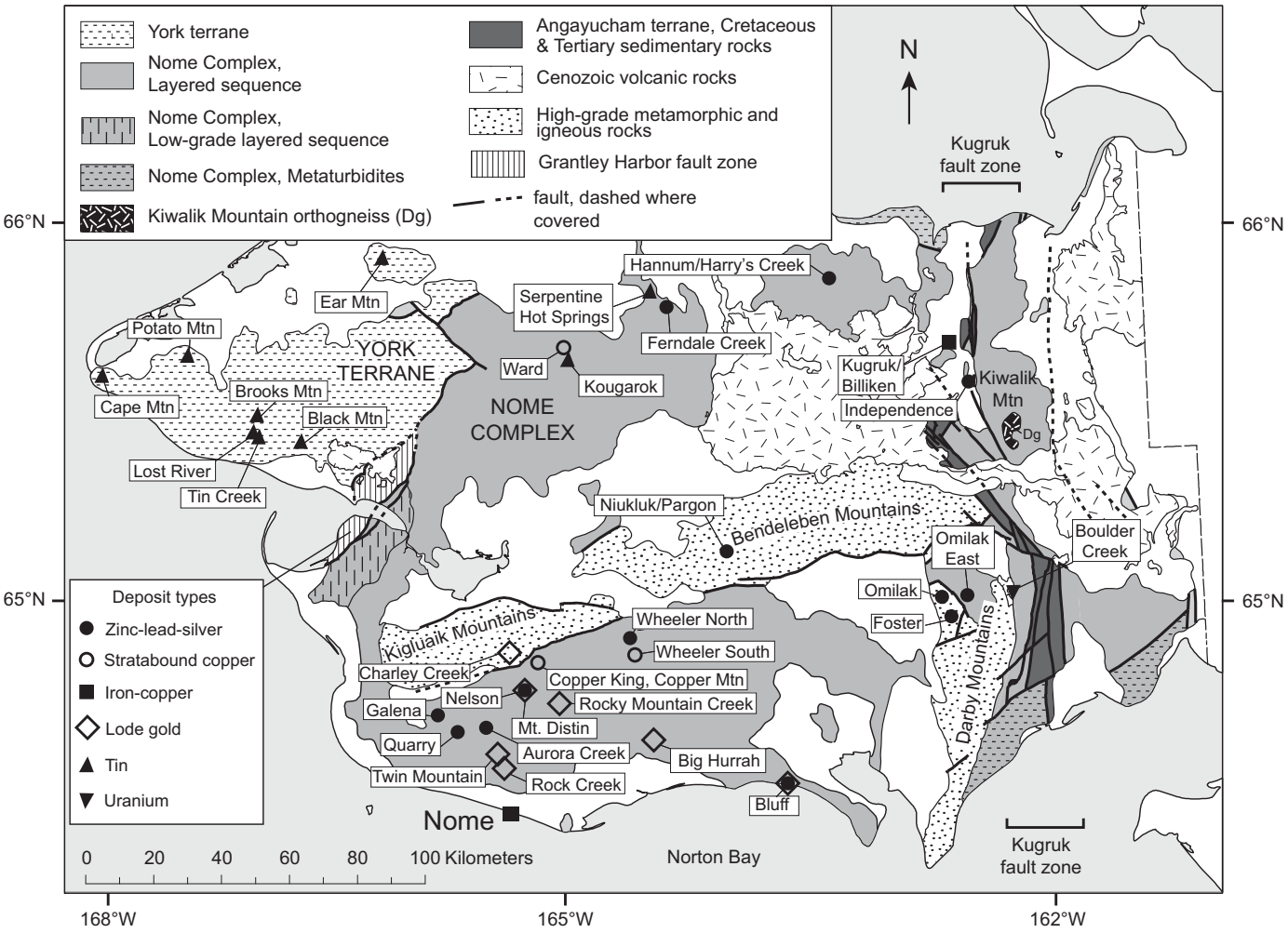


Figure 1. Simplified geologic map of Seward Peninsula showing major metallic mineral deposits. Geology from Till et al. (2011).

Downloaded from specialpapers.gsapubs.org on September 29, 2015

TABLE 1. SELECTED METALLIC MINERAL DEPOSITS AND OCCURRENCES IN THE NOME COMPLEX AND ASSOCIATED AMPHIBOLITE-FACIES METAMORPHIC ROCKS[1]

Name	Geometry	Principal metals	Ore minerals	Gangue minerals	Alteration
Premetamorphic					
Aurora Creek[2]	Stratabound lens	Zn, Ag, Au	Sph, Py, Asp, Gl, Po, Cp, Gd, Stb	Qtz, Ms, Bar, Fl, Ank, Dol, Mt, Chl	Ms, Chd, Qtz, Ank
Wheeler North	Stratabound lens	Pb, Ag, Au	Gl, Py, Po, Sph, Asp, Ss, Cp, Gd	Qtz, Ms, Fl, Ank, Mt, Bar	Ms, Chd, Qtz, Ank
Nelson	Stratabound lens	Pb, Zn, Ag	Py, Gl, Sph, Ss	Qtz, Ms, Cc	Ms, Chd, Qtz, Ank
Bluff	Stratabound lens	Pb, Zn	Sph, Gl, Py, Cp	Qtz, Ms, Cc	Qtz, Ms
Quarry	Deformed vein	Pb, Zn, Ag, Au	Gl, Tt, Asp, Cp, Ss	Qtz, Ms, Bar, Fl, Ank, Dol	Ms, Chd, Qtz, Ank
Galena	Deformed vein	Pb, Zn, Ag	Gl, Sph, Py	Qtz, Cc, Dol, Fl	Qtz, Dol(?)
Wheeler South[3]	Stratabound lens	Cu, Ag, Bi, Au	Cp, Bn, Py, Mal, Azu, Gl, Tt	Qtz, Cc, Ms	Qtz
Copper Mountain[3]	Stratabound lens	Cu, Pb, Ag, Au	Cp, Bn, Py, Gl, Azu, Mal	Qtz, Cc, Ms	Qtz, Ms
Copper King[3]	Stratabound lens	Cu, Pb, Ag, Bi, Au	Cp, Bn, Azu, Mal, Py, Gl, Tt	Qtz, Ms	Qtz
Postmetamorphic					
Hannum/Harry's Creek	Vein/replacement	Ag, Pb, Zn, Au	Gl, Sph, Ss, Py	Qtz	Qtz
Independence	Vein/replacement	Ag, Pb, Zn	Gl, Sph, Tt, Py	Qtz, Sid, Cc, Act(?)	Sid
Omilak/Omilak East	Vein/replacement	Ag, Pb, Sb, Au, Cu	Gl, Stb, Cp, Gd, Py, Po, Asp	Cc, Dol	
Foster	Vein/replacement	Ag, Pb, Zn, Au, Cu	Gl, Sph, Tt, Py, Cp, Po	Qtz	Qtz
Kugruk/Billiken	Skarn/replacement	Fe, Cu, Ag, Au	Cp, Gd, Py	Mt, Di, Dol, Ido, Olv, Srp, Clh, Phl	Srp, Phl, Grt
Rocky Mountain Creek	Discordant vein	Au, W	Gd, Sch	Qtz, Plg	
Rock Creek	Discordant vein	Au, Ag, Pb, Sb, W	Asp, Py, Gd, Gl, Sch, Ss	Qtz, Ank, Cc, Plg	Plg, Asp, Ms, Ank
Bluff	Discordant vein	Au, Ag, W	Py, Asp, Sch, Cp, Gd, Gl, Po	Qtz, Cc, Fl, Ms	Ms, Plg, Cc, Chl, Tur
Mount Distin	Discordant vein	Au, Ag, As, Sb	Py, Asp, Stb	Qtz, Cc, Ab	Qtz
Twin Mountain	Discordant vein	Au, W	Py, Asp, Gd	Qtz	
Niukluk-Pargon	Skarn/replacement	Ag, Pb, Zn, Cu	Gl, Sph, Cp, Py, Po	Act, Bt, Cc, Chl, Ep, Grt, Ms, Qtz	Ms, Act, Chl, Ep, Grt
Ferndale Creek	Discordant vein	Ag, Pb, Zn, Cu, Sn	Gl, Sph, Ss, Py	Qtz	
Charley Creek	Discordant vein	Au, Bi	Py, Asp	Qtz	
Big Hurrah	Discordant vein	Au, Sb	Gd, Stb	Qtz	Qtz

Note: Ore and gangue minerals are listed in decreasing order of abundance.

[1]Data from Slack et al. (this volume) and U.S. Geological Survey Alaska Resources Data Files (http://ardf.wr.usgs.gov).

[2]Includes Christophosen (strike extension of Aurora Creek).

[3]May be syn-metamorphic.

Mineral abbreviations: Ab—albite; Act—actinolite; Ank—ankerite; Asp—arsenopyrite; Azu—azurite; Bar—barite; Bt—biotite; Bn—bornite; Cc—calcite; Chd—chloritoid; Chl—chlorite; Clh—clinohumite; Cp—chalcopyrite; Di—diopside; Dol—dolomite; Ep—epidote; Fl—fluorite; Gd—gold; Gl—galena; Grt—garnet; Ido—idocrase; Mal—malachite; Ms—muscovite; Mt—magnetite; Olv—olivine; Phl—phlogopite; Plg—plagioclase; Po—pyrrhotite; Py—pyrite; Qtz—quartz; Sch—scheelite; Sid—siderite; Sph—sphalerite; Srp—serpentine; Ss—Ag-sulfosalts; Stb—stibnite; Tt—tetrahedrite; Tur—tourmaline.

Downloaded from specialpapers.gsapubs.org on September 29, 2015

ductile deformation and metamorphism at blueschist and subsequent greenschist facies during the Jurassic and Early Cretaceous Brookian orogeny. Metamorphic fabrics are characterized by mm- to cm-scale tight to isoclinal folds, common intrafolial folds, and well-developed stretching lineations (mineral streaks, quartz rods, and isoclinal fold axes). These features indicate that original stratigraphic relations have been thoroughly transposed. Remnants of primary igneous or sedimentary fabrics are rare but are locally preserved in deformation-resistant lithologies such as dolostone and gabbro.

Three major subdivisions are recognized within the Nome Complex: the Layered sequence, Scattered metacarbonate rocks, and Metaturbidites (Till et al., 2011; Till et al., this volume, Chapter 1). Stratabound base-metal sulfide deposits occur within the Layered sequence, which contains five mappable lithologic units (Fig. 2). Conodont and detrital zircon ages indicate that

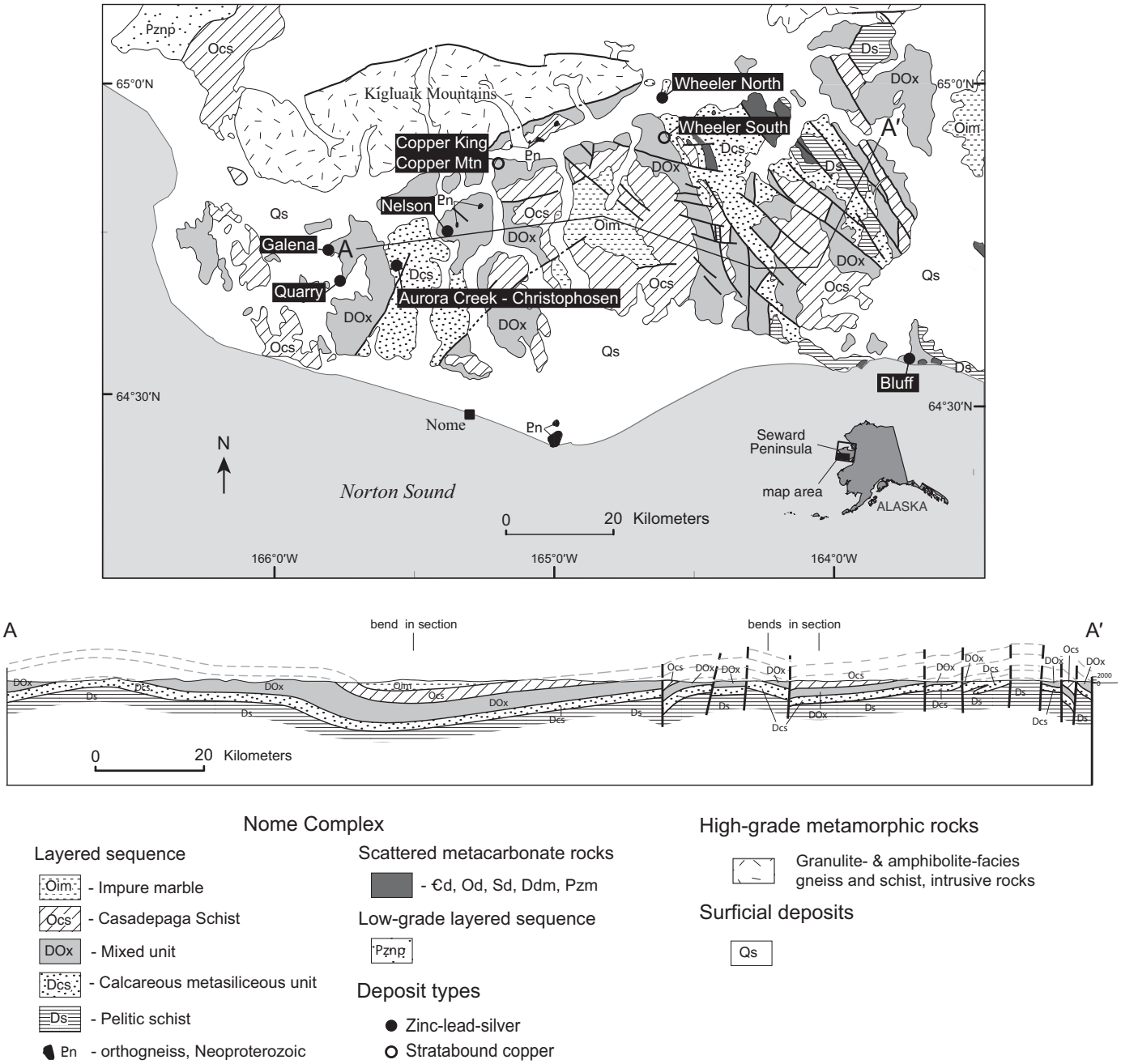


Figure 2. Geologic map of southwestern Seward Peninsula, showing units of the Nome Complex and location of base-metal sulfide deposits and occurrences. Geologic map from Till et al. (2011).

Downloaded from specialpapers.gsapubs.org on September 29, 2015

the older units (Impure marble [Oim], Casadepaga Schist [Ocs], and part of the Mixed unit [DOx]) are largely Ordovician in age; some Cambrian strata also are present based on fossil ages (Dumoulin et al., this volume). The Ordovician carbonate rocks are associated with a metasedimentary unit (Ocs) rich in calcareous, feldspathic, pelitic, and mafic detritus and mafic intrusive rocks (Fig. 3). Small bodies of Neoproterozoic orthogneiss are spatially associated with these older units, and may represent fragments of pre-metamorphic crystalline basement. The younger units lack significant carbonate material, and mafic rocks are extremely rare. The Calcareous metasiliceous unit (Dcs) is a mixture of graphitic siliceous schist, graphitic calcareous schist, thin marble, and pelitic schist. The Pelitic schist (Ds) is composed of pelitic and semipelitic material, with very minor amounts of carbonate. The younger units contain detrital zircons as young as Middle Devonian (Till et al., this volume, Chapter 4).

Till et al. (this volume, Chapter 1) interpreted the three older units as remnants of a continental margin that underwent an incipient rifting event during the Ordovician. The margin supported a carbonate platform from the late Neoproterozoic to the Middle Devonian (includes the Nome Complex and related rocks; Dumoulin et al., this volume). Mafic rocks in the Impure marble, Casadepaga Schist, and Mixed unit are related and possess geochemical characteristics that suggest formation during rifting of continental crust, which likely occurred during the Ordovician (Ayuso and Till, this volume). The rifting event was succeeded by a return to carbonate deposition, which lasted until the Middle Devonian (Dumoulin et al., this volume). Younger units of the Nome Complex—the Calcareous metasiliceous unit and Pelitic schist—represent a transition from a depositional system dominated by carbonate sedimentation to one characterized by an influx of terrigenous material (Till et al., this volume, Chapter 1). The nature of lithologic variation and some lithologies in the Calcareous metasiliceous unit led Till et al. (this volume, Chapter 1) to conclude that its protolith formed in several subbasins, some isolated from terrigenous input. They hypothesize that these subbasins formed during incipient rifting of the continental margin during or after the Middle Devonian.

Stratabound Zn- or Pb-rich deposits at Aurora Creek and Wheeler North occur within one of the younger units, the Calcareous metasiliceous unit (Dcs). Stratabound Pb- and/or Zn-rich deposits at Galena, Quarry, Nelson, and Bluff occur within the Mixed unit (DOx), in thick sequences of marble. Copper-rich deposits (Wheeler South, Copper King, and Copper Mountain) also occur within thick marbles of the Mixed unit. The age of the Mixed unit marbles that contain these deposits is unknown.

The protolith of the Nome Complex is thought to represent part of the same Paleozoic continental margin exposed in the Brooks Range, where it is less deformed (Till et al., this volume, Chapter 1). Paleozoic rocks in both areas record a period of Ordovician to Middle Devonian carbonate platform deposition. In the Brooks Range, carbonate deposition was succeeded by the development of widespread unconformities and basins in Middle Devonian–Mississippian time (Dumoulin et al., 2002; Young, 2004), a period interpreted as a time of extension. The younger units in the Nome Complex, the siliceous, calcareous, and pelitic schists of Dcs and Ds, are thought to record a similar transition

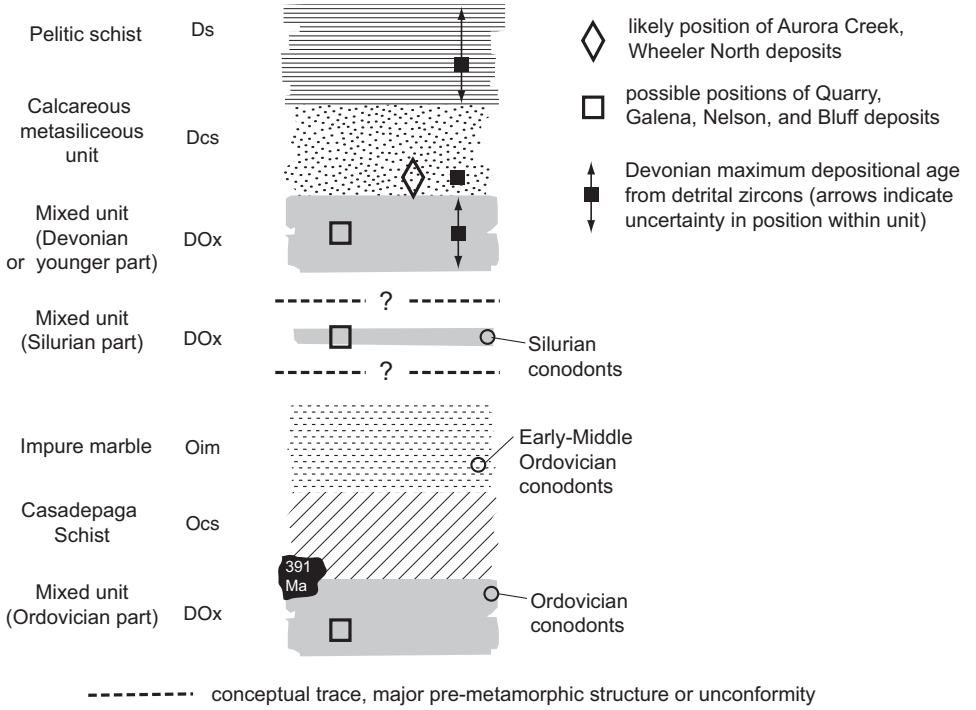


Figure 3. Interpreted stratigraphic sequence of metasedimentary rocks in the Nome Complex showing approximate positions of stratabound sulfide and deformed vein deposits. Modified from Till et al. (this volume, Chapter 1).

Downloaded from specialpapers.gsapubs.org on September 29, 2015

from carbonate to siliciclastic deposition in the Middle Devonian or later (Till et al., this volume, Chapter 1), and may also have formed in an extensional environment.

Mapped parts of Seward Peninsula indicate that older units in the Nome Complex Layered sequence (Oim and Ocs) are structurally above the younger units (Dcs and Ds; Fig. 2); Figure 3 shows the interpreted pre-metamorphic age relations of units within the Layered sequence.

PAST MINING AND EXPLORATION

History and Production

The largest sulfide deposit known in the study area is Aurora Creek, which was discovered in 1967 by the Alaska Division of Mines and Geology during a stream sediment geochemical survey (Herreid, 1968). Following early small-scale mining of placer gold in Aurora Creek (Record NM138, Hawley and Hudson, 2002), the area was later explored and drilled for base metals and gold in the 1970s by Cominco American Resources (Brown, 1977) and in the 1990s by Kennecott Exploration (Porterfield et al., 1996). The contiguous Christophosen deposit to the southeast was discovered prior to 1916, and explored by a shallow shaft (Mertie, 1918) and by pits and trenches in the 1970s and 1990s. The Wheeler North (informal name[1]) deposit was mined from a small pit, yielding possibly several tons of ore, but no shipment records exist (Smith, 1908). At the Quarry deposit, excavation of pits and driving of a shallow shaft were done prior to World War I (Herreid, 1970), followed by trenching in the 1960s to provide material for local road construction (Brobst et al., 1971). The Galena deposit, found prior to 1915 (Eakin, 1915), is exposed in several pits and shallow trenches (Mulligan and Hess, 1965; Herreid, 1966a). Among the Cu-rich deposits and occurrences, the Wheeler South (informal name[2]) deposit was most extensively developed utilizing adits, shafts, trenches, and pits (Smith, 1908), from which a total of ~25 tons of ore was mined prior to 1920 (Cathcart, 1922). No reserve or resource data are available for any of the above mineral deposits or occurrences.

Previous Genetic Models

Early workers including Smith (1908, 1910) described the base-metal deposits and occurrences of south-central Seward Peninsula as veins or replacements, linked in some cases to buried (but unknown) igneous intrusions as metal sources. Herreid (1970) compared these deposits with the carbonate-hosted F-Ba-Zn-Pb ores of the Illinois-Kentucky fluorspar district, which are widely considered to be epigenetic Mississippi Valley–type (MVT) deposits that formed long after sedimentation. Brobst et al. (1971) proposed a postmetamorphic origin for the Quarry deposit, coeval with the Late Cretaceous emplacement of tin granites on western Seward Peninsula. For the Aurora Creek deposit, Brown (1977) proposed an origin involving pre-metamorphic, syngenetic-exhalative processes distal from a volcanic center. Bundtzen et al. (1994) invoked a proximal volcanogenic massive sulfide (VMS) model for this deposit, based on the presence of inferred felsic metavolcanic rocks in the host sequence, an interpretation followed by Newberry et al. (1997). A very different conclusion was reached by Porterfield et al. (1996), who suggested that Aurora Creek is a pre-metamorphic carbonate replacement deposit (CRD), analogous to the large Santa Eulalia Ag-Pb-Zn-Cu ore body in Mexico, with an implied genetic link to a hidden granitic pluton (cf. Megaw et al., 1988).

SCOPE AND METHODS

Scope

This study provides a combined geological, mineralogical, and geochemical documentation of the stratabound sulfide deposits and occurrences and spatially related hydrothermally altered zones. Results presented here are based on field examination and sampling during the summers of 2004–2007, transmitted and reflected light petrography, whole-rock geochemistry for 65 major, trace, and rare-earth elements (REEs), scanning electron microscopy (SEM), and electron microprobe analysis (EMPA). The focus is on Zn-Pb(-Ag-Au-Ba-F) lenses, veins, and vein-breccias, with only limited study of the stratabound Cu-Bi-Sb-Pb-Ag-Au disseminations.

Access to drill core was very limited for this study; we were able to view and sample rocks from one skeletonized drill core from the Aurora Creek deposit and two drill cores from the Bluff prospect.

Analytical Methods

Whole-rock geochemical analyses were obtained on representative samples after removal of weathered surfaces and visible veins. For some of the muscovite-chloritoid schists, very small quartz veins could not be removed. All analyses were done at Activation Laboratories in Ancaster, Ontario, following pulverization of samples in an alumina-ceramic mortar. Major, selected trace, and REE were determined by inductively coupled plasma mass spectrometry (ICP-MS) on rock powders fused with lithium metaborate/tetraborate in order to insure complete acid dissolution of minerals such as zircon, rutile, monazite, xenotime, and barite prior to analysis. Two barite-rich samples from the Christophosen deposit were analyzed by high-resolution ICP-MS using an ion exchange technique in order to eliminate Ba interference on Eu. Instrumental neutron activation analysis (INAA) was used for Au, As, Sb, Sc, and Se; F and Hg were determined by specific ion electrode and flame atomic absorption, respectively. Other reported data include total C and S (LECO infrared analyzer), CO_2 (coulometry after digestion with

[1]Originally called Wheeler Lead (Cathcart, 1922).
[2]Originally called Wheeler Copper (Cathcart, 1922).

Downloaded from specialpapers.gsapubs.org on September 29, 2015

2N perchloric acid), graphitic and organic C (difference after CO_2 removal and ignition to 600 °C), and SO_4 (difference after roasting at 850 °C). Analyses were made on duplicate samples and 8–12 standards. Precision and accuracy for concentrations ~100× minimum detection limit (MDL) were generally better than ±5% relative, and for major elements were better than ±1% relative. For concentrations ~10× the MDL, precision and accuracy were about ±10%–20% relative depending on the method used. Details of the various analytical methods (including discussion of accuracy and precision) are available at www.actlabs.com. Results of whole-rock analyses are in the GSA Data Repository (mineralized rocks in Table DR1, muscovite-chloritoid-Fe-carbonate schists in Table DR2, and unaltered siliciclastic rocks in Table DR3)[3].

Mineral identifications were made at the U.S. Geological Survey (USGS) in Reston, Virginia, using standard petrography and a JEOL JSM-840 scanning electron microscopy (SEM) operated at 15 or 20 kV and a beam current of 40 nA. This instrument has a LaB6 electron emitter equipped with an EDAX energy-dispersive X-ray (EDS) analytical system, which provides qualitative and semiquantitative elemental data.

Quantitative electron microprobe analyses (EMPA) of major and minor elements were obtained at the USGS in Reston with a JEOL JXA-8900R five-spectrometer, fully-automated electron microprobe using wavelength-dispersive X-ray spectrometry. Analyses of chloritoid and mica were made at an accelerating voltage of 15 keV, 20 nA probe current, and peak counting times of 20–60 s, using a 10-µm-diameter probe spot. Carbonate analyses were made at 15 keV, 10 nA probe current, and peak counting times of 5–10 s, using a 20 µm spot. Natural and synthetic standard reference materials were used and the analyses were corrected for electron beam/matrix effects, and instrumental drift and dead time, using the phi-rho-Z (CITZAF; Armstrong, 1995) scheme supplied with the JEOL JXA-8900 electron microprobe. Relative accuracy of the analyses, based upon comparison between measured and published compositions of standard reference materials, is ~1%–2% for concentrations >1 wt% and ~5%–10% for concentrations <1 wt%. Elements analyzed as oxides (except Cl and F) and their detection limits (in wt%) at 3 sigma (background) are as follows: chloritoid and mica—MgO (0.02), Al_2O_3 (0.04), SiO_2 (0.06), CaO (0.03), TiO_2 (0.05), FeO (total) (0.04), MnO (0.04), Na_2O (0.03), K_2O (0.03), ZnO (0.06), BaO (0.04), SrO (0.04), F (0.05), and Cl (0.03); and carbonate—MgO (0.05), MnO (0.05), SrO (0.10), FeO (total) (0.08), CaO (0.07), ZnO (0.10), and BaO (0.10). All data are included in Tables DR4 and DR5 [see footnote 3].

[3]GSA Data Repository Item 2014227, Table DR1: Whole-rock analyses of mineralized rocks from base-metal sulfide deposits; Table DR2: Whole-rock analyses of muscovite-chloritoid-Fe-carbonate schists; Table DR3: Whole-rock analyses of unaltered siliciclastic metasedimentary rocks; Table DR4: Electron microprobe analyses of micas (phengite and biotite) from muscovite-chloritoid schists and mineralized rocks; Table DR5: Electron microprobe analyses of chloritoid from muscovite-chloritoid schists and mineralized rocks, is available at www.geosociety.org/pubs/ft2014.htm, or on request from editing@geosociety.org or Documents Secretary, GSA, P.O. Box 9140, Boulder, CO 80301-9140, USA.

STRATABOUND DEPOSITS AND OCCURRENCES

Aurora Creek

Geologic Setting

For the purposes of this study, we consider the Aurora Creek and Christophosen Zn-Au-Ba-F deposits (Fig. 4) to be parts of the same mineralized system, and they are here grouped as the Aurora Creek deposit. Both consist of disseminated to semi-massive sulfide accumulations that together form a discontinuous, nearly 4-km-long stratabound zone within siliciclastic metasedimentary rocks of the Nome Complex. Results from exploration drilling indicate that the metasedimentary rocks that host the mineralized zone (Dcs-m; Fig. 4) are structurally below a thick (2 km), massive marble unit (DOx) and above a sequence of variably graphitic and albitic schists (Dcs; Fig. 4; Brown, 1977). The thick massive marble is part of the Mixed unit (DOx, Fig. 2); metasedimentary rocks that host mineralization and the schists that lie structurally below them are part of the Calcareous metasiliceous unit (Dcs, Fig. 2).

The metasedimentary sequence associated with mineralization is between 250 and 700 m thick (Fig. 4). This sequence is composed of: (1) quartz-muscovite-chloritoid-chlorite schist with as much as 20 vol% calcite, dolomite, or Fe-carbonate; (2) graphitic and micaceous impure marble; and (3) albitic and chloritic impure marble, graphitic mica schist, quartz-rich schist, graphitic quartz-rich schist, chlorite-albite schist, and schistose carbonate-clast conglomerate or breccia. The matrix of the schistose conglomerate is lithologically identical to the graphitic and micaceous impure marble. The conglomerate is exposed at the structural top of the mapped sequence and has also been encountered in drill core lower in the sequence, in sparsely mineralized rocks above the main sulfide zone (Fig. 4; Brown, 1977).

Detrital zircon ages from mineralized drill core samples and outcrop at Aurora Creek provide a limit to the age of mineralization (Till et al., this volume, Chapter 4). A drill core sample taken just above the main zone of mineralization (AC17/66) and muscovite-chloritoid schist (05AD24G), interpreted as part of the alteration zone a few kilometers south of the deposit, yield Devonian detrital zircon populations (Fig. 4). The drill core sample contains a population of five Middle Devonian zircons, the youngest population collected from the Nome Complex to date; the muscovite-chloritoid schist and nearby schist from Dcs (05AD25C) contains populations of Early Devonian zircons. Other samples, collected from the schistose carbonate conglomerate and the quartz-rich schist, contain only Mesoproterozoic zircons. The mineralization at Aurora Creek, based on detrital zircon geochronology, is Middle Devonian or younger.

Sulfide Zones

Based on exploration drilling, four sulfide-bearing zones of the Aurora Creek deposit are recognized (Brown, 1977; Porterfield et al., 1996), each occurring within quartz-ankerite rocks that thin to the north and together grade into unmineralized micaceous marble. The main sulfide zones extend for ~245 m along

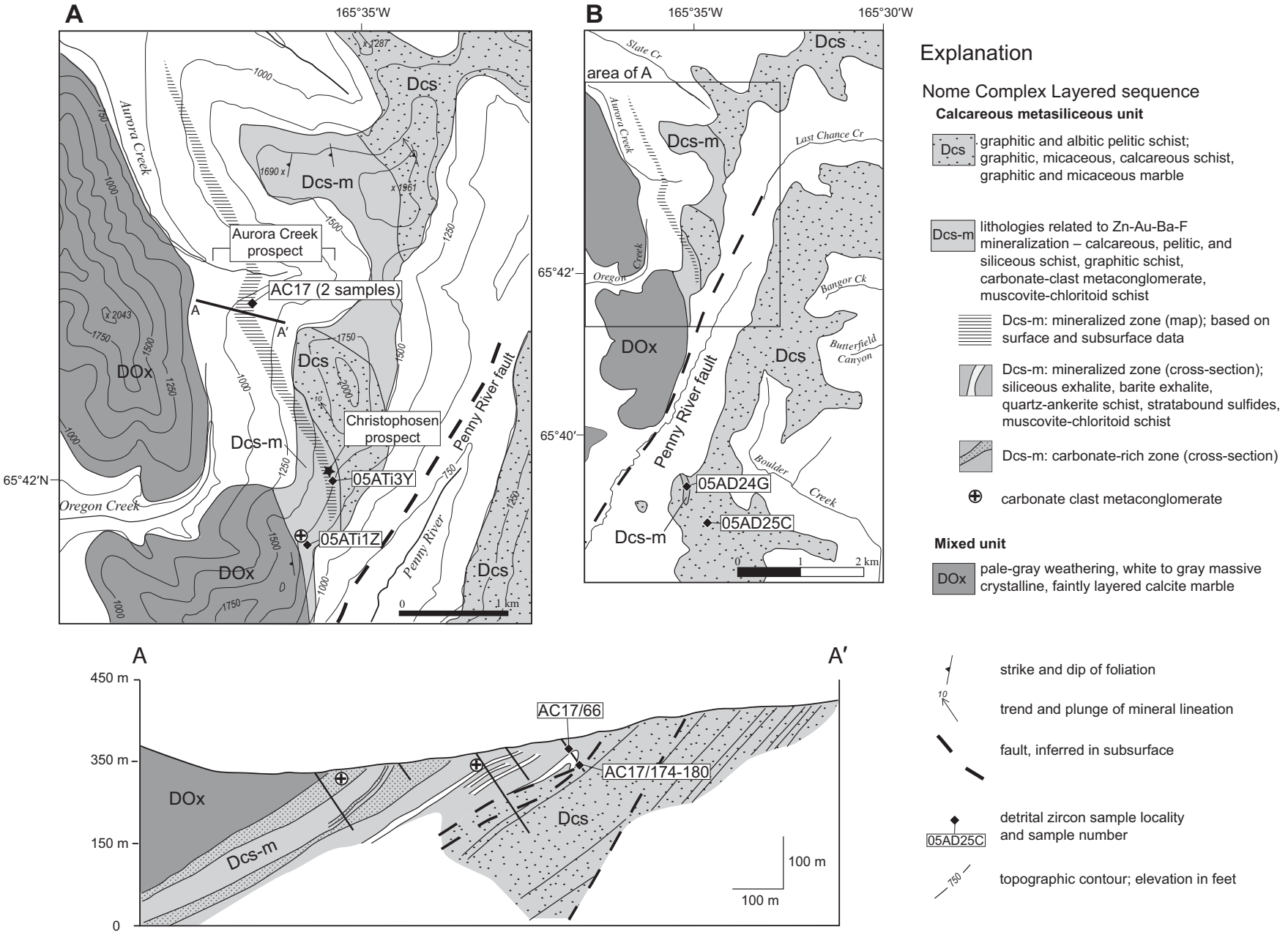


Figure 4. Geologic setting of the Aurora Creek Zn-Au-Ba-F deposit: (A) Geologic map and cross section (A–A′) of the deposit; locations of five drill holes (inclined) are shown. (B) Regional map showing extent of rocks thought to represent alteration lithologies. Geology modified from Till et al. (2011).

Downloaded from specialpapers.gsapubs.org on September 29, 2015

Downloaded from specialpapers.gsapubs.org on September 29, 2015

strike, dip mainly 35° to the southwest, and range in thickness typically from <1–2 m; much thicker zones (up to 19.5 m) occur in fold hinges. Proportions of sulfide vary from several vol% in disseminated zones to ~30–50 vol% in semi-massive zones; true massive sulfide (>50 vol%) is apparently rare. The best drill hole intercepts are 24.8 m of 5.5% Zn and 0.007 oz/t Au, 4.6 m of 8.5% Zn, and 7.6 m of 2.6% Zn and 0.244 oz/t Au; thicknesses and grades of Zn + Au increase from the south and north toward Aurora Creek (Porterfield et al., 1996). Mineralogical zoning, recognized by Brown (1977), is characterized by an outer low-grade zone of minor sphalerite and galena, a middle higher-grade zone of abundant sphalerite, and an inner high-grade zone of abundant sphalerite with minor pyrite and gold.

Mineralogy

Sphalerite, as the major sulfide mineral, forms disseminations, breccia fillings, and lenses. Disseminated sphalerite occurs in both silicate and carbonate host rocks, as red-brown grains typically <1 cm in length. Brecciated carbonate rock, from Aurora Creek, shows a distinctive crackle texture in which sphalerite fills the matrix of angular fragments of carbonate (Fig. 5A). Semi-massive zones containing abundant sphalerite are reported in drill cores (Porterfield et al., 1996) but are not present in the cores that we studied. Network veins consist of sphalerite and quartz with local chlorite (Fig. 6A), chloritoid (Fig. 6B), or zoned tourmaline (Fig. 6C). Within quartz-rich schist, sphalerite typically is aligned in the major foliation (Fig. 6D). Regardless of textural setting, all of the sphalerite is unzoned both in transmitted light and in SEM backscattered electron (BSE) images.

Abundant pyrite occurs in fine-grained disseminations and locally as coarse (1 cm) euhedral crystals that contain inclusions of pyrrhotite and sparse galena. Pyrrhotite also forms separate grains, and in a few samples is the predominant iron sulfide. Magnetite is common in irregular masses up to 2 cm in length, or as euhedral crystals enclosed in sphalerite or gangue minerals. Galena, chalcopyrite, and arsenopyrite (Fig. 6E) are generally sparse, although a few samples contain minor (~3%–5%) galena as intergrowths with sphalerite and pyrite, and as inclusions in pyrite (see Ayuso et al., this volume). Gold and electrum, where present, form isolated small (<10 μm) grains in pyrite and sphalerite (Fig. 7A); appreciable Ag concentrations occur in some of the gold, based on semiquantitative analyses by SEM-EDS. Rare constituents include cassiterite, tetrahedrite, and one or more unidentified Pb-Sb and Ag-Pb sulfosalts. Gangue minerals are chiefly quartz, siderite, and dolomite; calcite is generally minor. Some sulfide-bearing samples contain minor tourmaline, barite (Fig. 7B), hyalophane (Ba-rich K-feldspar), fluorite, chloritoid, apatite, monazite, allanite, epidote, or rutile. The carbonate gangue typically consists of siderite that replaces earlier dolomite (Fig. 7C); siderite locally shows prominent growth zoning (Fig. 7D).

Stratiform Siliceous and Baritic Rocks

Stratiform layers and lenses of siliceous and baritic rocks occur on Christophosen Ridge at the southeastern end of the Aurora Creek deposit (Fig. 4). The barite-rich layers have been found only in a small prospect pit on the east side of the ridge, in a structural position below the main zone of mineralization.

The siliceous layers are 10–30 cm thick in a small outcrop on Christophosen ridge. Tight to isoclinal folds are evident both in outcrop and hand specimens. Layering dips steeply (Fig. 5B). Predominant is fine-grained, microcrystalline quartz with minor pyrite and muscovite, sparse ankerite and barite, and traces of sphalerite and galena. Thin (<1 mm) laminae containing disseminated ankerite and/or pyrite define the layering. In places, the microcrystalline quartz layers contain 1–2 cm clots of Fe-carbonate and interspersed, fine-grained sphalerite.

The barite-rich zone, estimated to be 0.5 m thick, is commonly layered and typically displays open to tight folds (Fig. 5C). Characteristic are alternating layers of cream-colored barite and orange-weathering dolomite, the latter locally forming 1–5 cm fragments in the former. Calcite and quartz are minor. Sulfide minerals occur as sparse disseminations of pyrite, sphalerite, or galena; one coarse (3–5 cm) clot of magnetite and pyrite is also present. Grains of euhedral hyalophane ~300 μm long are locally intergrown with fine-grained barite and variably replaced by quartz (Fig. 7E).

Hydrothermal Alteration

In the Aurora Creek area, hydrothermal alteration varies in style and intensity owing to the diversity of wall rock lithologies. Due to scarcity of outcrops and degree of deformation, the geometry of altered rocks is poorly defined and thus variations in thickness and mineralogy with proximity to the sulfide deposit are unknown. Within micaceous metasedimentary rocks, hydrothermal alteration produced a distinctive assemblage in schist composed of muscovite, chloritoid, and quartz, minor chlorite and ankerite, and sparse pyrite, galena, chalcopyrite, barite, hyalophane, fluorite, tourmaline, monazite, xenotime, and ilmenite. This assemblage, hereafter referred to as muscovite-chloritoid schist, is estimated to extend tens of meters from the sulfide zone; based on information from drill cores, the schist also extends outward from less altered, intervening lithologies such as quartzite. Muscovite contents range widely, in tandem with varying amounts of quartz including thin (<1 cm) discontinuous quartz lenses. Muscovite, and to a lesser extent chloritoid, typically contains myriad small inclusions of ilmenite and zircon (Fig. 7F), plus rutile, monazite, and xenotime. The muscovite is in most cases compositionally zoned (Fig. 7G); some grains have lamellae and aggregates of hyalophane (Fig. 7H).

The matrix of the conglomerate southwest of the sulfide zone (Fig. 4) may be hydrothermally altered. Scanning electron microscopy study of the heavy-mineral fraction of this conglomerate, used initially in obtaining detrital zircons for SHRIMP U-Pb geochronology (Till et al., this volume, Chapter 4), shows the presence of minor pyrite together with sparse barite and galena. Textural evidence does not support a detrital origin for the barite or galena; hence a hydrothermal origin for these minerals is inferred.

Downloaded from specialpapers.gsapubs.org on September 29, 2015

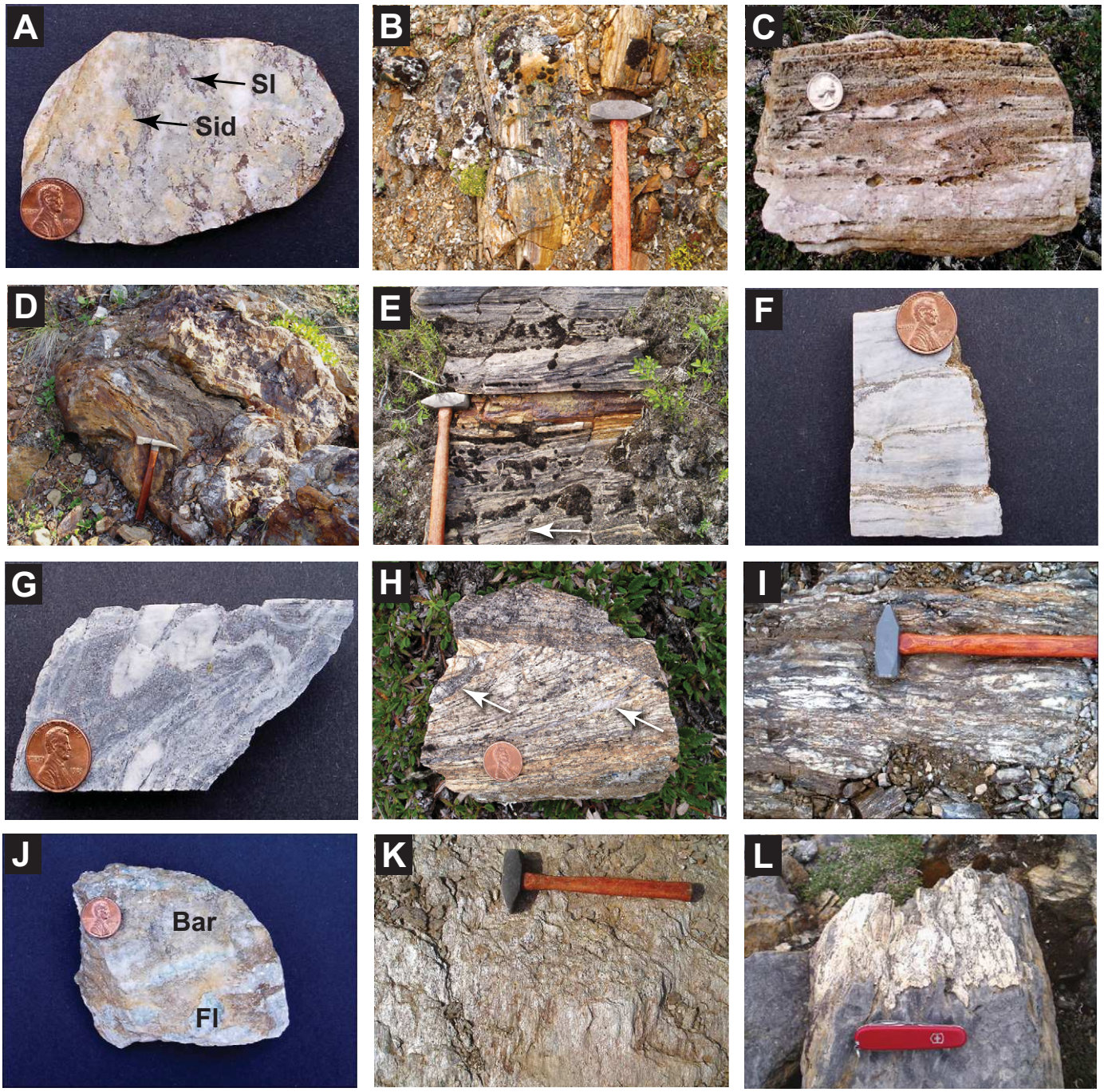


Figure 5. Field and hand specimen photographs of base-metal sulfide deposits and occurrences. (A) Disseminated sphalerite (Sl) and siderite (Sid) in quartz-carbonate gangue, Aurora Creek deposit; (B) layered siliceous rock (exhalite), Christophosen deposit; (C) folded barite-carbonate rock (exhalite), Aurora Creek deposit; (D) folded sulfide-magnetite-fluorite-carbonate lens in marble, Wheeler North deposit; (E) iron-stained pyritic layer, Wheeler North deposit; note isoclinal folds in unmineralized and mineralized zones (arrow at bottom); (F) seams of disseminated sphalerite and galena in dolostone, Nelson occurrence; (G) folded quartz-sulfide layer, Bluff occurrence; (H) quartz and disseminated sulfides in silicified carbonate, Copper King deposit; note presence of quartz-sulfide veins in shear planes (arrows) and along upper sheared contact; (I) banded quartz-carbonate-sulfide-sulfosalt-fluorite vein in marble, Quarry deposit; (J) coarse barite (Bar)-fluorite (Fl) from remobilized vein, Quarry deposit; (K) muscovite-quartz-chloritoid-chlorite-carbonate schist (tiny black grains are chloritoid), Quarry deposit; (L) folded mylonitic quartz vein, Galena deposit.

Downloaded from specialpapers.gsapubs.org on September 29, 2015

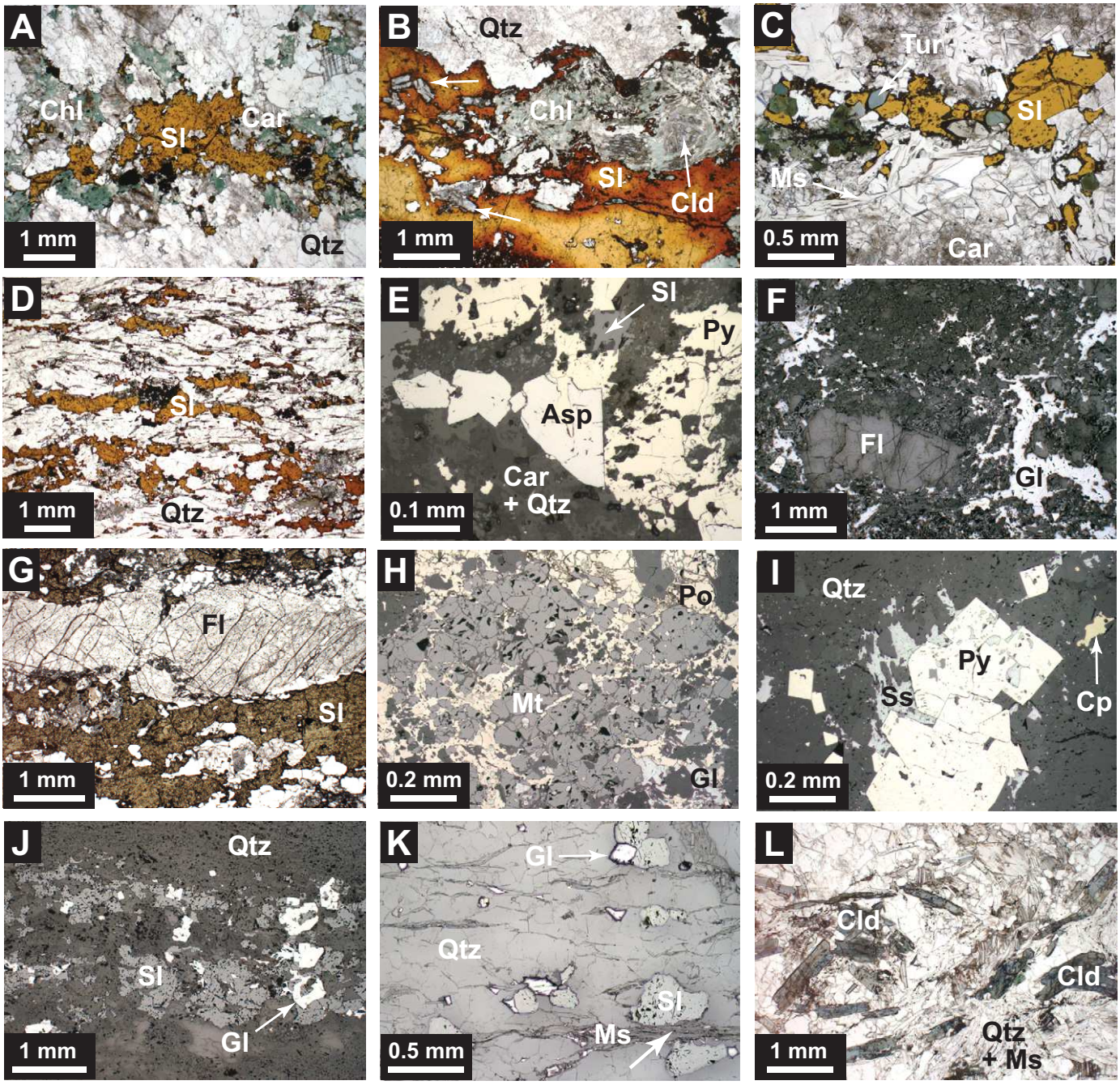


Figure 6. Photomicrographs of mineralized samples, all in plane transmitted light unless otherwise noted. (A) Sphalerite (Sl), chlorite (Chl), and carbonate (Car) in a quartz (Qtz) matrix; Aurora Creek deposit, sample JS-07-8E; (B) relict chloritoid (Cld, arrows) enclosed in chlorite and sphalerite (Sl) with quartz matrix; Aurora Creek deposit, sample AC-8/60.0 ft; (C) tourmaline (Tur) with sphalerite (Sl) in matrix of carbonate, muscovite (Ms), and quartz; Aurora Creek deposit, sample JS-07-8D; (D) sphalerite (Sl) grains aligned in the principal metamorphic foliation; matrix is quartz with minor muscovite and carbonate; Aurora Creek deposit, sample AC-8/18.5 ft; (E) arsenopyrite (Asp) with pyrite (Py) and minor sphalerite (Sl) in matrix of carbonate and quartz; Aurora Creek deposit, sample AC-8/60.0 ft (reflected light); (F) galena (Gl) and minor pyrite with coarse fluorite (Fl) in matrix (dark gray) of quartz, fluorite, and muscovite; Wheeler North deposit, sample JS-07-18C (reflected light); (G) fluorite and sphalerite with minor quartz; Wheeler North deposit, sample JS-05-77E; (H) magnetite (Mt) with pyrrhotite (Po) and minor pyrite and galena, with matrix quartz; Wheeler North deposit, sample JS-04-15G (reflected light); (I) euhedral pyrite with inclusions and intergrowths of unidentified Ag-Sb-S sulfosalt (Ss) mineral, in matrix of quartz and sparse chalcopyrite (Cp); Wheeler North deposit, sample JS-07-18B (reflected light); (J) sphalerite, pyrite, and minor galena (Gl, white arrow) in matrix of quartz and minor carbonate; Nelson occurrence, sample JS-06-18A (reflected light); (K) sphalerite and minor galena in foliated matrix of quartz and muscovite; note truncation of sphalerite grains in lower right by foliated muscovite (large arrow) and tiny galena grains within muscovite seams; Nelson occurrence, sample JS-06-18A (reflected light); (L) euhedral chloritoid in matrix of quartz, muscovite, and minor carbonate, Quarry deposit, sample JS-07-1G.

Downloaded from specialpapers.gsapubs.org on September 29, 2015

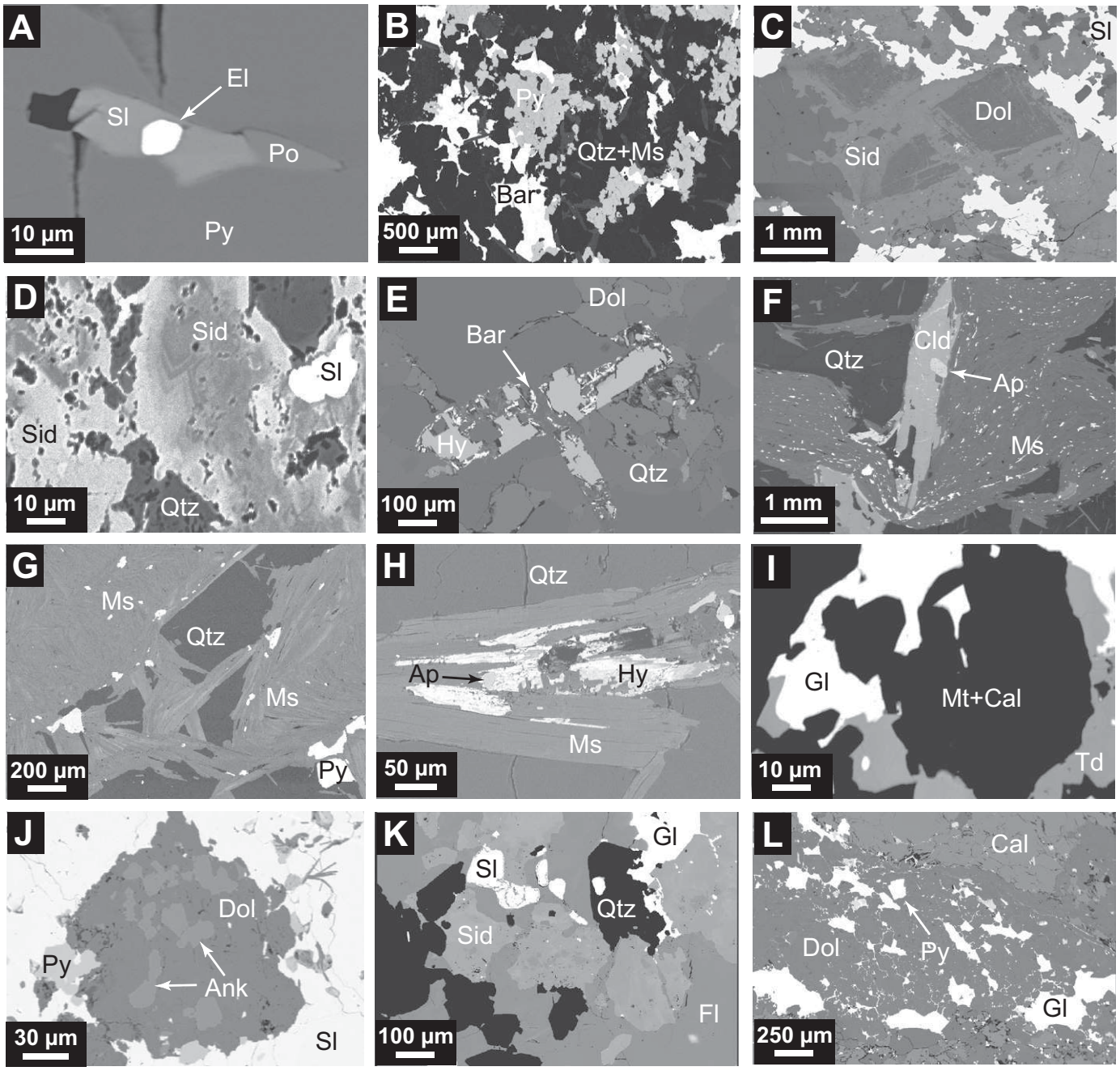


Figure 7. Scanning electron micrographs of mineralized samples. (A) Electrum (El) in sphalerite (Sl) within pyrite (Py), Aurora Creek deposit, sample AC-17/102.0; (B) intergrown pyrite and barite (Bar), Aurora Creek deposit, sample JS-07-27; (C) siderite (Sid) replacing dolomite (Dol) in sphalerite-rich breccia, Aurora Creek deposit, sample JS-07-8D; (D) zoned siderite gangue in thin sphalerite-rich lens, Aurora Creek deposit, sample AC-8/60.0; (E) bladed hyalophane (Hy) and interstitial barite, Aurora Creek deposit, sample JS-05-66A; (F) coarse chloritoid (Cld) and inclusion-rich muscovite (Ms) with sparse apatite (Ap) in muscovite-chloritoid schist (small white inclusions are mostly ilmenite and zircon), Aurora Creek deposit, sample AC-17/88.6; (G) zoned muscovite with pyrite, Aurora Creek deposit, sample AC-17/178.0; (H) hyalophane (Hy) inclusions in muscovite, Aurora Creek deposit, sample JS-07-27; (I) Ag-rich tetrahedrite (Td) with galena (Gl), Wheeler North deposit, sample JS-07-18C; (J) ankerite (Ank) replacing dolomite within sphalerite, Wheeler North deposit, sample JS-05-77H; (K) fluorite (Fl) and zoned siderite with sphalerite and galena, Wheeler North deposit, sample JS-04-15H; (L) galena and minor pyrite in a dolomite matrix bordered by calcite (Cal), Nelson occurrence, sample JS-07-19B.

Downloaded from specialpapers.gsapubs.org on September 29, 2015

A small metabasite dike or sill in Aurora Creek, ~3 m thick and 10 m long, is pervasively altered to an assemblage of tremolite + chlorite + ilmenite + carbonate + pyrite ± magnetite ± chalcopyrite. This apparent intrusive body is weakly foliated, but its relationship with surrounding pelitic and muscovite-chloritoid schists is unknown.

Tremolite-chlorite-hematite-apatite schist with minor pyrite, chalcopyrite, and magnetite is exposed in a resistant, blocky-weathering lens, ~100 m across, east of Aurora Creek near peak 1690 (Fig. 4). Along the ridgeline as far as peak 1961, muscovite-chloritoid schists are common, and essentially identical to the schists encountered in Aurora Creek adjacent to the sulfide mineralization. Similar muscovite-chloritoid schist occurs in a section of calcareous and graphitic pelitic schists ~6 km south of the Aurora Creek deposit (Fig. 4B).

The pre-deformational extent of the alteration zone surrounding the Aurora Creek deposit cannot be characterized. Both the penetrative ductile deformation and brittle fault movement (Penny River fault, Fig. 4) have modified the geometry of the deposit, perhaps significantly.

Wheeler North

Geologic Setting

The Wheeler North Pb-Zn-Ag-Au-F deposit is southeast of the Kigluaik Mountains (Fig. 2) within the Calcareous metasiliceous unit (Dcs), the same unit of the Nome Complex Layered sequence that hosts the Aurora Creek deposit. Like the Aurora Creek deposit, the Wheeler North deposit is near the contact of the Calcareous metasiliceous unit with structurally overlying thick, massive marbles of the Mixed unit (DOx) (Fig. 8).

Earliest references to the Wheeler North deposit describe prospect pits on both the northwest and southeast banks of the Pilgrim River, near the mouth of Iron Creek (Fig. 8). Smith (1908) described three pits on the south side of the river, one of which exposed a 1.2-m-thick lens of galena in limestone. On the northwest bank of the river, Cathcart (1922) recorded exposures of galena in a 9-m-long cut. Both Smith (1908) and Cathcart (1922) noted that mineralization was concentrated along or near contacts between limestone and schist. Each reported the presence of greenstone on the south side of the river, near the contact between limestone and schist.

Well-foliated marble with north-northeast–trending mineral lineations and isoclinal fold axes is exposed adjacent to mineralization on both sides of the river. Schists spatially associated with the sulfide deposit are typically calcareous, dominated by varying amounts of calcite, siderite, or ankerite with muscovite (typically barium-rich), quartz, chloritoid, and accessory minerals that include dolomite, pyrite, albite, apatite, and fluorite. Study by EMPA and SEM reveals that small (<0.1 mm) grains of sphalerite, galena, chalcopyrite, barite, tetrahedrite, pyrrhotite, xenotime, florencite, zircon, rutile, and monazite are characteristic of these rocks. Schists exposed along both banks of the river 100–1000 m from the prospect are typically calcareous (quartz-calcite-muscovite-chloritoid) or pelitic (quartz-muscovite-chloritoid-chlorite), and contain minor pyrite and/or siderite, together with trace amounts of sphalerite, galena, chalcopyrite, xenotime, and tetrahedrite. Several outcrops of black-weathering graphitic siliceous schist are exposed on the south side of the river. Less common near the deposit, on both sides of the river, are large angular blocks of dark-green chlorite-albite schist, which may be the greenstone reported by Smith (1908) and Cathcart (1922).

Mineral lineations and axes of folds trend north-northwest at the deposit, and are similar to those measured in schists several kilometers along trend to the north and south (Fig. 8). Schists along strike are similar in composition to those near the prospect, and they include pelitic and calcareous varieties that are chloritoid-bearing, together with thin layers of marble and chlorite-albite schist. The southern exposures also contain a 0.5-m-thick siliceous schist that yielded Mesoproterozoic detrital zircons (sample 07ATi21D, Fig. 8; Till et al., this volume, Chapter 4).

Sulfide Zone

The main mineralized zone consists of a ~0.5-m-thick sulfide-rich layer enclosed by marble and schist and deformed by an open, northeast-plunging fold (Fig. 5D). In places, sulfide layers occur both above and below a thin marble unit. Sulfides vary from minor disseminations of pyrite, sphalerite, or galena in schist and carbonate rock to semi-massive to nearly pure (>90 vol%) pyrite or galena. Early assays reported by Wimmler (1926) include results on a 0.7 m channel sample containing 3.0 wt% Pb, 2.3 oz/t Ag, and 0.30 oz/t Au, and a single high-grade grab sample having 22.9 wt% Pb and 20.0 oz/t Ag. An irregular, undeformed quartz-carbonate-sulfide vein up to 30 cm thick cuts the sulfide layer. In outcrops ~100 m to the east, thin pyritic layers and host siliciclastic metasedimentary rocks display tight to nearly isoclinal folds (Fig. 5E).

Mineralogy

Fine- to coarse-grained galena is the principal sulfide, accompanied by variable amounts of pyrite and lesser sphalerite. Both galena and sphalerite are intergrown with fluorite, the latter locally occurring as gray lenses up to 1 cm thick (Figs. 6F and 6G). In places, the mineralized lens consists nearly entirely of massive pyrite with sparse interstitial quartz. Pyrite also commonly forms euhedral crystals with inclusions of galena or sparse pyrrhotite. Magnetite is locally abundant, forming discrete grains or aggregates (Fig. 6H) and segregations in pyrite- and galena-rich lenses. Tetrahedrite occurs as intergrowths with galena (Fig. 7I) and inclusions in euhedral pyrite. Sparse phases include arsenopyrite, pyrrhotite, chalcopyrite, and unidentified Ag-Sb-S (Fig. 6I), Pb-Sb-S, and Pb-Sb-Ag-S sulfosalts. No gold was found. Major gangue minerals are quartz and carbonates including dolomite, ankerite, and siderite (Figs. 7J and 7K). Fluorite commonly occurs as massive gray lenses up to 3 cm thick, as disseminated grains, and as the matrix to abundant galena or sphalerite. Sparse hyalophane is locally intergrown with sphalerite.

Downloaded from specialpapers.gsapubs.org on September 29, 2015

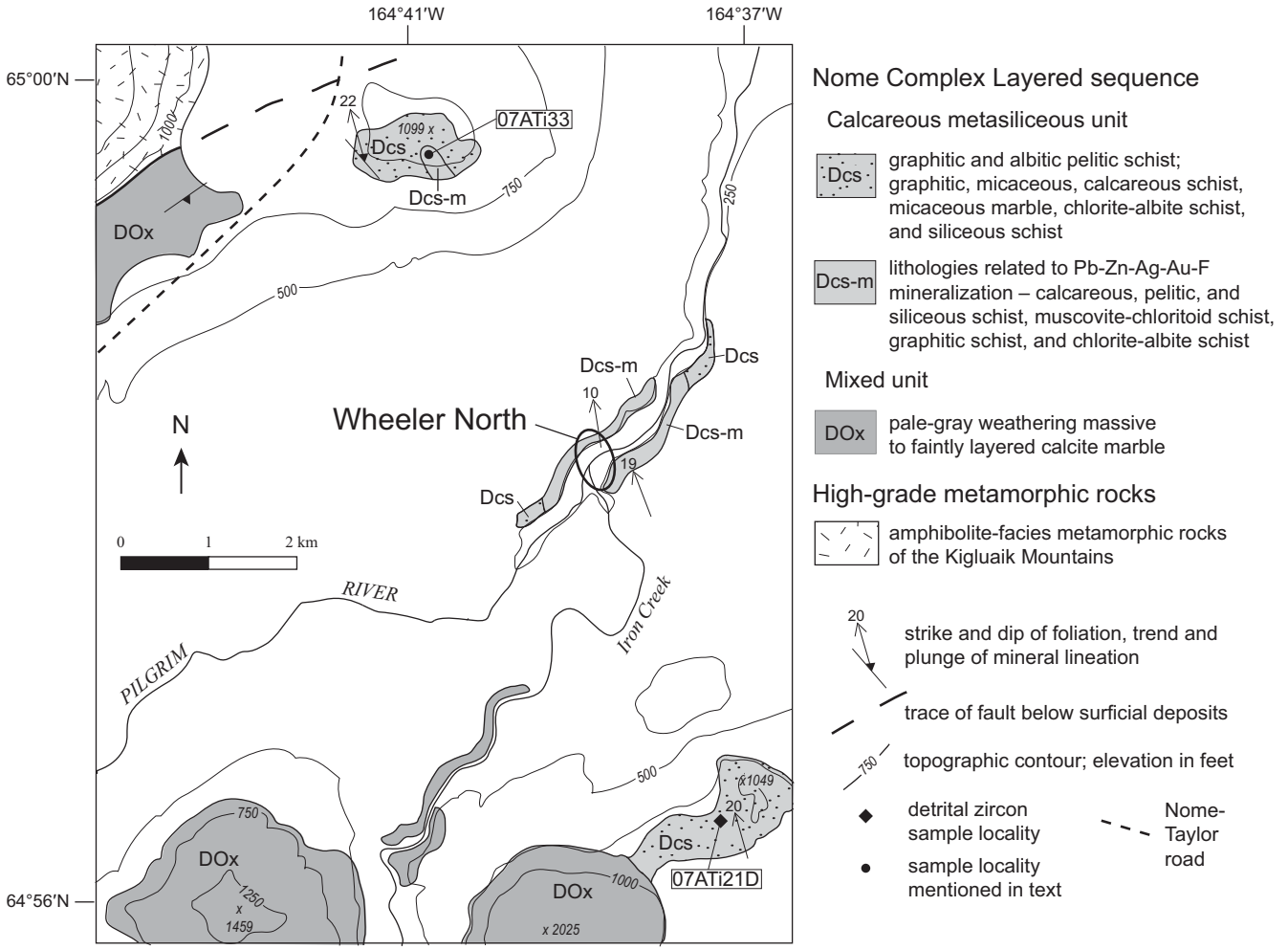


Figure 8. Geologic map of the Wheeler North Pb-Zn-Ag-Au-F deposit area. Geology modified from Till et al. (2011).

Hydrothermal Alteration

Muscovite-chloritoid schist, similar to the lithology at the Aurora Creek deposit, is exposed at the Wheeler North deposit and is a common lithology up to a kilometer upstream and downstream (Fig. 8). Significantly, it is also present 3.5 km to the north-northwest (Fig. 8). In the vicinity of the deposit, on the north side of the Pilgrim River, muscovite-chloritoid schist alternates with less aluminous pelitic schist and minor dolostone. Siliceous layers with disseminated fine-grained pyrite and purple fluorite occur locally. Within the muscovite-chloritoid schist, small deformed quartz veins less than 1 cm thick have concentrations of chloritoid and tourmaline(?) along contacts with the host schist. On the south side of the Pilgrim River, muscovite-chloritoid schists are spatially associated with graphitic marble and with pelitic schist as far as several hundred meters downstream from the deposit.

Chalcopyrite, galena, and sphalerite occur as fine-grained accessory minerals and inclusions within pyrite in muscovite-chloritoid schist along the river hundreds of meters downstream (on the south side) and upstream (on the north side) from the deposit. Chalcopyrite is present in muscovite-chloritoid schist at a separate locality 3.5 km to the north (07ATi33; Fig. 8).

Nelson

Geologic Setting

The Nelson Zn-Pb occurrence is due north of Nome and, unlike the Aurora Creek and Wheeler North deposits, is hosted within the Mixed unit (Fig. 2). The prospect sits on Steep Creek, on the south face of Mount Distin (Fig. 9). At Mount Distin, the Mixed unit is comprised of two thick sections dominated by cliff-forming marble separated by an interval of interlayered schists, marble, and dolomitic marble (Fig. 9). Sulfide mineralization is within the interval of mixed lithologies, which locally include 1–10-m-thick layers of platey-weathering gray marble, calcareous schist, tan dolomitic marble, chlorite-albite schist, and white-weathering muscovite schist. Platey marbles contain lenses of dolostone and chlorite-albite schist. Cathcart (1922) described a sulfide-bearing zone nearly 2 m thick in “bleached limestone.”

Downloaded from specialpapers.gsapubs.org on September 29, 2015

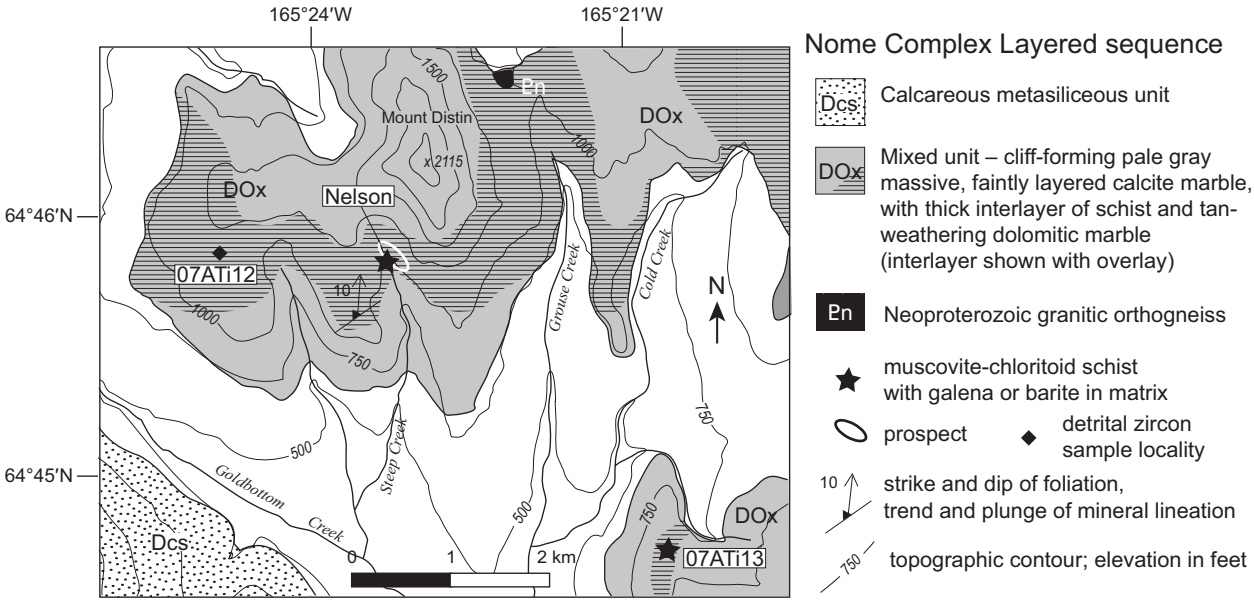


Figure 9. Geologic map of the Nelson Zn-Pb occurrence area. Geology modified from Till et al. (2011).

Sulfide Zone

Sulfide minerals form disseminations and veinlets in siliceous dolomitic marble; no semi-massive or massive sulfide has been found. Sphalerite, galena, and lesser pyrite are concentrated in thin lenses less than 1 cm thick that are parallel to layering in the host marble (Figs. 5F and 6J). Pb-Sb-S and Pb-Sb-Ag-S sulfosalt minerals are minor; trace amounts of arsenopyrite occur as tiny inclusions in pyrite. Secondary smithsonite is present in small amounts. Gangue minerals comprise quartz, dolomite, and calcite (Fig. 7L), with lesser F-phlogopite and muscovite, and traces of fluorite and talc.

No hydrothermal alteration zone has been identified in the vicinity of the prospect. However, muscovite-chloritoid schist within 20 m structurally below the prospect contains barite as inclusions in pyrite. An outcrop of similar schist over 3 km to the southwest has galena inclusions in barite (Fig. 9). Accessory minerals in these schists (apatite, rutile, zircon, monazite, and xenotime) and their textural relations with enclosing muscovite, chloritoid, and carbonate are similar to those in muscovite-chloritoid schists associated with mineralization at Aurora Creek and Wheeler North.

Bluff

Geologic Setting

Stratabound sulfides were encountered during exploration for gold at the Bluff prospect (Ford, 1993), which is located on the coast east of Nome (Fig. 2). The area surrounding the prospect is underlain by rocks of the Mixed unit and Devonian marbles (Ddm) that are part of the Scattered metacarbonate unit (Figs. 2 and 10). Drilling results at the prospect show that upper and lower sections of color-laminated gray marble are separated by an interval of variably calcareous and graphitic quartz-mica schists and graphitic marble (Ford, 1993). The stratabound sulfides occur within the quartz-mica schist.

Sulfide Zone

Base-metal sulfides occur in cores that were drilled for gold exploration. Paragenetically early sulfide minerals are localized in 1- to 3-cm-thick layers that in some intervals are folded together with adjacent quartz veins (Fig. 5G). The sulfide-bearing layers, conformable with lithologic layering in the host quartz-muscovite schist, consist of disseminated sphalerite and galena with subordinate pyrite and sparse chalcopyrite in a gangue of quartz, carbonate, and minor muscovite. Apatite and rutile are trace constituents.

Copper Mountain, Copper King, and Wheeler South

Geologic Setting

Copper mineralization associated with silica-rich zones in massive marble has been found at several localities dispersed over a broad area in central Seward Peninsula (see record TE071 in Hudson, 1998). The Cu- and silica-rich zones are typically within thick, massive marble of the Mixed unit. They are most common along a broad north-south zone that stretches from the vicinity of the Ward prospect in the north to a small prospect near Big Hurrah in the south, and west of Salmon Lake in the vicinity of Copper King (Fig. 1).

Sulfide Zones

Copper-rich stratabound sulfide deposits occur at Copper Mountain, Copper King, and Wheeler South (Fig. 2). These deposits differ from other base-metal deposits within the Nome

Downloaded from specialpapers.gsapubs.org on September 29, 2015

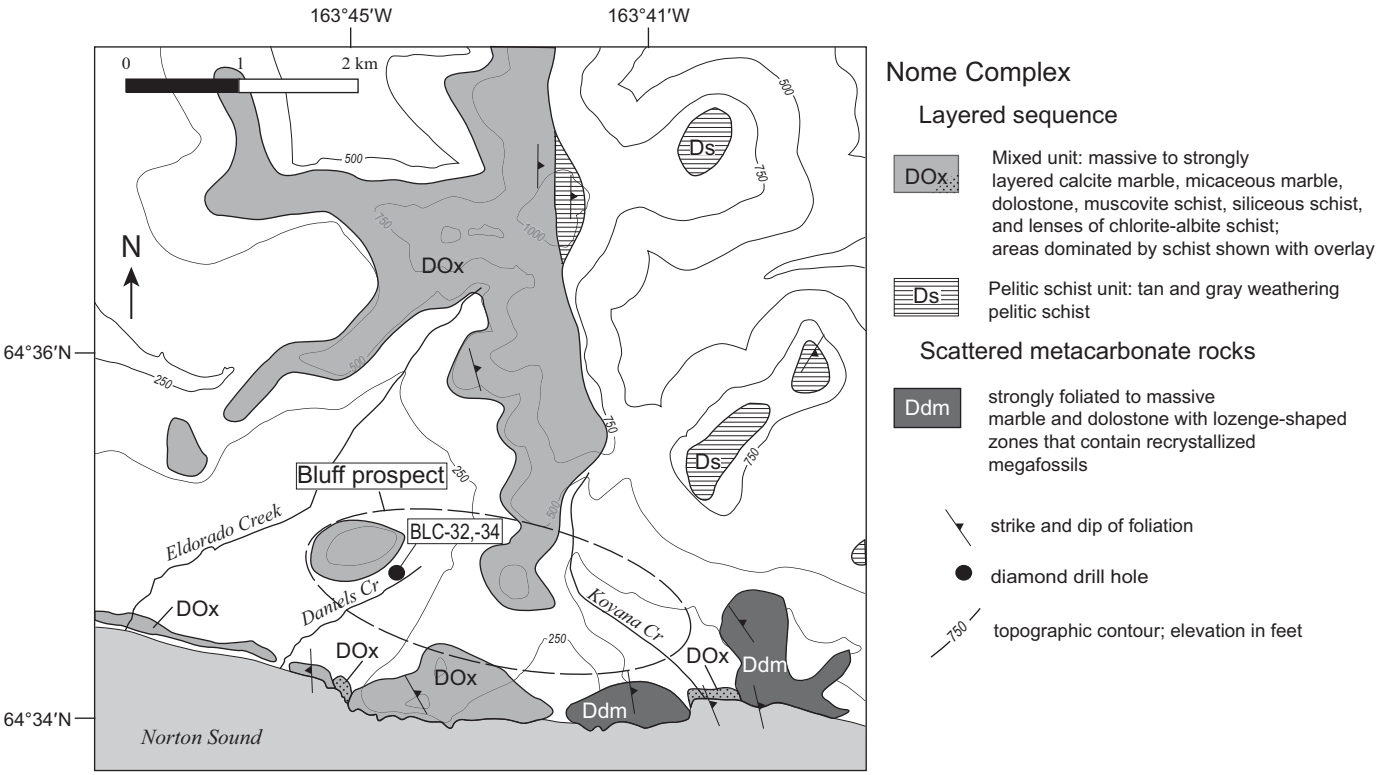


Figure 10. Geologic map of the Bluff prospect area. Geology modified from Till et al. (2011).

Complex in having predominant Cu with or without subordinate Pb, Ag, and Au, and no known Zn, Ba, or F concentrations. Early shipments of handpicked oxidized ore from the Wheeler South deposit contained up to 35.7 wt% Cu, 5.16 oz/t Ag, and 1.82 oz/t Au (Wimmler, 1926). The sulfide zones form stratabound layers and lenses up to ~10 m thick within marble and especially at marble-schist contacts (Smith, 1908; Cathcart, 1922). Hypogene sulfide minerals, chiefly chalcopyrite and bornite with locally abundant pyrite and galena, form disseminations and small veinlets in stratabound siliceous zones. At the Copper King deposit, mineralized zones are in places discordant to lithologic contacts (Fig. 5H). At Wheeler South, finely laminated quartz-rich layers and associated sulfide mineralization trace centimeter- to meter-scale folds. Gangue minerals are mainly quartz, with minor calcite and white mica.

DEFORMED Zn-Pb(-Ag-Au-Ba-F) VEINS

Quarry

Geologic Setting

The Quarry Zn-Pb-Ag-Ba-F deposit is exposed adjacent to the Nome-Teller road ~30 km northwest of Nome. It is part of the Sinuk mining district, which includes a variety of gossans, geochemical anomalies, and prospects with sulfide mineralization (Herreid, 1970). The deposit occurs in the Mixed unit, at the edge of a north-northwest–trending belt of gray-weathering calcite marble, near its southwest contact with a thick unit of schists (also part of the Mixed unit). At the deposit, the predominant lithology is gray- to orange-weathering marble with mm- to cm-thick concentrations of white mica and quartz defining the foliation, traces of intrafolial isoclinal folds, and stretching lineations (Fig. 11). Lenses of mineralized rock occur within a tan- to reddish-orange–weathering quartz-rich schist with mm-scale laminations of iron oxide, carbonate, and muscovite, which lies structurally above and is folded in with the marble (Fig. 11). The quartz-rich schist locally contains dark red, cm-scale equant concentrations of hematite or magnetite, has small amounts of hyalophane, barite, Ba-muscovite, and rare sphalerite, and is barren of zircons. The structurally highest lithology at the deposit is gray- to tan-weathering, locally calcareous, muscovite-chloritoid schist with rare black tourmaline. Lozenges and pods of dolostone, locally brecciated, sit in this mica-rich schist (Fig. 11). Subvertical faults, veins, and crenulations of the foliation, oriented N70E, are fairly common; locally, mineralization was remobilized within these brittle structures.

Sulfide Zone

Stratabound veins and lenses occur within a broad zone above the contact between layered marble and the overlying schists (Fig. 11). Following conventional usage, veins are defined here as generally planar structures, whereas lenses are irregular structures that pinch and swell along strike. Dimensions of the veins and lenses vary widely, from only a few centimeters thick

Downloaded from specialpapers.gsapubs.org on September 29, 2015

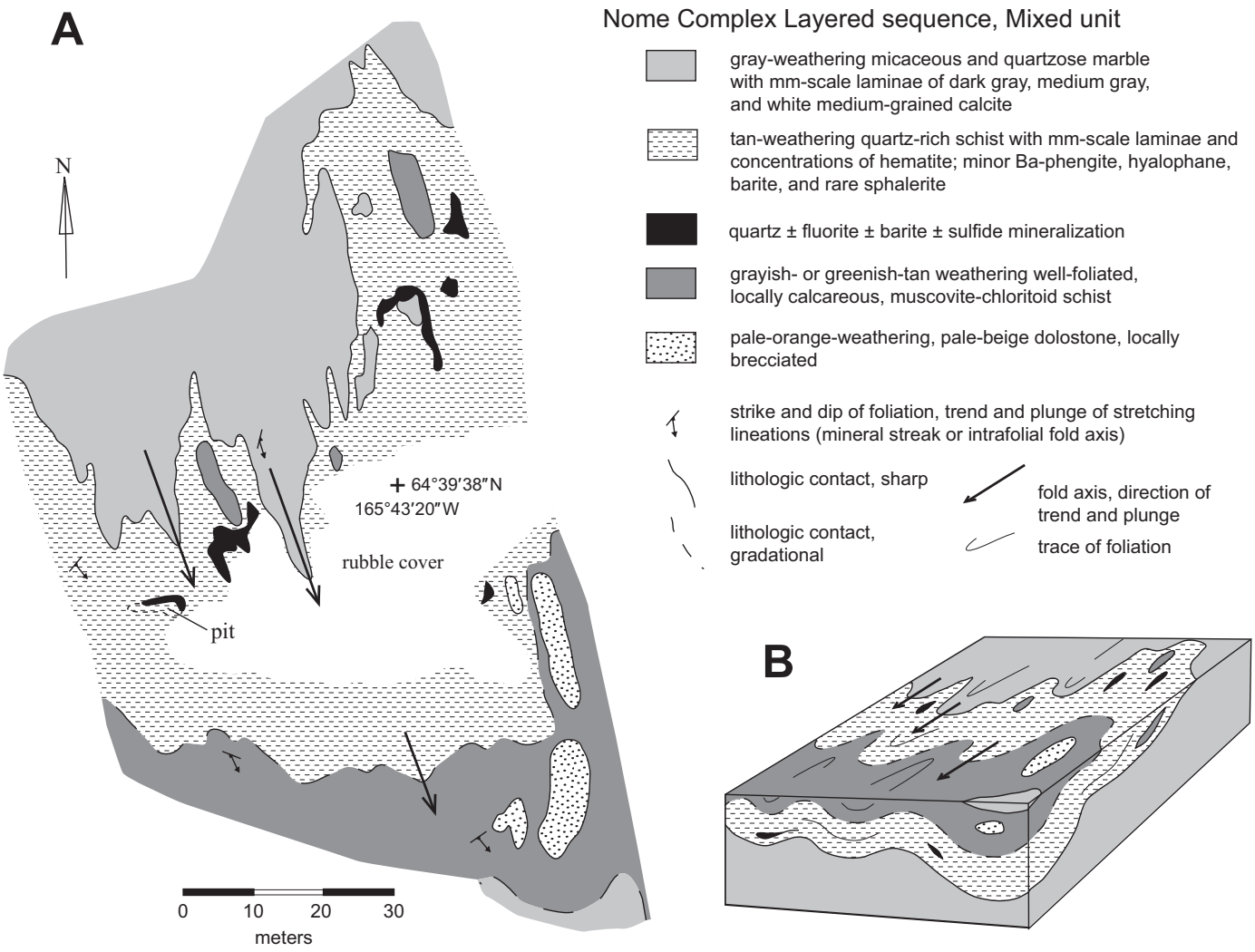


Figure 11. (A) Geologic map of the Quarry Zn-Pb-Ag-Ba-F deposit area (modified from Herreid, 1970). (B) Interpretative block diagram illustrating structural relations at the deposit.

and <1 m in length, up to larger structures as much as 2 m thick and 10 m long. The mineralized zone, variably silicified, consists mostly of quartz, fluorite, barite, and sulfides in veins and lenses that are conformable with the dominant foliation in the quartz-rich schist (Fig. 5I). Sulfides also form disseminations in schist and brecciated dolomite (Brobst et al., 1971). Geometric relations in surface exposures suggest that these veins and lenses also are folded together with enclosing strata. Paragenetically early veins (quartz + carbonate + sulfide ± sulfosalt ± fluorite) are characterized by a banded structure (Fig. 5I); late remobilized veins are composed mainly of coarsely crystalline quartz or barite + fluorite (Fig. 5J).

Mineralogy and Hydrothermal Alteration

Major sulfide minerals are galena and sphalerite that occur as disseminated grains in quartz or carbonate gangue and grain aggregates aligned within the dominant metamorphic foliation. Brobst et al. (1971) reported the presence of boulangerite, which was not found in our study. The quartz-sulfide veins likely contain some arsenopyrite, chalcopyrite, and gold (or electrum), based on whole-rock analyses in Brobst et al. (1971, Tables 1 and 2) that include up to 2000 ppm As, 700 ppm Cu, and 3.6 ppm Au. Scanning electron microscopy work in our study also documents the presence of minor apatite, rutile, and monazite. Coarse clots of limonite and goethite up to 3 cm in diameter occur in some veins; the primary, unoxidized precursor of these clots is unknown, and could be pyrite, magnetite, or siderite.

Muscovite-chloritoid schist is common in the Quarry prospect area as lenses within the well-foliated micaceous schist that are structurally above the mineralized zone (Fig. 11). The typical assemblage is muscovite + quartz + chloritoid ± Fe-carbonate ± chlorite ± tourmaline ± rutile ± ilmenite ± monazite. Euhedral blades of chloritoid are distinctive both in surface exposure (Fig. 5K) and thin section (Fig. 6L) and are randomly oriented

TABLE 2. REPRESENTATIVE ANALYSES OF MINERALIZED ROCKS IN THE NOME COMPLEX

Sample	1	2	3	4	5	6	7	8	9	10	11	12	13	14
Deposit	A.C.	A.C.	A.C.	A.C.	A.C.	W.N.	W.N.	Nelson	Bluff	W.S.	Quarry	Quarry	Galena	Galena
Major elements (wt%)														
SiO_2	33.10	8.83	85.19	40.57	26.67	19.10	9.32	13.39	68.62	24.24	67.10	64.13	89.85	48.85
Al_2O_3	0.34	0.83	2.76	0.57	0.30	2.19	1.51	1.30	2.64	0.09	0.60	0.65	0.50	0.46
$Fe_2O_3^T$	1.79	25.91	3.40	8.33	3.10	39.57	16.06	3.69	1.23	11.32	13.63	1.03	1.30	13.74
MnO	0.082	0.650	0.006	0.264	0.094	1.347	0.914	0.476	0.004	0.193	0.300	0.031	0.047	0.230
MgO	2.29	9.19	0.10	4.65	2.03	1.25	0.96	9.42	0.12	0.12	0.05	0.63	0.04	0.27
CaO	10.80	17.73	0.03	11.95	6.90	10.89	26.76	25.29	0.66	26.37	2.39	16.69	4.15	0.46
Na_2O	<0.01	0.04	0.04	<0.01	<0.01	<0.01	0.25	0.04	0.05	0.08	0.08	0.07	0.06	0.08
K_2O	0.07	0.16	0.35	0.18	0.07	0.04	0.32	0.18	0.47	<0.01	0.02	0.03	<0.01	0.07
TiO_2	0.011	0.004	0.157	0.031	0.010	0.050	0.087	0.036	0.132	0.001	0.022	0.019	0.004	0.009
P_2O_5	<0.01	<0.01	0.03	0.03	<0.01	<0.01	0.02	<0.01	0.07	<0.01	0.09	0.03	0.07	<0.01
LOI	11.81	14.12	3.42	10.78	10.00	9.50	–1.20	38.57	3.70	19.59	5.67	6.76	4.44	12.02
Total	60.29	77.46	95.48	77.36	49.17	83.94	55.00	92.39	77.70	82.00	89.95	90.07	100.46	76.19
F	0.08	0.05	0.06	0.03	2.60	0.69	22.3	0.14	0.03	<0.01	3.30	10.9	0.03	0.03
C total	3.19	7.90	0.07	5.29	2.35	4.84	2.77	9.09	0.19	6.03	0.46	0.7	1.06	2.09
Corg	<0.05	0.06	<0.05	<0.05	0.06	0.07	0.21	0.60	0.05	0.69	0.49	0.08	0.11	2.14
CO_2	11.4	28.8	0.04	21.7	7.32	17.6	9.69	33.0	0.32	22.0	1.43	2.34	3.82	<0.01
S	6.43	11.8	1.67	4.65	15.6	2.70	3.63	3.56	4.19	0.68	0.24	1.12	0.25	2.16
SO_4	18.9	19.4	0.50	9.40	24.6	7.50	10.5	8.70	0.30	2.38	0.88	3.10	<0.3	0.55
Trace elements (ppm)														
Be	1	<1	<1	<1	<1	<1	<1	<1	<1	<1	<1	<1	<1	<1
Sc	0.7	1.8	1.4	1.6	0.9	2.9	1.4	0.3	0.9	1.0	0.8	0.6	0.9	1.0
V	<5	14	14	7	<5	19	11	7	26	<5	<5	5	<5	<5
Cr	<5	<5	190	<5	45	<5	29	<5	16	18	<5	162	40	<5
Zr	11	<4	113	10	2	15	27	10	35	<4	7	12	<4	<4
Hf	0.5	<0.1	3.3	0.2	<0.1	0.2	0.9	0.2	1.2	<0.1	0.3	0.3	<0.1	0.1
Nb	0.8	0.2	2.9	0.4	<0.2	0.4	6.6	0.4	2.9	<0.2	0.5	1.1	<0.2	0.4
Ta	0.38	0.04	0.43	0.03	<0.01	<0.01	2.30	0.15	0.35	<0.01	0.10	0.15	<0.01	0.03
Th	1.12	0.07	2.74	0.43	0.62	0.66	2.15	0.17	2.19	0.08	0.47	0.32	0.11	0.18
U	0.38	0.08	0.66	0.30	0.09	0.21	0.68	0.48	4.11	6.28	3.26	0.53	0.29	0.99
Co	<1	1	4	6	10	1	1	<1	21	<1	1	1	<1	3
Ni	6	7	11	<20	<20	<20	<20	<20	13	16	5	<20	3	3
Cu	<10	79	655	10	90	10	40	30	304	82,600	162	30	19	10
Zn	4770	59,700	8290	79,400	301,000	32,800	410	36,500	102,000	81	9360	790	535	160,000
Pb	243	11	7810	21	62	18	218,000	70,900	40,400	82	87,300	98,900	52,000	93
Ag	<0.5	1.4	6.8	0.6	<0.5	0.9	700	26	34.5	10.1	113	100	50.1	1.8
Au (ppb)	<2	8660	116	<2	<2	<2	102	75	36	34	18	13	<2	36
Hg (ppb)	237	6190	2490	15,100	61,500	2780	37	554	23,800	227	1350	890	83	24,500
Tl	2.93	<0.05	1.26	0.07	<0.05	0.98	13.0	0.16	0.20	0.06	0.76	<0.05	0.18	0.19
Bi	<0.1	<0.1	1.3	<0.1	<0.1	<0.1	0.1	<0.1	1.8	6220	3.0	<0.1	1.1	<0.1
Mo	<2	<2	3	<2	<2	<2	<2	<2	<2	3	<2	14	<2	<2

(*Continued*)

Downloaded from specialpapers.gsapubs.org on September 29, 2015

Downloaded from specialpapers.gsapubs.org on September 29, 2015

TABLE 2. REPRESENTATIVE ANALYSES OF MINERALIZED ROCKS IN THE NOME COMPLEX (*Continued*)

Sample	1	2	3	4	5	6	7	8	9	10	11	12	13	14
Deposit	A.C.	A.C.	A.C.	A.C.	A.C.	W.N.	W.N.	Nelson	Bluff	W.S.	Quarry	Quarry	Galena	Galena
Trace elements (ppm) (*Continued*)														
In	<0.1	1.0	1.0	0.3	3.3	0.2	<0.1	<0.1	<0.1	3.9	0.7	<0.1	<0.1	0.1
Sn	<1	<1	7	2	40	11	11	16	2	82	10	<1	<1	6
W	5.1	1.3	2.6	<0.5	<0.5	0.5	1.4	<0.5	<0.5	0.6	0.6	<0.5	<0.5	<0.5
As	3.8	285	67.6	2.5	10.1	9.6	108	137	16.2	18.5	35.6	2.5	14.6	6.6
Sb	4.9	4.0	255	1.1	5.3	13.3	906	408	50.2	19.4	240	104	60.2	3.0
Se	<3	<3	<3	<3	<3	<3	3	<3	<3	<3	<3	<3	<3	<3
Ga	<1	3	6	4	11	5	3	1	13	<1	1	1	<1	4
Ge	4.7	<0.5	6.2	1.2	2.6	2.5	<0.5	<0.5	2.2	2.5	5.6	6.3	10.0	3.4
Rb	3	11	15	6	2	2	19	5	23	<1	<1	2	2	3
Cs	0.4	1.1	1.2	1.2	0.1	0.2	2.2	0.1	1.3	<0.1	0.1	<0.1	0.4	0.3
Sr	1363	186	73	83	245	112	27	210	22	60	142	42	55	11
Ba	230,900	1679	15,410	85	8227	27,400	2939	59	74	21	2617	173	84	681
Y	11.7	6.2	1.4	6.1	8.7	9.7	112	2.2	2.8	13.5	13.2	25.3	0.7	0.6
La	5.24	1.11	13.2	3.70	1.04	8.54	5.82	2.61	5.72	12.5	1.61	1.55	0.44	0.63
Ce	9.55	1.90	22.3	4.81	2.89	14.5	11.9	4.79	10.2	17.6	2.94	2.99	0.78	0.93
Pr	1.07	0.26	2.14	0.44	0.37	1.51	1.67	0.51	1.03	1.98	0.43	0.43	0.11	0.13
Nd	4.05	1.23	7.02	1.63	1.71	5.66	15.0	1.71	3.69	7.14	2.41	2.71	0.51	0.65
Sm	1.07	0.36	0.92	0.38	0.50	1.39	8.93	0.37	0.61	1.57	0.86	1.09	0.14	0.21
Eu	0.500	0.243	0.398	0.127	0.312	2.050	16.10	0.242	0.138	1.150	1.060	1.770	0.099	0.128
Gd	1.44	0.55	0.45	0.48	0.71	1.51	23.2	0.37	0.47	1.71	1.36	2.07	0.14	0.13
Tb	0.25	0.11	0.05	0.10	0.15	0.27	2.64	0.06	0.08	0.32	0.26	0.36	0.02	0.02
Dy	1.50	0.77	0.25	0.75	0.94	1.56	11.6	0.31	0.50	1.91	1.55	2.11	0.11	0.10
Ho	0.29	0.17	0.05	0.18	0.18	0.31	1.82	0.06	0.10	0.36	0.28	0.40	0.02	0.02
Er	0.78	0.56	0.19	0.61	0.47	0.85	3.94	0.17	0.32	0.95	0.69	1.03	0.06	0.05
Tm	0.101	0.091	0.038	0.104	0.058	0.114	0.412	0.025	0.057	0.125	0.081	0.119	0.008	0.008
Yb	0.53	0.60	0.34	0.72	0.33	0.70	1.80	0.14	0.41	0.68	0.43	0.53	0.05	0.05
Lu	0.073	0.083	0.061	0.114	0.045	0.110	0.192	0.016	0.062	0.086	0.055	0.062	0.009	0.008
Ce/Ce*	0.929	0.816	0.953	0.824	1.050	0.923	0.876	0.955	0.962	0.802	0.813	0.842	0.817	0.749
Eu/Eu*	1.964	2.382	2.600	1.268	2.222	6.369	6.467	3.020	1.119	3.104	4.372	5.506	3.406	3.287

Abbreviations, sample numbers, and locations: A.C.—Aurora Creek; W.N.—Wheeler North; W.S.—Wheeler South; 1—JS-05-66A, layered barite-carbonate rock, Christophosen prospect; 2—AC-17-106.5, sphalerite-ankerite-dolomite rock with minor pyrite, arsenopyrite, and gold, drill core at 106.5 ft depth; 3—JS-06-14, siliceous rock with disseminated sphalerite + galena + hyalophane(?), outcrop along trend of Aurora Creek deposit; 4—JS-07-8D, disseminated sphalerite in brecciated dolomite-ankerite-quartz rock, Aurora Creek (see Fig. 5A); 5—JS-7-23A, sphalerite-rich quartzose rock with minor pyrite + fluorite + barite, Aurora Creek; 6—JS-07-17D, sphalerite-rich massive sulfide with minor quartz + siderite + barite, Wheeler North dump; 7—JS-07-18C, galena- and fluorite-rich massive sulfide with minor pyrite + sphalerite + tetrahedrite + quartz + carbonate, Wheeler North dump; 8—JS-07-19B, seams and thin layers of galena + sphalerite with minor pyrite and dolomite in marble, Nelson prospect; 9—BLC-34-175.5, quartz-rich schist containing abundant sphalerite and galena, with minor pyrite, Bluff prospect drill core at 175.5 ft depth; 10—JS-04-13D, brecciated and silicified marble containing chalcopyrite and bornite with minor bismuthinite(?), Wheeler South dump; 11—JS-04-5A, deformed quartz vein containing galena and minor sphalerite, Pb-sulfosalts, and fluorite, Quarry deposit; 12—JS-07-1C, deformed quartz vein containing galena and fluorite, and minor Pb-sulfosalts and carbonate, Quarry deposit; 13—JS-05-78B, deformed quartz vein containing abundant galena, Galena deposit dump; 14—JS-05-79A, deformed sphalerite-quartz vein, Galena deposit dump (Oso claim). Ce and Eu anomalies are calculated by shale normalization (SN) using data for average post–Archean Australian shale (PAAS; Taylor and McLennan, 1985); $Ce/Ce^*_{(SN)} = 2Ce_{SN}/(La_{SN} + Pr_{SN})$; $Eu/Eu^*_{(SN)} = 2Eu_{SN}/(Sm_{SN} + Gd_{SN})$.

Downloaded from specialpapers.gsapubs.org on September 29, 2015

or aligned within the dominant foliation. Where so aligned, the chloritoid lineation is parallel to mineral streaks and fold axes elsewhere in the prospect (Fig. 11).

Galena

Geologic Setting

Like the Quarry prospect, the Galena Pb-Zn prospect occurs in the Mixed unit, in a north-northwest–trending belt of gray-weathering calcite marble, near its southwest contact with a thick unit of Mixed unit schists. It consists of two claims or mineralized zones (Sunrise and Oso), both of which show a spatial association of quartz-rich lenses in marble with mineralization. At the Sunrise Pb claim, strongly foliated quartz-rich layers and minor layers of quartz-mica schist are associated with the gray-weathering marble. The quartz-mica schist contains muscovite with abundant inclusions of rutile, iron oxide, zircon, and tourmaline, and a few grains of sphalerite; locally, it also contains up to 50% calcite. At the Oso Zn claim, silica-rich rocks have orange and white banding, reflecting variations in concentration of iron oxides.

Sulfide Zones

At the Sunrise claim, galena forms disseminated grains in highly deformed quartz veins (Fig. 5L), whereas at the Oso claim, disseminations and coarse (1–3 cm) aggregates of sphalerite occur together with pyrite and local fluorite (Mertie, 1918). The mineralized zones are chiefly in marble but in places occur in schist; silicification appears to be the main type of wall rock alteration. Herreid (1966a) reported up to 5.8 wt% Zn, 1.0 wt% Pb, and 0.85 oz/t Ag in different samples. Reconnaissance SEM study of sulfide-rich samples shows the presence of rare grains of cassiterite and celsian, respectively 100 µm and 50 µm in diameter.

WHOLE-ROCK GEOCHEMISTRY

Mineralized Samples

Weakly mineralized (Zn+Pb <1 wt%) samples from the Aurora Creek and Wheeler North deposits and vicinity contain elevated Ba (to 3.0 wt% ppm) or F (to 4.3 wt%). Petrographic and SEM studies of these samples indicate residence of the Ba mainly in barite, with minor hyalophane; the F is principally contained in fluorite. One galena-rich sample from the Galena deposit contains 10 ppm Hg; a fluorite-quartz-calcite-sulfide–bearing sample from Quarry has 3.3 ppm Hg (Brobst et al., 1971). Covariance between Zn and Hg (r = 0.92) suggests residence of the Hg in sphalerite. A strong correlation between Pb and Ag (r = 0.95) is consistent with the Ag occurring in sulfosalt inclusions and, perhaps, in lattice sites of galena, although the latter possibility is constrained by limited solubility for coupled substitutions of Ag phases in PbS (Sharp and Buseck, 1993; Renock and Becker, 2011). Barite-rich samples from the Quarry deposit have very high Sr (up to 4446 ppm). Among all of the sulfide deposits, high Tl contents occur only at the Aurora Creek (up to 5.0 ppm) and Wheeler North (up to 26.6 ppm) deposits, in contrast to Tl in the other deposits that is uniformly low (<1.0 ppm) and in unaltered clastic metasedimentary rocks of the Nome Complex (<2.8 ppm; $n = 18$).

Analyses of three sphalerite- and galena-rich samples from the Bluff drill cores show significant differences in trace-metal contents relative to those present in syn-metamorphic, gold-bearing veins of this prospect. The three base-metal samples (e.g., Fig. 5G) have 16.2–29.6 ppm As, 38.8–50.2 ppm Sb, and 7150–23,800 ppb Hg, which contrasts with the uniformly high As (>5000 ppm), generally elevated Sb (>100 ppm), and low Hg (<100 ppb) that characterize the local gold-bearing veins (Ford, 1993).

A limited number of whole-rock analyses ($n = 4$) of Cu-rich samples from the Copper King, Copper Mountain, and Wheeler South deposits show distinctively high contents of several metals including up to 6220 ppm Bi and up to 327 ppm Sn for the Wheeler South deposit (Table DR1 [see footnote 3]). These samples are also noteworthy for having uniformly low F (maximum 400 ppm) and Ba (maximum 1703 ppm).

Stratiform siliceous and baritic rocks at the Aurora Creek deposit have distinctive geochemical signatures. The siliceous type has high contents of Zn (2990 ppm), Pb (894 ppm), Ba (1.09 wt%), Ge (15.9 ppm), and Tl (3.8 ppm), which distinguish it from all unaltered clastic metasedimentary rocks of the Nome Complex, including quartz-rich siltstones and sandstones (e.g., Ge <3.5 ppm). This siliceous rock contains a small population of euhedral zircon grains that have a range of Proterozoic ages as determined by sensitive high-resolution ion microprobe (SHRIMP) U-Pb analysis (Till et al., this volume, Chapter 4). The barite-rich type is noteworthy for having high Zn (up to 4740 ppm), Sr (up to 2041 ppm), Tl (up to 5.0 ppm), and Ge (up to 6.4 ppm).

Shale-normalized REE data for representative sulfide-rich samples show diverse patterns typically with positive Eu anomalies (Fig. 12). No significant Ce anomalies, either positive or negative, are evident. Sulfide-rich samples from the Aurora Creek and Wheeler North deposits (Fig. 12A) display relatively flat patterns and moderate to large positive Eu anomalies (Eu/Eu* mainly 1.5–8.9; Table 2). Barite- and quartz-rich layered units from the Aurora Creek deposit (Fig. 12B) have hump-shaped patterns; only the quartz-rich type has a positive Eu anomaly. Rare-earth–element patterns for sulfide-rich samples from the Quarry and Galena deposits (Fig. 12C) are similar to those for Aurora Creek and Wheeler North although at slightly lower abundance levels. Comparable patterns are shown by sulfide-rich samples from the Nelson occurrence, but those from the Bluff prospect differ in having no or only small positive Eu anomalies (Fig. 12D). None of these mineralized samples displays a REE pattern like those of the unaltered clastic metasedimentary rocks of the Nome Complex; some of the Bluff samples are broadly similar but have higher La/Lu ratios.

Downloaded from specialpapers.gsapubs.org on September 29, 2015

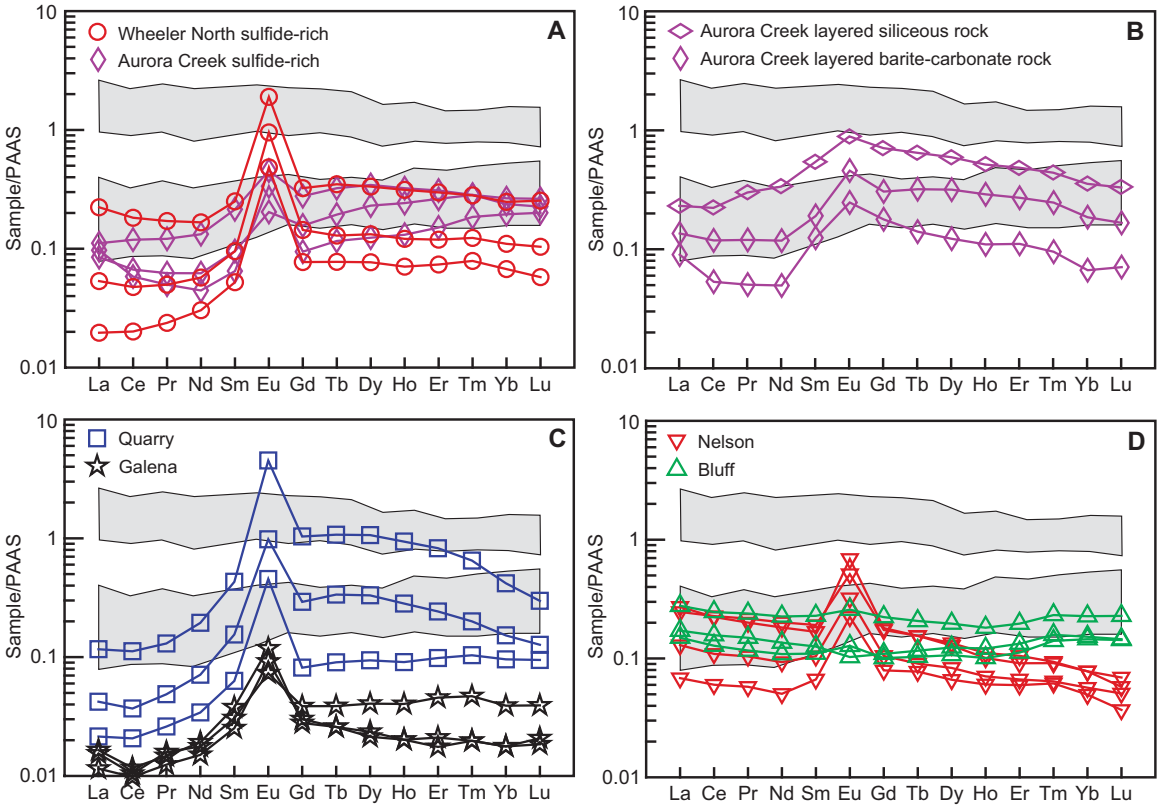


Figure 12. Shale-normalized rare-earth–element plot of representative mineralized samples. (A) Aurora Creek and Wheeler North sulfide-rich samples; (B) Aurora Creek layered siliceous and barite-carbonate rocks; (C) Quarry and Galena sulfide-rich samples; (D) Nelson and Bluff sulfide-rich samples. Data are normalized to average post–Archean Australian shale (PAAS; Taylor and McLennan, 1985). Pale-gray fields show range of data for unaltered siliciclastic metasedimentary rocks (n = 18) of the Nome Complex; upper field represents more aluminous rocks, whereas lower field represents more quartzose rocks (see text).

Aluminous Muscovite-Chloritoid Schists

Whole-rock analyses of the muscovite-chloritoid schists show aluminous compositions up to 20.1 wt% Al_2O_3 and an average of 13.3 ± 2.98 wt% Al_2O_3 (Table DR2 [see footnote 3]). These schists are distinguished from most unaltered clastic metasedimentary rocks of the Nome Complex by lower SiO_2/Al_2O_3 ratios and higher $Fe_2O_3^T/MgO$ ratios (Fig. 13A), and by lower CaO and Na_2O contents. Total $Fe_2O_3^T$ + MgO is not a discriminator (Fig. 13B). The SiO_2/Al_2O_3 ratios are variably affected by the inclusion in some analyzed samples of small deformed quartz veins and quartz-rich host rock; subsamples lacking this material would have lower ratios. For evaluation of possible geochemical differences with proximity to mineralized zones, the muscovite-chloritoid schists are divided into proximal (<300 m from such zones) and distal settings.

Broad correlations exist between Al_2O_3 and several relatively immobile trace elements such as Nb (r = 0.53; Fig. 13C), consistent with clastic metasedimentary rocks of the Nome Complex being the predominant protolith of the muscovite-chloritoid schists. However, other possible protoliths that are unknown in the Nome Complex, such as arkose and rhyolite, cannot be excluded. The deposit-proximal muscovite-chloritoid schists can also be distinguished from metasedimentary rocks of the Nome Complex by trace-metal concentrations, including Zn >150 ppm (Fig. 14A), Cu >50 ppm (Fig. 14B), and Sb >5 ppm (Fig. 14C). Shale-normalized REE data for the deposit-proximal schists display mostly flat patterns without Eu anomalies and abundance levels that broadly match those of the muscovite-chloritoid schists from deposit-distal locations within the Nome Complex, and those of quartz-poor unaltered clastic metasedimentary rocks of the Nome Complex (Fig. 15).

Average mass changes were calculated for 12 samples each of deposit-proximal and deposit-distal muscovite-chloritoid schists, determined relative to the compositional average for unaltered clastic metasediments of the Nome Complex. Calculations are based on average Al-normalized data (inferred immobility of Al), using volatile-free compositions of major elements, for both the muscovite-chloritoid schists and unaltered clastic metasedimentary rocks (n = 13). Several geochemically anomalous samples were screened from the database, including one highly aluminous (30.0 wt% Al_2O_3) pelitic schist, one siltstone,

Downloaded from specialpapers.gsapubs.org on September 29, 2015

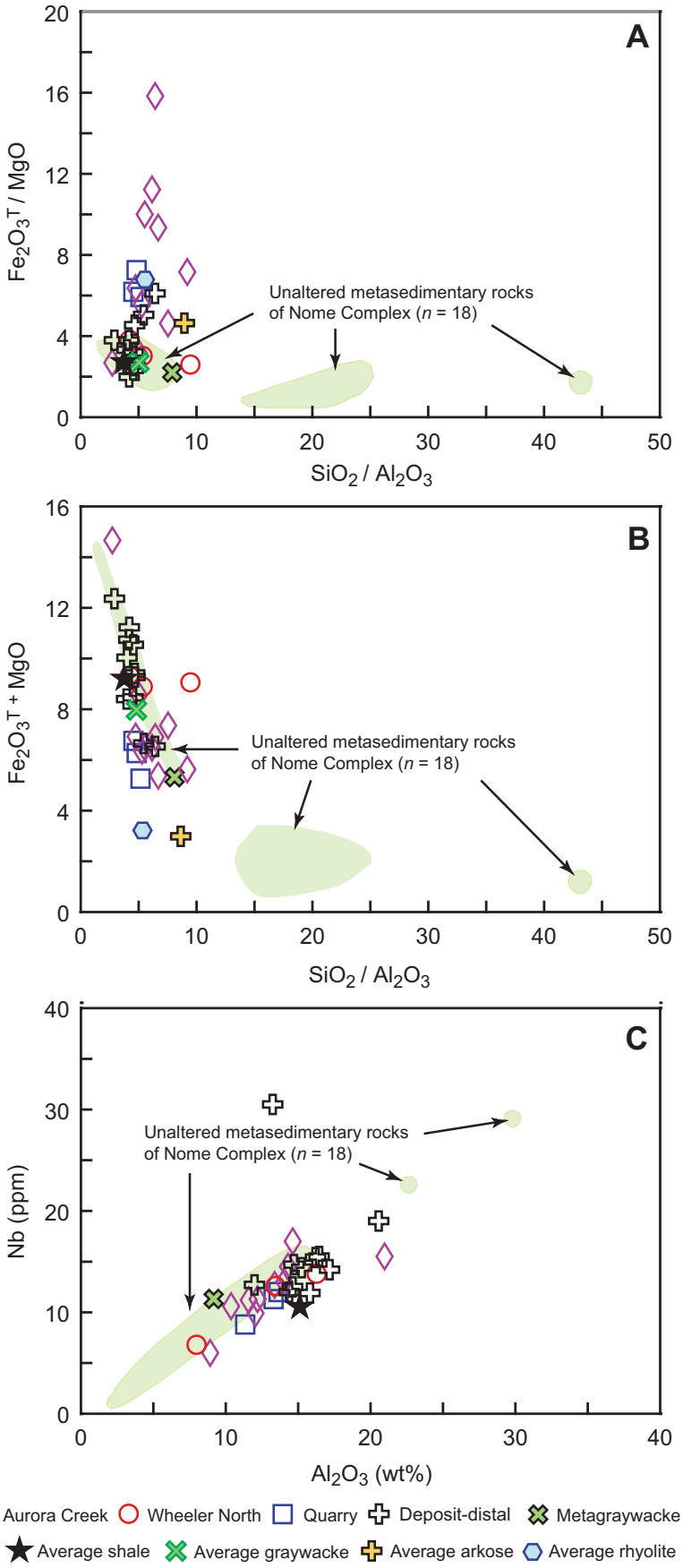


Figure 13. Bivariate plots of bulk compositions of major elements in muscovite-chloritoid schists compared to those of unaltered siliciclastic metasedimentary rocks of the Nome Complex and other lithologies (all volatile-free basis). (A) SiO_2/Al_2O_3 versus $Fe_2O_3^T/MgO$; (B) SiO_2/Al_2O_3 versus $Fe_2O_3^T$+MgO; (C) Al_2O_3 versus Nb. Data sources: average shale (Krauskopf and Bird, 1995); average arkose and graywacke (Pettijohn, 1963); average rhyolite (Le Maitre, 1976).

Downloaded from specialpapers.gsapubs.org on September 29, 2015

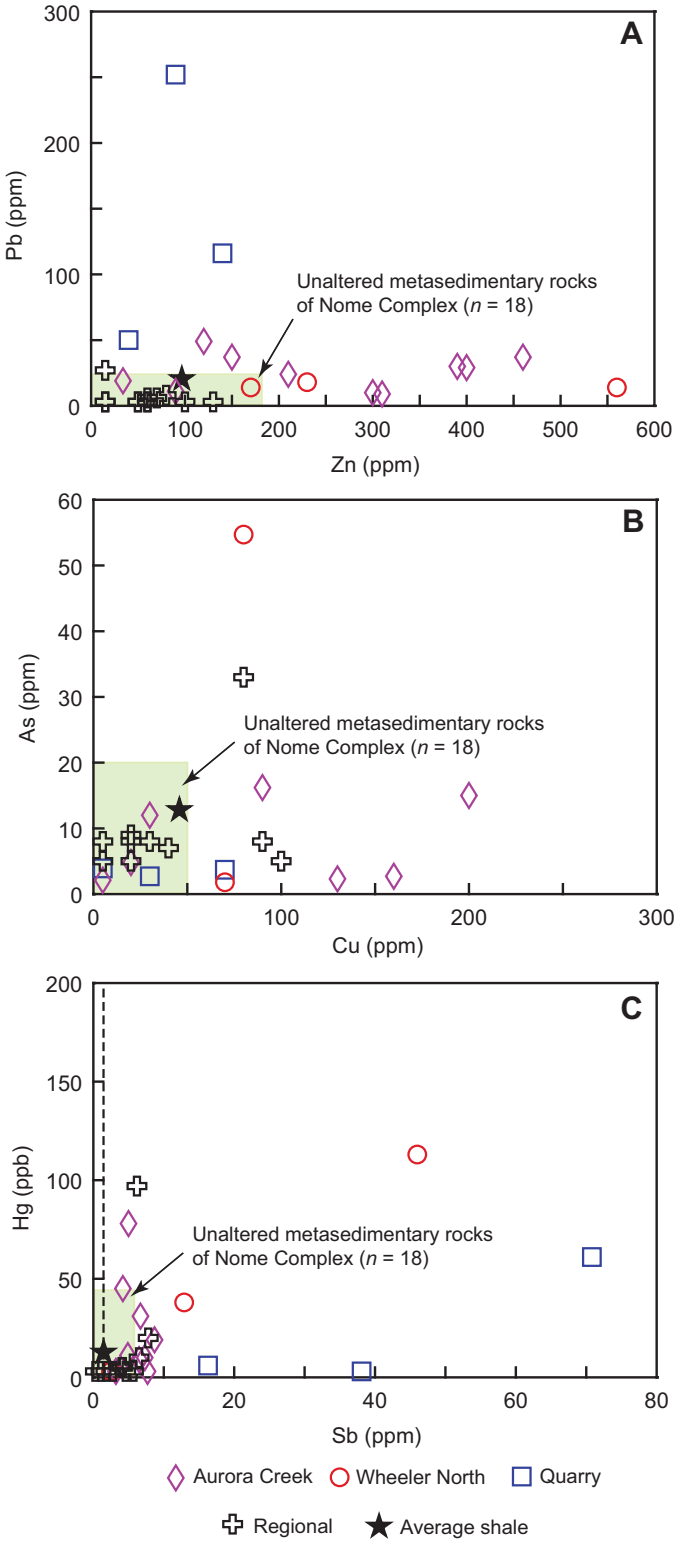


Figure 14. Bivariate plot of bulk metal contents of trace metals in muscovite-chloritoid schists compared to those of unaltered siliciclastic metasedimentary rocks of the Nome Complex. (A) Zn versus Pb; (B) Cu versus As; (C) Sb versus Hg. Dashed line in (C) reflects poorly defined Hg content of average shale. Average shale data from Krauskopf and Bird (1995).

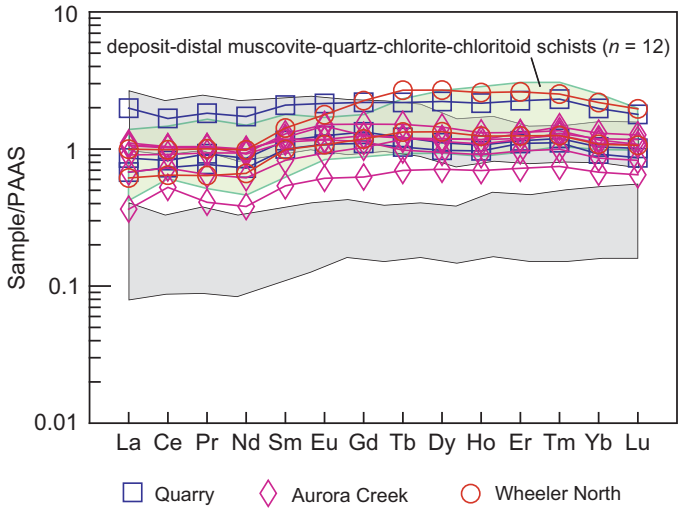


Figure 15. Shale-normalized, rare-earth–element plot of representative samples of muscovite-chloritoid schists from sulfide deposits and prospects. Green field shows range of data for mineralogically similar samples from deposit-distal locations in the Nome Complex. Gray fields represent range of data for unaltered clastic metasedimentary rocks of the Nome Complex, higher and lower abundances reflecting less and more quartzose samples, respectively (see text). Note overlap of upper gray field and pale-green field. All data are normalized to post–Archean Australian shale (PAAS; Taylor and McLennan, 1985).

and one metachert (>91.5 wt% SiO_2), and two very calcite-rich (>12.5 wt% CaO) schists. Concentrations reported as not detected were assigned values equal to one-half the analytical detection limit (Sanford et al., 1993). The average mass changes include major increases (>50%) in Cu, Zn, Pb, Sb, and Hg, accompanied by moderate increases (10%–50%) in Fe, Mn, K, and Co; major decreases (>50%) are displayed by Ca, Na, Sr, and Ba, with moderate decreases (10%–50%) in Si, Mg, P, U, V, Ni, and Tl (Fig. 16). Average mass changes for deposit-distal muscovite-chloritoid schists show moderate increases in Fe, K, Sc, Cu, and Sb; major decreases occur for Ca, Na, Sr, Ba, Zn, and Pb, with moderate decreases displayed by Si, Mg, P, F, La, U, V, As, and Tl.

MINERAL CHEMISTRY

Carbonate

Average compositions of carbonate grains in mineralized samples show three principal groupings that comprise siderite + rhodochrosite, dolomite-ankerite, and calcite (Fig. 17). Most samples have <5 mol% $MnCO_3$ except one paragenetically late veinlet (14.0 mol% $MnCO_3$) in an ankerite-siderite-pyrrhotite-magnetite-sphalerite-pyrite-fluorite rock from the Wheeler North deposit (JS-05-77A-b; Table 4). A few samples from the Aurora Creek and Wheeler North deposits have 1–2 mol% $ZnCO_3$. Siderite, which in sulfide-rich samples is typically intergrown with ankerite and Fe-rich dolomite (Fig. 5A), occurs preferentially at the Aurora Creek and Wheeler North deposits. Carbonate

Downloaded from specialpapers.gsapubs.org on September 29, 2015

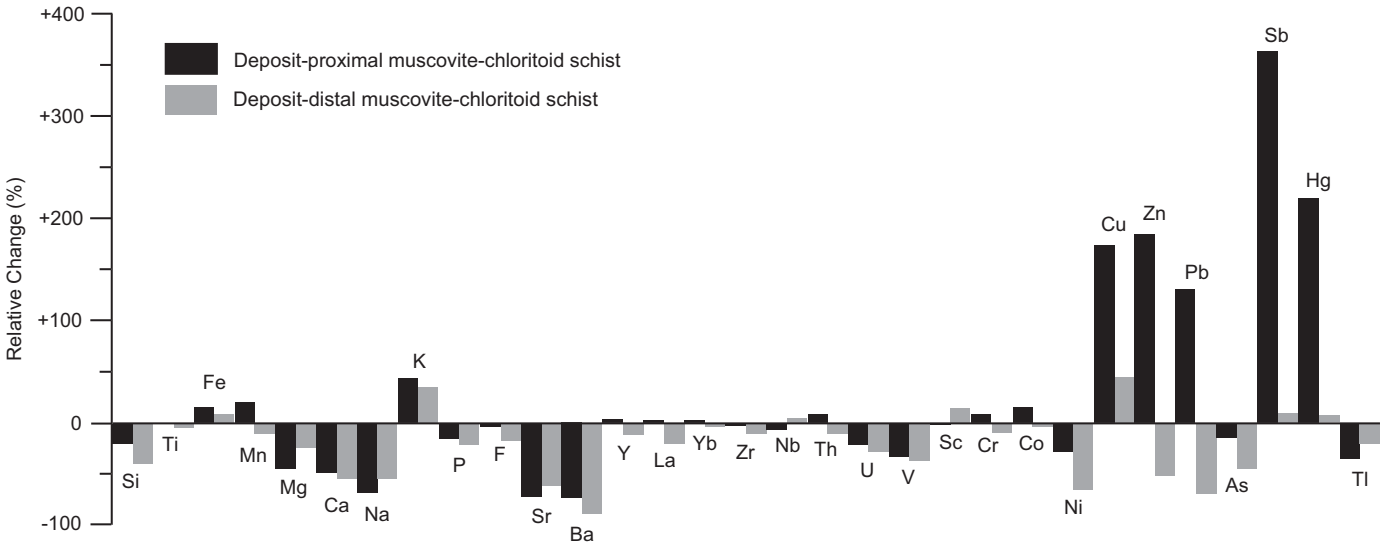


Figure 16. Enrichment and depletion diagram showing net mass changes during formation of the muscovite-chloritoid schists, both for samples proximal to sulfide deposits and occurrences, and in settings distal to the deposits. See text for methods used.

associated with paragenetically early base-metal sulfides at the Bluff prospect is reportedly siderite (Millrock Resources, 2010), but our single analyzed sample contains only dolomite and calcite. Dolomite also occurs in sulfide-rich samples at the Nelson occurrence, and in layered barite with subordinate calcite at the Aurora Creek deposit (Fig. 5C).

Muscovite

Mica from muscovite-chloritoid schists is phengitic, with Si atoms per formula unit (apfu) ranging from 6 to 7 (on an 11 oxygen basis; Table 5). The composition of the phengites largely overlaps that of phengite in Nome Complex pelitic

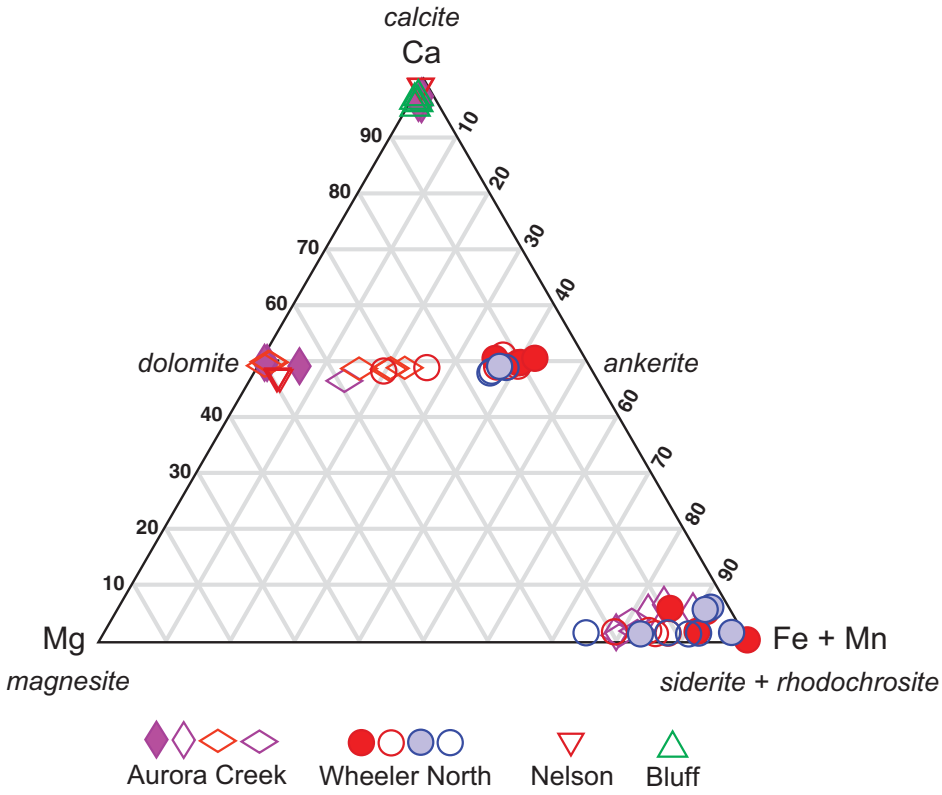


Figure 17. Ternary Ca-Mg-(Fe + Mn) plot showing average compositions of carbonate minerals in mineralized samples from the stratabound sulfide deposits and occurrences. Different symbols represent different samples, each an average of, in most cases, three to nine analyses (total 174); filled diamond symbol represents sample of layered barite.

Downloaded from specialpapers.gsapubs.org on September 29, 2015

TABLE 3. REPRESENTATIVE WHOLE-ROCK ANALYSES OF MUSCOVITE-CHLORITOID SCHISTS IN THE NOME COMPLEX

Sample	1	2	3	4	5	6	7
Major elements (wt%)							
SiO_2	64.43	71.72	68.89	67.10	60.50	74.75	56.92
Al_2O_3	13.57	11.63	7.27	12.53	12.51	11.63	19.52
$Fe_2O_3^T$	5.55	5.67	5.96	6.23	5.05	5.44	9.28
MnO	0.058	0.084	0.134	0.079	0.074	0.024	0.047
MgO	0.87	0.51	2.30	2.06	0.70	0.89	2.45
CaO	4.15	1.98	3.88	2.46	8.51	0.28	0.39
Na_2O	0.23	0.20	0.10	0.26	0.13	0.13	0.34
K_2O	2.93	2.68	1.91	1.68	3.09	2.97	4.74
TiO_2	0.862	0.773	0.487	0.753	0.931	0.745	1.055
P_2O_5	0.11	0.09	0.18	0.16	0.16	0.16	0.19
LOI	6.14	3.08	8.52	5.84	8.65	1.99	4.14
Total	98.90	98.42	99.63	99.15	100.31	99.01	99.07
F	0.05	0.07	0.07	0.05	0.21	0.09	0.13
C total	1.26	0.45	2.27	1.20	1.88	0.04	0.07
C org	0.15	0.06	0.18	0.05	0.06	<0.05	<0.05
CO_2	4.00	1.46	7.88	4.11	6.63	0.10	0.19
Total S	0.19	0.03	0.23	0.04	<0.01	<0.01	<0.01
SO_4	0.40	<0.3	0.60	<0.3	<0.3	<0.3	<0.3
Trace elements (ppm)							
Be	2	2	1	2	2	2	4
Sc	12.0	11.7	8.5	10.5	12.8	12.8	22.2
V	116	114	85	124	120	110	164
Cr	80	182	132	76	164	98	125
Zr	322	227	157	245	298	252	278
Hf	8.7	5.9	4.2	6.4	7.8	6.4	7.2
Nb	17.0	11.3	6.8	12.6	12.0	12.7	19.0
Ta	1.11	0.97	0.57	1.00	1.10	1.01	1.47
Th	12.7	10.8	8.31	12.6	20.3	9.97	15.7
U	4.85	3.43	2.26	4.92	2.54	2.64	3.63
Co	10	16	11	17	10	18	25
Ni	31	30	30	40	40	60	10
Cu	160	130	80	70	70	100	5
Zn	460	300	560	230	90	60	130
Pb	37	10	14	18	252	<5	<5
Ag	1.4	<0.5	<0.5	<0.5	2.6	0.6	<0.5
Au (ppb)	9	<2	46	<2	<2	13	<2

(*Continued*)

schists (Table 5); this is to be expected, as phengitic muscovite is typical of high-pressure and low-temperature metamorphic terranes (Spear, 1993). Evans and Patrick (1987) report similar ranges in Si apfu in phengite from pelitic schist of the Nome Complex.

A ternary plot of large interlayer cations (K-Na-Ba) shows most phengites in the muscovite-chloritoid schists have little paragonite component and some have a minor enrichment in Ba (Fig. 18A). Ba enrichment is limited to phengite in surface and core samples from the Aurora Creek deposit; these samples typically contain accessory barite. Barite in the phengites is elevated up to 0.068 Ba apfu. Muscovite in other samples analyzed in this study and in pelitic schist in the literature typically contains 0.01–0.03 Ba apfu; Ba contents up to 0.10 apfu are documented in metamorphic muscovite (Guidotti, 1987).

Mica from sulfide-rich quartz and/or carbonate schists collected at five deposits and prospects is also phengitic but is compositionally more complex. Many of these phengites have additional Fe enrichment and some have a significantly larger paragonite component (Fig. 18B). Some contain significantly more Ba than phengite in muscovite-chloritoid schist, up to 0.48 apfu (Fig. 18B); these samples contain barite as a minor phase.

Chloritoid

Bulk composition influences the Fe-Mg ratio of chloritoid in muscovite-chloritoid schists; analyses from individual samples tend to cluster on the Fe–Mg join of a ternary diagram (Fig. 19). All chloritoids are relatively iron rich, and many overlap in composition with chloritoids typical of Nome Complex pelitic schist (Table 6). Chloritoids in muscovite-chloritoid schist from the Aurora Creek deposit are more Fe-rich than others analyzed (Fe 2.028 apfu); chloritoid from drill core samples contains small amounts of Zn (0.020 apfu; Table 6; Fig. 19); sphalerite is present in these samples. The highest values of Zn measured in chloritoid are from a siderite-quartz-ankerite rock in Aurora Creek drill core that contains minor sphalerite (0.038 apfu, sample AC-8-60; Fig. 19; Table 6).

Downloaded from specialpapers.gsapubs.org on September 29, 2015

TABLE 3. REPRESENTATIVE WHOLE-ROCK ANALYSES OF MUSCOVITE-CHLORITOID SCHISTS IN THE NOME COMPLEX (*Continued*)

Sample	1	2	3	4	5	6	7
Trace elements (ppm) (*Continued*)							
Hg (ppb)	n.a.	78	113	38	61	20	<5
Tl	1.20	0.69	0.77	0.69	1.67	1.85	3.15
Bi	0.2	0.2	<0.1	0.3	0.1	1.1	<0.1
Mo	50	3	<2	12	4	<2	<2
In	<0.1	<0.1	<0.1	<0.1	<0.1	<0.1	<0.1
Sn	3	3	2	3	2	3	4
W	2.5	1.4	1.6	1.4	3.5	2.8	3.4
As	<5	2.3	54.7	1.8	3.7	5.0	8.0
Sb	9.7	3.2	59.1	6.5	72.8	5.9	3.0
Se	<3	<3	<3	<3	<3	<3	<3
Ga	17	14	10	17	16	15	27
Ge	3.6	1.8	1.5	2.3	3.1	2.4	1.9
Rb	157	144	83	72	176	139	251
Cs	21.9	14.1	8.3	4.3	63.5	11.4	20.4
Sr	121	38	93	72	68	24	31
Ba	2150	1438	731	577	859	456	815
Y	38.6	38.3	33.8	76.5	61.3	28.9	31.8
La	40.9	34.6	23.5	38.1	75.8	22.7	47.4
Ce	90.8	72.7	51.3	78.6	133	52.2	96.1
Pr	9.62	8.26	5.65	8.86	16.1	5.67	12.3
Nd	36.7	31.7	22.5	33.4	58.5	19.4	38.0
Sm	7.76	7.16	5.50	7.90	11.6	4.12	7.27
Eu	1.37	1.63	1.16	1.92	2.32	0.923	1.22
Gd	6.82	7.08	5.52	10.5	10.2	4.03	6.03
Tb	1.19	1.17	1.03	2.08	1.69	0.71	0.93
Dy	7.07	6.77	6.25	12.6	10.4	4.59	5.61
Ho	1.35	1.30	1.23	2.56	2.14	1.01	1.16
Er	3.99	3.76	3.55	7.45	6.41	3.22	3.64
Tm	0.58	0.551	0.508	1.020	0.936	0.494	0.535
Yb	3.87	3.28	3.05	6.16	5.57	3.17	3.39
Lu	0.632	0.469	0.461	0.851	0.775	0.483	0.530
Ce/Ce*	1.056	0.992	1.027	0.987	0.878	1.061	0.917
Eu/Eu*	0.831	1.048	0.924	0.922	0.957	1.012	0.836

Note: Ce/Ce* and Eu/Eu* are shale-normalized Ce and Eu anomalies, respectively, as calculated in Table 1 footnote. Abbreviations: LOI—loss on ignition; n.a.—not analyzed.

Sample numbers and locations: 1—AC-17-66.5, drill core from Aurora Creek deposit; 2—JS-07-24, outcrop in Aurora Creek; 3—JS-07-29, outcrop 1 km upstream from Wheeler North deposit; 4—JS-07-30, outcrop 0.8 km upstream from Wheeler North deposit; 5—JS-07-1E, outcrop at Quarry deposit; 6—05AD24G, outcrop ~4 km SSE of Aurora Creek deposit (see Fig. 4); 7—07ATi22E, outcrop 0.8 km downstream from Wheeler North deposit.

DISCUSSION

Stratabound Zn-Pb(-Ag-Au-Ba-F) Lenses

A variety of field and laboratory data suggest that the base-metal sulfide deposits in the Nome Complex formed by diverse seafloor hydrothermal processes. The stratabound and locally stratiform lenses at Aurora Creek (Zn-Au-Ba-F) and Wheeler North (Pb-Zn-Ag-Au-F) are interpreted to be deformed and metamorphosed SEDEX deposits, based on the presence at these deposits of stratiform layers of semi-massive to massive sulfide, siliceous rock, and barite; the folded nature of the sulfide layers; and alignment of sphalerite grains within the dominant foliation (Figs. 5B–5D and 6D). The uniformly moderate to large positive Eu anomalies in mineralized samples from these deposits, and from the Nelson deposit (Figs. 12A and 12D), are strong evidence of a major hydrothermal component (Bau, 1991; Lottermoser, 1992); similar Eu anomalies occur in sulfide ores of the Sullivan deposit in British Columbia and the Red Dog deposits in Alaska (Slack et al., 2000; Slack et al., 2004b). Layered barite like that at Aurora Creek is also present in many other SEDEX deposits worldwide (e.g., Goodfellow and Lydon, 2007). Occurrence of euhedral porphyroblasts of pyrite (Fig. 6I) and other minerals including arsenopyrite and magnetite (not shown) suggest metamorphic recrystallization of preexisting Fe-As-S and Fe-O phases, respectively.

Alternative origins for the stratabound sulfide lenses, invoked by previous workers, are considered unlikely as follows: (1) a pre-metamorphic VMS model (Brown, 1977; Bundtzen et al., 1994; Newberry et al., 1997) is not preferred because the host strata to the deposits lack metavolcanic rocks including metamorphosed volcaniclastic strata; (2) a pre-metamorphic MVT model (Herreid, 1970) is similarly discounted owing to the occurrence at Aurora Creek of layered barite, which is unknown in MVT deposits; (3) a pre-metamorphic CRD model (Porterfield et al., 1996) is undermined also by the presence of this layered barite and its very high sulfur isotope ($\delta^{34}S$) values of 25.5‰–26.3‰ that suggest a major component of seawater sulfate (Shanks et al., this volume); these

Downloaded from specialpapers.gsapubs.org on September 29, 2015

TABLE 4. REPRESENTATIVE ELECTRON MICROPROBE ANALYSES OF CARBONATE MINERALS IN SULFIDE-RICH SAMPLES FROM THE NOME COMPLEX

Sample	1	2	3	4	5	6	7
CaO	2.71	27.15	29.35	25.77	0.88	28.92	53.21
MgO	2.07	11.44	21.44	5.97	9.19	21.42	1.31
FeO^T	54.34	15.61	0.78	19.86	40.66	2.16	0.32
MnO	1.64	0.63	0.02	5.04	9.37	0.92	0.09
SrO	0.00	0.00	0.00	0.00	0.00	0.00	0.00
ZnO	0.08	0.92	0.02	0.12	0.08	0.15	0.12
BaO	0.00	0.02	0.03	0.05	0.00	0.00	0.02
CO_2*	38.73	44.23	46.94	42.09	41.48	48.04	43.50
Total	99.57	100.00	98.59	98.89	101.68	101.62	98.56
Cations on the basis of 6 oxygens							
Ca	0.220	1.926	1.962	1.921	0.067	1.889	3.839
Mg	0.234	1.129	1.994	0.619	0.967	1.947	0.132
Fe	3.437	0.865	0.041	1.156	2.401	0.110	0.018
Mn	0.105	0.035	0.001	0.297	0.561	0.048	0.005
Sr	0.000	0.000	0.000	0.000	0.000	0.000	0.000
Zn	0.004	0.045	0.001	0.006	0.004	0.007	0.006
Ba	0.000	0.000	0.001	0.001	0.000	0.000	0.000
C	2.000	2.000	2.000	2.000	2.000	2.000	2.000
Total	6.000	6.000	6.000	6.000	6.000	6.000	6.000
End members (mol%)							
$CaCO_3$	5.50	48.15	49.05	48.03	1.67	47.22	95.97
$MgCO_3$	5.84	28.22	49.85	15.47	24.17	48.67	3.29
$FeCO_3$	85.92	21.62	1.02	28.90	60.03	2.75	0.45
$MnCO_3$	2.62	0.88	0.03	7.42	14.02	1.19	0.12
$SrCO_3$	0.00	0.00	0.00	0.00	0.00	0.00	0.00
$ZnCO_3$	0.11	1.12	0.03	0.15	0.11	0.17	0.15
$BaCO_3$	0.00	0.01	0.02	0.03	0.00	0.00	0.01

Notes: *CO_2 values are calculated assuming stoichiometry. Total iron determined as FeO.

Sample numbers and locations: 1—AC-8-60.0, siderite in sphalerite-rich drill core, Aurora Creek deposit; 2—JS-07-8D, ankerite-dolomite in sphalerite-rich brecciated carbonate rock, Aurora Creek (see Figs. 5A and 7C); 3—JS-07-8D, dolomite in sphalerite-rich brecciated carbonate rock, Aurora Creek deposit (see Figs. 5A and 7C); 4—JS-05-77A, ankerite in sulfide-magnetite-fluorite rock, Wheeler North deposit; 5—JS-05-77A, Mn-rich siderite in galena-rich rock, Wheeler North deposit; 6—JS-07-19B, dolomite in sphalerite- and galena-rich rock, Nelson deposit; 7—BLC-34-174.0, calcite in sphalerite- and galena-rich rock, Bluff prospect.

$\delta^{34}S$ values cannot reflect sulfur in CRD barite, which typically has values of less than 12‰ due to a predominance of magmatic sulfur (cf. Thompson and Beaty, 1990); and (4) a postmetamorphic epigenetic model related to Late Cretaceous tin granites (Brobst et al., 1971) is ruled out because of the deformed and metamorphosed nature of the deposits and because the tin granites on Seward Peninsula were emplaced after Jurassic–Cretaceous penetrative deformation and metamorphism related to the Brooks Range orogeny (see Hudson and Arth, 1983). The weight of available evidence—geological, textural, chemical, and isotopic—indicates that the stratabound Zn(-Pb-Ag-Au-Ba-F) lenses at Aurora Creek and Wheeler North are pre-metamorphic SEDEX deposits that formed contemporaneously with their Late Devonian–Mississippian(?) metasedimentary host rocks. An alternative analogy with Broken Hill–type (BHT) Zn-Pb-Ag deposits (e.g., Broken Hill and Cannington, Australia; Beeson, 1990; Walters et al., 2002) is permissive based on their local fluorite gangue but is discounted here because of the characteristic abundance in BHT deposits of Mn-rich silicate gangue and close spatial association with felsic metavolcanic rocks, both of which are absent from the base-metal sulfide deposits of the study area.

By comparison with well-characterized sediment-hosted stratiform deposits worldwide (e.g., Leach et al., 2005; Goodfellow and Lydon, 2007), our SEDEX model permits sulfide deposition both on the seafloor and in the shallow subsurface. Support for seafloor mineralization comes from the presence of layered semi-massive to massive sulfide at Wheeler North (Fig. 5D), although such sulfide-rich rock also can form by subseafloor replacement of chemically reactive strata such as carbonate or barite (e.g., Kelley et al., 2004a, 2004b). Evidence for mineralization in the shallow subsurface is the occurrence of disseminated sulfides within brecciated carbonate at Aurora Creek (Fig. 5A). Layered siliceous and barite-rich rocks at Aurora Creek (Figs. 5B and 5C) are interpreted as metamorphosed exhalites that precipitated on the paleoseafloor; the clots of Fe-carbonate and sulfide that occur within them may have originated as clasts eroded from mineralized mounds on the seafloor. However, it is also possible that these layered units formed by subseafloor replacement, as in well-studied occurrences elsewhere such as the siliceous cap rock at the Myra Falls Zn-Pb-Ag-Au-Ba deposit in British Columbia (Jones et al., 2006) and the layered barite at the Anarraaq Zn-Pb-Ag deposit in Alaska (Kelley et al., 2004a).

The origin of the other sulfide accumulations in the Nome Complex is less certain. At the Nelson occurrence, stratabound Zn-Pb-Ag mineralization has a similar sulfide mineralogy to the Wheeler North and Aurora Creek deposits—comprising

Downloaded from specialpapers.gsapubs.org on September 29, 2015

TABLE 5. REPRESENTATIVE ANALYSES OF MICA, NOME COMPLEX

	Phengite in muscovite-chloritoid schist						Phengite in other mineralized lithologies			F-phlogopite
Location	Aurora Creek		Wheeler North		Quarry	Nelson	Aurora Creek	Wheeler North	Galena	Nelson
Sample number	AC17-66	JS07-8B	07ATi8B	07ATi7A	07ATi1B	06ATi25F	JS-07-9	JS-07-17A	JS-05-79	JS-07-19B
Number of analyses averaged	[2]	[3]	[3]	[3]	[3]	[3]	[2]	[3]	[3]	[5]
Oxide (wt%)										
SiO_2	46.96	47.10	48.75	45.93	46.59	48.34	49.13	43.70	43.17	42.97
TiO_2	0.11	0.17	0.05	0.08	0.07	0.05	0.12	0.59	0.18	0.18
Al_2O_3	32.07	32.13	32.59	35.59	31.93	33.14	31.10	34.64	32.31	13.40
FeO	3.64	4.24	1.07	2.19	4.05	1.16	1.42	2.35	3.80	1.53
MnO	0.00	0.01	0.01	0.01	0.01	0.00	0.00	0.00	0.00	0.03
MgO	1.15	1.00	1.90	0.54	1.16	1.66	2.03	1.00	1.40	27.07
CaO	0.00	0.00	0.00	0.00	0.01	0.00	0.01	0.00	0.03	0.09
ZnO	0.07	0.04	0.03	0.00	0.03	0.03	0.64	0.05	0.24	0.31
BaO	1.24	0.88	0.46	0.23	0.23	0.10	0.83	5.33	6.49	0.19
Na_2O	0.48	0.31	0.38	1.21	0.29	0.34	0.36	0.51	0.78	0.10
K_2O	9.66	9.95	9.68	9.37	10.50	10.60	10.02	8.59	7.31	9.17
F	0.06	0.01	0.18	0.00	0.19	0.16	0.84	0.42	0.51	3.81
Cl	0.01	0.01	0.00	0.00	0.01	0.01	0.00	0.00	0.00	0.01
Ox sum	95.43	95.79	95.09	95.15	95.06	95.60	96.49	97.17	96.22	98.86
O≡ F, Cl	0.02	0.01	0.08	0.00	0.08	0.07	0.35	0.18	0.22	1.61
H_2O calc	4.38	4.44	4.35	4.49	4.24	4.36	3.71	3.99	3.80	0.69
Total	99.78	100.22	99.36	99.64	99.21	99.89	99.84	100.99	99.80	97.95
Cations per 11 oxygens										
Si	3.174	3.170	3.237	3.066	3.164	3.204	3.268	2.984	3.020	2.991
Al	0.826	0.830	0.763	0.934	0.836	0.796	0.732	1.016	0.980	1.009
∑T	4.000	4.000	4.000	4.000	4.000	4.000	4.000	4.000	4.000	4.000
Al	1.730	1.722	1.787	1.866	1.720	1.793	1.706	1.771	1.684	0.091
Ti	0.005	0.008	0.002	0.004	0.003	0.003	0.006	0.030	0.009	0.010
Fe	0.206	0.239	0.059	0.122	0.230	0.064	0.079	0.134	0.222	0.089
Mn	0.000	0.001	0.000	0.000	0.000	0.000	0.000	0.000	0.000	0.002
Mg	0.116	0.100	0.188	0.053	0.117	0.164	0.201	0.102	0.146	2.809
Zn	0.005	0.003	0.002	0.000	0.002	0.002	0.045	0.004	0.018	0.023
∑R	2.062	2.074	2.039	2.046	2.074	2.026	2.037	2.041	2.079	3.024
Ca	0.000	0.000	0.000	0.000	0.000	0.000	0.001	0.000	0.002	0.007
Ba	0.033	0.023	0.012	0.006	0.006	0.003	0.022	0.143	0.178	0.005
Na	0.062	0.041	0.049	0.157	0.038	0.044	0.046	0.068	0.105	0.014
K	0.833	0.856	0.820	0.798	0.910	0.896	0.850	0.748	0.652	0.815
∑A	0.928	0.920	0.881	0.962	0.955	0.943	0.919	0.959	0.938	0.840
Cation sum	6.990	6.994	6.920	7.008	7.028	6.969	6.956	7.000	7.018	7.864
Mg#	0.361	0.297	0.759	0.303	0.337	0.719	0.719	0.433	0.397	0.969

Note: All iron assumed to be Fe^{2+}; Mg# = Mg/(Mg + Fe + Mn); H_2O calculated by stoichiometry.

mainly sphalerite, galena, and pyrite, as well as sparse amounts of fluorite in places—but is hosted in schists and marbles of the Mixed unit; the geologic setting is apparently not the same as at Wheeler North and Aurora Creek. Rare-earth–element data for sulfide-rich samples from Nelson also are broadly like those for these two stratabound sulfide deposits including moderate positive Eu anomalies (Fig. 12D). However, carbonate gangue analyzed by EMPA in one sample from Nelson consists of dolomite and calcite, without the ankerite and/or siderite that characterize the gangue mineralogy of Aurora Creek and Wheeler North (Fig. 17). Moreover, Pb isotope compositions of Nelson galena are more radiogenic and require one or more different Pb sources than those inferred for the Aurora Creek and Wheeler North deposits (Ayuso et al., this volume).

The genesis of base-metal sulfides at the Bluff prospect is enigmatic. Sphalerite, galena, and minor pyrite occur in layers that are deformed by folds (Fig. 5G). These sulfides are not spatially associated with high gold contents in the same drill cores, and they lack the high As and Sb contents that characterize the gold-bearing veins. Nevertheless, the timing of base-metal mineralization within the layers is uncertain and may be syn-metamorphic based on detailed structural studies by Ford (1993). Also relevant is the presence of very small or no positive Eu anomalies in all three mineralized samples analyzed from this prospect, which contrast with the uniformly moderate to large positive Eu anomalies in samples from the other stratabound Zn- or Pb-rich lenses and from the deformed veins in the Nome Complex (Fig. 12). Additional differences at Bluff, relative to these other lenses and veins, include an apparent lack of associated aluminous alteration zones (see Ford, 1993) and more radiogenic Pb isotope ratios in galena (Ayuso et al., this volume).

Downloaded from specialpapers.gsapubs.org on September 29, 2015

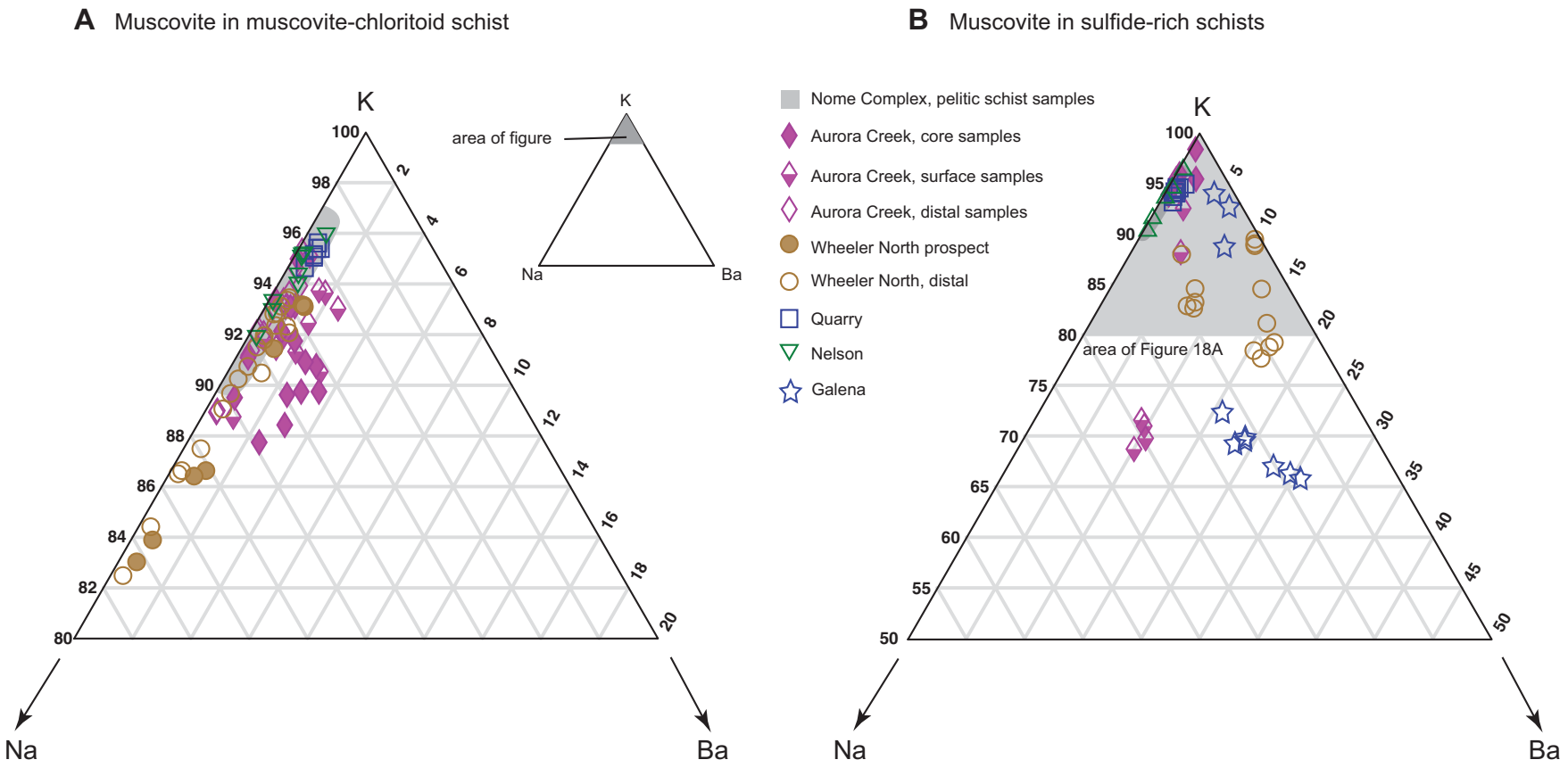


Figure 18. Ternary K-Na-Ba plot of muscovite compositions in (A) muscovite-chloritoid schist and (B) mineralized rocks. Note that both plots represent a portion of the full ternary near the K apex.

Downloaded from specialpapers.gsapubs.org on September 29, 2015

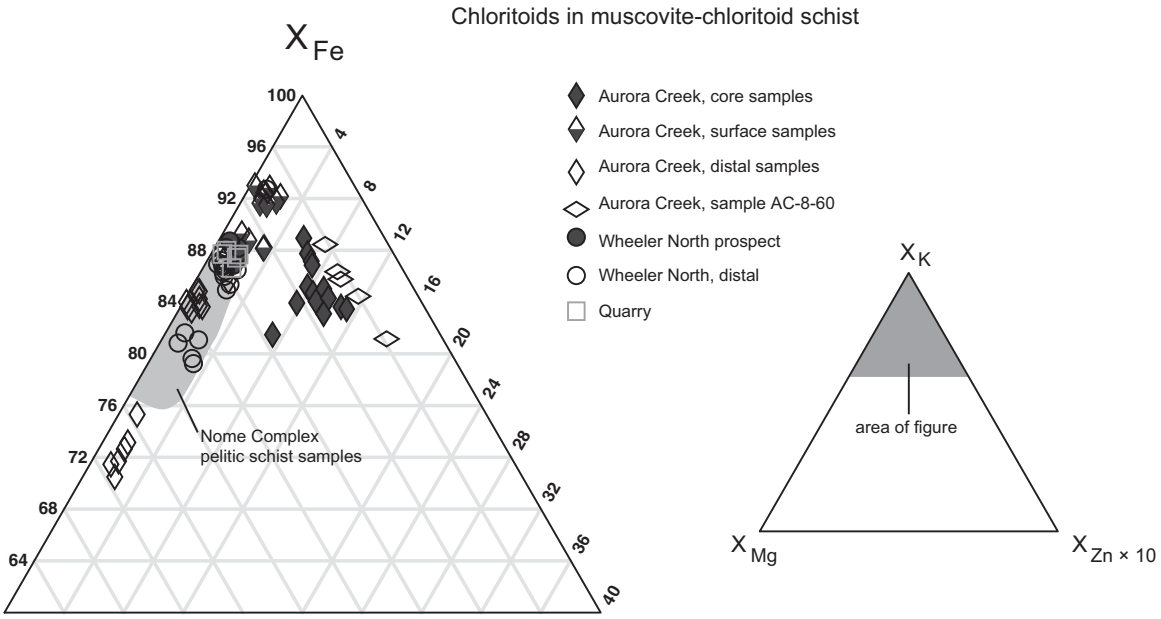


Figure 19. Ternary Mg-Fe-Zn plot of chloritoid compositions in mineralized and unmineralized rocks.

Deformed Zn-Pb(-Ag-Au-Ba-F) Veins

The deformed base-metal veins at Quarry and Galena are interpreted to be deep subsurface components of a mineralizing system similar to the ones that generated the stratabound Aurora Creek and Wheeler North lenses. These deformed veins and the stratabound lenses have a very similar ore and gangue mineralogy and aluminous alteration zones. The Galena prospect is an exception. No aluminous alteration zone has been identified there, although concentrations of very fine-grained rutile, zircon, and other minerals in muscovite are typical of the very minor quartz-muscovite schists at the prospect and of aluminous alteration zones at the other deposits and prospects. An additional strong link is provided by the high sulfur isotope values of barite at Quarry (26.1‰–30.3‰) and Aurora Creek (25.5‰–26.3‰), both of which document a major component of seawater sulfate (Shanks et al., this volume). This indication of seawater sulfate in the hydrothermal fluids at Quarry does not require a shallow depth of mineralization below the seafloor, however, because in modern ocean basins that lack abundant unreactive organic matter, seawater sulfate is not quantitatively reduced to sulfide during early diagenesis and can persist in pore fluids to significant depths (e.g., Emerson and Hedges, 2003; Meister et al., 2013). The maximum preservation depth of sulfate-rich pore fluids within sedimentary strata of the Mixed unit during the Devonian–Mississippian(?) is unknown, but on analogy with data from deep drill cores in marine sediments of the southwest Pacific Ocean (Böttcher et al., 2004), could have been 600 m or more. Faults or other high-permeability structures that focused mineralization at Quarry and Galena apparently had access to hydrothermal fluids that were compositionally similar to those that formed the Aurora Creek and Wheeler North deposits, based on their common metal signature of Zn (±Pb) and F among all four deposits, and also the local abundance of Ba at Aurora Creek and Quarry.

However, these compositional similarities are not reflected in Pb isotope ratios for galena collected from the stratabound lenses and deformed veins (Ayuso et al., this volume). All four stratabound lenses yielded distinct Pb isotope ratios. Amongst the lenses, only Nelson has a Pb isotope signature wholly like that of the deformed veins (Quarry and Galena). The least radiogenic Pb isotope ratios for Aurora Creek are similar to those of Nelson, Quarry, and Galena, possibly reflecting a common source; however, the Pb isotope data for Aurora Creek as a whole reflect mixing with a younger reservoir of fluid, likely that associated with Cretaceous gold veins (Ayuso et al., this volume). Lead-isotope ratios for Wheeler North require different Pb sources and a slightly younger age of mineralization. The Wheeler North Pb isotope signature wholly overlaps that of the Red Dog district (Ayuso et al., this volume).

Genetic Model for Mineralization

Figure 20 shows a schematic model for Zn-Pb(-Ag-Au-Ba-F) deposits and occurrences in the Nome Complex. This model includes SEDEX mineralization both on the seafloor and in the shallow subsurface, as represented by Aurora Creek and Wheeler North, which are interpreted to have formed as exhalative chemical sediments and subseafloor replacements during Late Devonian–Mississippian(?) time, contemporaneously with siliciclastic and lesser carbonate sedimentation in the Calcareous metasiliceous unit (Fig. 3). Stratabound mineralization at Nelson and vein mineralization at Quarry and Galena formed deep

Downloaded from specialpapers.gsapubs.org on September 29, 2015

TABLE 6. REPRESENTATIVE ANALYSES OF CHLORITOID, NOME COMPLEX

	Chloritoid in muscovite-chloritoid schist			Chloritoid in mineralized lithology
Location	Aurora Creek			Aurora Creek
Sample number	JS07-8B	07ATi4A-F	AC-17-66.5	AC-8-60
Number of analyses averaged	[3]	[4]	[3]	[3]
Oxide (wt%)				
SiO_2	24.26	24.80	24.02	24.06
TiO_2	0.07	0.05	0.03	0.03
Al_2O_3	40.21	40.62	40.67	41.62
FeO	29.53	23.35	27.87	26.81
MnO	0.20	0.29	0.16	0.24
MgO	0.98	4.55	1.28	0.70
ZnO	0.05	0.07	0.32	0.57
CaO	0.00	0.01	0.00	0.01
Total	95.33	93.72	94.36	94.05
Cations on the basis of 12 oxygens				
Si	1.993	2.009	1.980	1.979
Al	3.000	3.000	3.000	3.000
Al	0.892	0.879	0.950	1.036
Ti	0.005	0.003	0.002	0.002
Fe^{2+}	2.028	1.582	1.921	1.845
Mn	0.014	0.020	0.011	0.017
Mg	0.120	0.549	0.158	0.085
Zn	0.003	0.004	0.020	0.035
Ca	0.000	0.000	0.000	0.001
Cation sum	8.055	8.047	8.042	8.000
X_{Fe}	0.937	0.734	0.911	0.931
X_{Mn}	0.006	0.009	0.005	0.008
X_{Mg}	0.055	0.255	0.075	0.043
X_{Zn}	0.001	0.002	0.009	0.018

Note: All iron as Fe^{2+} (no Fe^{+3} because Al^{VI} is > 1); $X_{Fe} = Fe/(Mg + Mn + Fe + Zn)$; $X_{Mg} = Mg/(Mg + Mn + Fe + Zn)$; $X_{Mn} = Mn/(Mg + Mn + Fe + Zn)$; $X_{Zn} = Zn/(Mg + Mn + Fe + Zn)$.

in the subsurface, within the stratigraphically underlying Mixed unit, by filling of faults or other high-permeability structures or sediments that focused the flow of hydrothermal fluids. This interpretation is consistent with Pb isotope data (Ayuso et al., this volume) and with a scenario in which the Quarry and Galena deposits were deep feeders for the SEDEX mineralization at Aurora Creek; formation of the Nelson deposit is attributed to replacement in the deep subsurface, contemporaneous with mineralization at Aurora Creek, Quarry, and Galena. In Figure 20, the schistose carbonate-clast conglomerate at the Aurora Creek deposit is interpreted as a fault-scarp breccia deposited during SEDEX mineralization. The matrix of the carbonate-clast conglomerate contains minor disseminated pyrite, barite, and galena; it also has detrital zircons with ages similar to those of detrital zircons contained in the siliceous layered rock (inferred exhalite) at Aurora Creek.

A similar model involving surface and deep subsurface mineralization was proposed by Werdon (2000) for Mississippian SEDEX Pb-Zn-Ag deposits (e.g., Red Dog and Drenchwater) and stratigraphically lower Zn-Pb-Cu-Ag vein breccias (e.g., Kady and Husky) in the Brooks Range of Alaska. Although these vein breccias occur as much as 1 km below the stratigraphic level of the Red Dog deposits, they contain galena with similar Pb isotope compositions (Ayuso et al., 2004) and have Ar-Ar and other age constraints (Werdon et al., 2004) that suggest mineralization by the same hydrothermal fluids. However, among the sulfide deposits in the Nome Complex, the possibility of a common fluid for the all of the stratabound lenses and deformed veins is undermined by their different Pb isotope compositions (Ayuso et al., this volume), which require different Pb sources and probably slightly different ages, at least in some cases. These data nevertheless permit a model in which the deformed veins at Quarry and Galena, and the stratabound deposit at Nelson, formed as deep subsurface facies of a SEDEX hydrothermal system very similar in fluid composition to the system(s) that produced the Aurora Creek, and Wheeler North deposits, but at a different stratigraphic level, possibly including the formation of related stratiform deposits that are unexposed or eroded. Such a model would require that the relative influence of fluid components sourced in Proterozoic basement in the deformed veins differed from that in the stratabound lenses. However, sulfur isotope data for the deposits and for Paleozoic seawater sulfate allow for a different genetic model and different ages, in which the Aurora Creek and Wheeler North deposits formed in the Late Devonian–Mississippian(?), with the Nelson, Quarry, and Galena deposits having formed in the Ordovician or Silurian (Shanks et al., this volume). If this model is correct, then the deformed veins at Quarry and Galena could not have served as deep feeders for the Aurora Creek or Wheeler North deposits.

Downloaded from specialpapers.gsapubs.org on September 29, 2015

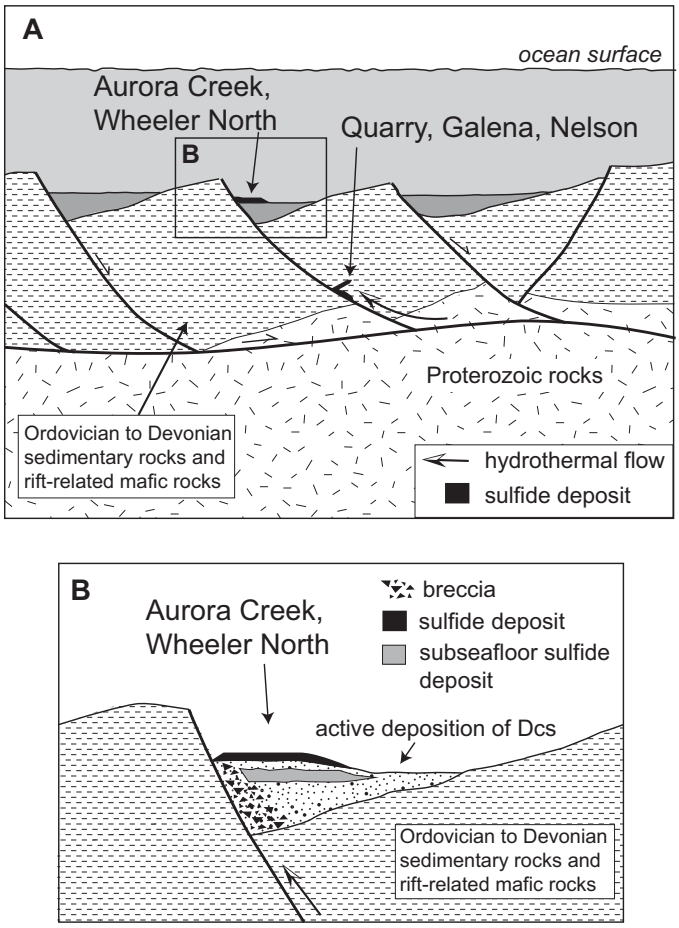


Figure 20. Schematic models for the origin of Zn-Pb(-Ag-Au-Ba-F) mineral deposits in the Nome Complex. Both panels were drawn to illustrate the setting of mineralization and do not represent single mineralizing systems: (A) Formation of the deformed veins at Quarry and Galena and the stratabound lens at Nelson is inferred to have occurred within the deep subsurface, while Aurora Creek and Wheeler North formed at the seafloor or in the shallow subsurface; Nelson probably formed by replacement of permeable carbonate strata. Seafloor or shallow subsurface mineralization at Aurora Creek may have been synchronous with the deeply formed deposits. Setting for the Zn-Pb occurrence at Bluff is not shown, because this mineralization likely formed during the early stages of Cretaceous deformation (see text). Arrows show generalized flow paths for hydrothermal fluids. Proterozoic rocks include ca. 870 Ma, ca. 680 Ma, and ca. 565 Ma felsic igneous rocks and older rocks, possibly of Mesoproterozoic age. (B) Formation of the stratabound sulfide lenses at Aurora Creek and Wheeler North is interpreted to have occurred on the seafloor or in the shallow subsurface; the schistose conglomerate at Aurora Creek is interpreted as a fault-related breccia in this reconstruction.

Mineralogical Similarities to Other SEDEX Deposits

The stratabound and locally stratiform Zn-Pb(-Ag-Au-Ba-F) lenses in the Nome Complex have both similarities and differences with SEDEX deposits elsewhere. Base-metal contents and proportions of the Aurora Creek, Wheeler North, and Nelson deposits are within the range of those documented for SEDEX deposits worldwide, and the occurrence of layered barite at Aurora Creek is common in this deposit type (e.g., Leach et al., 2005; Goodfellow and Lydon, 2007). Accessory Ba-rich muscovite (phengite) and Ba-rich feldspar (hyalophane) that occur in the Aurora Creek deposit (Figs. 7E and 7H) are also present in the ore zones and altered wall rocks of some SEDEX deposits, including the giant George Fisher ore body in the Mount Isa district, Australia (Chapman, 2004), the large Jason deposit in Yukon Territory (Turner, 1990), and the large Dengjiashan deposit in China (Ma et al., 2007), and in small deposits at Aberfeldy, Scotland (Coats et al., 1980), Rozna, Czech Republic (Kříbek et al., 1996), and Zamora, Spain (Moro et al., 2001), among others. Such Ba-rich silicate minerals probably are more common in SEDEX deposits than is reported in the literature, having been misidentified as muscovite and orthoclase without thorough documentation by EMPA or SEM.

Ferroan carbonate minerals that occur in the Aurora Creek and Wheeler North mineralized lenses are characteristic of SEDEX deposits worldwide (e.g., Goodfellow et al., 1993). Most such deposits contain minor to locally abundant siderite and/or ankerite, within the sulfide ores and in footwall feeder zones, as fillings of fractures and pore spaces, and as replacements of other minerals (e.g., calcite and feldspar). Examples include the Tom deposit, Yukon Territory (Goodfellow and Rhodes, 1990), the Century and Lady Loretta deposits in Queensland (Broadbent et al., 1998; Large and McGoldrick, 1998), and the Rammelsberg deposit, Germany (Large and Walcher, 1999). The presence in footwall zones below these deposits of brecciated carbonate with a siderite- or ankerite-rich matrix is similar to the occurrence at Aurora Creek (Figs. 5A, 7C, and 7D), adding further support to a SEDEX origin for this deposit. The lack of Mn-rich carbonate in the Aurora Creek and Wheeler North samples (Table 4) is consistent with a proximal setting for both deposits, based on the zoning pattern of carbonate gangue recognized in some SEDEX ore bodies, from predominantly siderite in the core of the vent complex (feeder zone) to peripheral ankerite to distal Mn-carbonate (e.g., Large and McGoldrick, 1998).

The stratabound sulfide lenses in the Nome Complex are noteworthy for having locally high contents of Au and F (Table 2). At Aurora Creek, one mineralized zone contains an average of 7.6 g/t Au (Porterfield et al., 1996), and at Wheeler North a short (0.7 m) channel sample has 9.3 g/t Au (Wimmler, 1926). Fluorite is abundant in both deposits, and especially at Wheeler North (up to 22.3 wt% F; Table DR1 [see footnote 3]). As summarized by Emsbo (2000), known gold-rich SEDEX deposits are limited to Rammelsberg in Germany (Zn-Pb-Cu-Ag-Au-Ba), Triumph in Idaho (Zn-Pb-Ag-Au), Rodeo in Nevada (Zn-Pb-Ag-Au), and those of the Anvil district in Yukon Territory (Zn-Pb-Ag-Au-Ba). Deposits of the Anvil district are especially relevant because of the nature of the footwall lithostratigraphic sequence there that includes abundant calcareous metapelite and minor metabasite (Jennings and Jilson, 1986). In the Nome Complex, calcareous pelitic schist and mafic metaigneous rocks (metabasites) are common in the Casadepaga Schist, which probably was deposited during the Ordovician (Till et al., this volume, Chapter 1). The Casadepaga

Downloaded from specialpapers.gsapubs.org on September 29, 2015

Schist likely was in the subsurface at the time that the Aurora Creek and Wheeler North deposits were formed (Fig. 3). Such metabasites could have served as enriched source rocks for gold, based on the generally higher background gold contents of mafic igneous rocks relative to siliciclastic sediments. Mafic rocks in the Casadepaga Schist are tholeiitic basalts that formed during incipient rifting of continental crust (Ayuso and Till, this volume). Stolz and Large (1992) identified compositionally similar continental tholeiites as the source for gold within Au-rich VMS deposits in Tasmania. The stratabound Zn-Pb deposits of Seward Peninsula occur within a highly productive placer gold district; Cretaceous veins in the Nome Complex are the apparent source for this gold (Apodoca, 1994; Ford and Snee, 1996). Oxygen isotope data indicate that the fluids involved in vein formation were metamorphic (Ford, 1993). Clearly, metamorphic rocks of the Nome Complex and related high-grade rocks of Seward Peninsula were significant sources of gold for the veins, and it follows that their protoliths also may have been the source of gold in the Zn-Pb deposits. In addition to the continental tholeiitic basalts that may have served as enriched source rocks for the gold in the Zn-Pb deposits, other factors also likely played a role in generating this mineralization, including the involvement of reduced H_2S-rich brines during hydrothermal transport of the gold (see Large et al., 1996; Emsbo, 2000). However, despite textural evidence for paragenetically early gold (e.g., electrum in sphalerite, Fig. 7A), it is also possible that the gold (and electrum) present locally in some of the deposits (e.g., Aurora Creek, Wheeler North, and Quarry), is genetically unrelated to Devonian–Mississippian(?) mineralization, instead having formed later from overprinting metamorphic fluids during the Jurassic–Cretaceous Brookian orogeny. Relatively radiogenic lead isotope compositions of most galena from the Aurora Creek deposit, compared to those from the Wheeler North, Nelson, Quarry, and Galena deposits, also suggest that much of the lead present in Aurora Creek galena was introduced epigenetically during the Brookian orogeny (Ayuso et al., this volume).

On a global basis, F-rich SEDEX deposits are also uncommon but unlike the Au-rich examples described above include several giant high-grade ore bodies. Prime examples are in Australia at Broken Hill in New South Wales (Plimer, 1984) and Cannington in Queensland (Walters et al., 2002) where F resides principally in fluorite gangue. The F present in other, much smaller SEDEX deposits similarly is concentrated in fluorite as at the Drenchwater deposit in the Brooks Range of Alaska (Werdon, 1996), the Vulcan deposit in Northwest Territories (Mako and Shanks, 1984), the Dariba deposit in India (Deb and Pal, 2004), deposits in the Arditurri and Vera de Bidasoa-Modesta districts in northern Spain (Pesquera and Velasco, 1989), and the Tripi and related deposits in Sicily (Ferla and Omenetto, 2000).

Source of the Fluorine

The widespread presence of fluorite in the stratabound sulfide lenses and deformed veins of the Nome Complex records the involvement of F-rich hydrothermal fluids during mineralization. Such fluids could reflect high temperatures or pressures and/or high salinities (Rimstidt, 1997), or F-bearing source rocks at depth. Based on the general scarcity of fluorite or other F-rich minerals in SEDEX deposits worldwide (e.g., Goodfellow et al., 1993; Leach et al., 2005), and similarities in ore and gangue mineralogy among these deposits to those of the Nome Complex, an enriched source is plausible. A magmatic component has been invoked to explain the abundance of fluorite in SEDEX deposits that are spatially associated with alkaline plutons, such as Drenchwater, Alaska (Werdon, 1996), and in MVT and rift-related deposits with or without associated plutons (Plumlee et al., 1995; Partey et al., 2009). However, no plutons of appropriate age (Devonian–Mississippian[?]) are known in the vicinity of the Nome Complex sulfide deposits (Fig. 2), hence a magmatic-hydrothermal source for the fluorine in these deposits is considered unlikely. An alternative possibility, preferred here, involves F-rich strata in the deep footwall of the sulfide deposits, where circulating hydrothermal fluids could have leached fluorine to form the fluorite-rich deposits at Aurora Creek, Wheeler North, and Quarry. In this model, the most likely source would be sedimentary fluorapatite, present either in disseminated grains or beds of phosphorite. Both types of fluorapatite occur within Mississippian black shale of the Brooks Range (Slack et al., 2004a; Dumoulin et al., 2011), but no evidence exists for the presence of lithologically correlative strata in the Nome Complex (Till et al., this volume, Chapter 1). However, this constraint does not preclude derivation of the fluorine from strata of the Nome Complex, a possibility supported by the occurrence of 5%–10% secondary phosphate in a thin graphitic siliceous schist in the Calcareous metasiliceous unit, the same unit that hosts the stratabound sulfide lenses (Till et al., this volume, Chapter 1). Following the recent model of Davis et al. (2011), we speculate that the fluorine present within the stratabound sulfide and deformed veins was leached from disseminated sedimentary fluorapatite by basinal brines, during the Devonian–Mississippian(?), and was deposited on the seafloor and in the shallow subsurface as fluorite, together with sulfides, quartz, Fe-carbonate, and other constituents. A slightly different model involving the leaching of fluorine from F-bearing Proterozoic basement rocks within or beneath the Nome Complex cannot be ruled out, given the possible contribution of Proterozoic source rocks to the Pb isotope evolution of the base-metal sulfide deposits in the study area (see Ayuso et al., this volume).

Aluminous Alteration Zones

The aluminous alteration zones that surround most of the sulfide deposits are important to understand in terms of genesis and for insights into the associated mineralization. Occurrences of these zones at both the stratabound lenses (Aurora Creek and Wheeler North) and discordant veins (Quarry) indicates formation at two different levels, respectively at or near the paleoseafloor and in the deep subsurface. However, despite this difference in primary setting, the common mineralogy of the aluminous rocks (muscovite + quartz ± chloritoid ± chlorite ± carbonate ±

Downloaded from specialpapers.gsapubs.org on September 29, 2015

hyalophane ± tourmaline) and their similar trace-metal concentrations (Zn, Pb, and Sb; Fig. 14) suggest deposition from compositionally similar hydrothermal fluids. This interpretation is supported by the presence in these rocks of minor barite, hyalophane, and/or celsian, which occur in some SEDEX deposits, as discussed above. The deposit-distal alteration zones, which extend along strike up to several kilometers beyond the known limits of the sulfide deposits, are also interpreted as products of hydrothermal alteration in the shallow subsurface, based on the similarity of mineral assemblages and Al_2O_3-$\delta^{18}O$ trend relative to those for the deposit-proximal zones (Fig. 6 in Shanks et al., this volume).

Possible non-hydrothermal origins for these aluminous chloritoid-bearing rocks, such as metamorphism of laterite or bauxite (Franceschelli et al., 2003; Verlaguet et al., 2011), are discounted because of close spatial association with the sulfide deposits, typical enrichment of the same metals (Zn, Pb, and Sb) that are present in the deposits, and uniformly low $Fe_2O_3^T$ contents of ≤10 wt% (Table 3; Table DR2 [see footnote 3]) relative to contents of >20 wt% $Fe_2O_3^T$ that characterize known metalaterites and metabauxites (Franceschelli et al., 2003, Table 1). A third possible origin involves deposition from syn-metamorphic fluids (e.g., Cox et al., 1987; Sutton and Land, 1996), a model supported by the common occurrence of small deformed quartz veins and lenses within the aluminous schists. However, this scenario is considered unlikely because of the close spatial association of these schists in the Nome Complex to the Zn- and Pb-rich sulfide deposits, which formed prior to the Jurassic–Cretaceous regional metamorphism in the region.

Our favored genetic model for the muscovite-chloritoid schists (Slack et al., 2013) involves a high flux of hydrothermal fluids focused within permeable sedimentary units during formation of the stratabound sulfide lenses and mineralogically similar veins (Fig. 20). This model resembles that proposed for aluminous chloritoid-bearing schists that occur in the stratigraphic footwall of several VMS deposits, being termed by some workers "semi-conformable alteration zones" (e.g., Galley, 1993). One important example occurs below the large Mattabi ore body in Ontario (Franklin et al., 1975), where rocks consisting of chloritoid + sericite + quartz + Fe-carbonate ± chlorite ± andalusite form stratabound zones tens of meters thick and up to 1800 m long (Groves, 1984). Several other, smaller VMS deposits have alteration zones with comparable mineral assemblages, such as Gossan Hill in Western Australia (Sharpe and Gemmell, 2001), and the Kozak occurrence in Ontario (Lockwood et al., 1985). Noteworthy is the fact that net mass changes calculated for the muscovite-chloritoid schists of the Nome Complex, relative to average unaltered clastic metasedimentary rock in the region (Fig. 16), show similar enrichments and depletions in major and trace elements—especially the significant losses of CaO and Na_2O—compared to those in the footwall alteration zones of VMS deposits (e.g., MacLean and Barrett, 1993). Aluminous chloritoid-bearing altered rocks are apparently rare in the vicinity of SEDEX deposits, one of the few described occurrences being at small Zn-Pb-Ag-Au deposits in the Casario area of northern Italy, where chloritoid-carbonate mica schist (±pyrite ± sphalerite ± tourmaline) forms stratabound lenses up to 30–40 m thick and at least 300 m long (Rossetti and Ferrero, 2008).

Several protoliths are possible for the aluminous altered rocks of the Nome Complex. In VMS systems, detailed geologic and geochemical studies have identified rhyolite tuff as the likely protolith of lithologically similar rocks, based on field relations and the inference of high permeability in such tuffs during influx of hydrothermal fluids beneath the seafloor. A rhyolite protolith cannot be ruled out for the Nome Complex aluminous rocks, given the composition of average rhyolite in terms of SiO_2/Al_2O_3-$Fe_2O_3^T$/MgO variations (Fig. 13A). However, no rhyolite of any type has been found in the Paleozoic strata of the Nome Complex during our studies (Till et al., this volume, Chapter 1), and zircons separated from a muscovite-chloritoid schist in drill core from the Aurora Creek deposit are all rounded and clearly detrital; no euhedral igneous zircons were found (Till et al., this volume, Chapter 4). In addition, SEM study reveals the common occurrence in the aluminous rocks of accessory rutile, zircon, ilmenite, apatite, xenotime, and monazite in fine layers (Fig. 7F) that suggest an appreciable detrital component. Considered in total, these data do not support a rhyolitic protolith for the muscovite-chloritoid schists.

The most likely protolith was some type of coarse-grained and permeable sediment. A shale protolith is discounted owing to the low permeability of precursor clay-rich muds (e.g., Davis, 1969) and hence an inability to permit major fluid flow in the subsurface. Arkose (a feldspar-rich sandstone) is a possible protolith, but no metaarkose has been recognized in the Calcareous metasiliceous rocks, host unit to the Aurora Creek and Wheeler North deposits. Plagioclase is a significant, but not dominant component of metasandstones in that unit. The best candidate is graywacke, based on several factors. First, rocks that are likely metamorphosed graywacke occur within the Calcareous metasiliceous unit in areas far from known sulfide deposits or occurrences (Till et al., 2011; Till et al., this volume, Chapter 1). Second, the composition of average graywacke (Pettijohn, 1963) and of the one analyzed metagraywacke in our collection (JS-06-11; Table DR3 [see footnote 3]) both have low SiO_2/Al_2O_3 and $Fe_2O_3^T$/MgO ratios (Fig. 13B) that are consistent with similar lithologies being protoliths of the aluminous altered rocks. Third, prior to deep burial and metamorphism, graywacke would have had the relatively high permeability (e.g., Davis, 1969) needed for transport of large volumes of hydrothermal fluid during SEDEX mineralization. We therefore conclude that graywacke was the protolith to the aluminous altered rocks in the study area (see also Slack et al., 2013). If this interpretation is valid, and if metagraywacke sample JS-06-11 is representative of the protolith, the subseafloor hydrothermal alteration that formed the aluminous schists produced a net mass loss in most cases, based on Al_2O_3-Nb relationships (Fig. 13C) and assuming relative immobility of Al and Nb during this alteration process.

Downloaded from specialpapers.gsapubs.org on September 29, 2015

Stratabound Cu Deposits

The stratabound Cu-rich deposits have significantly different textures, metal signatures, and alteration styles compared to the other base-metal concentrations described in this study. At the Copper King deposit, for example, chalcopyrite and bornite plus quartz occur in stratabound lenses that contain mm- to cm-wide zones of disseminated to semi-massive sulfide within silicified carbonate rock (Fig. 5H). This deposit and other Cu-rich deposits in the area (Copper Mountain and Wheeler South) are characterized by prominent silicification within and adjacent to the mineralized zones (Cathcart, 1922; this study); such silicification of wall rocks is uncommon in the stratabound Zn- and/or Pb-rich lenses. The Cu-rich nature of these deposits, and elevated Bi (Table 2), also contrasts with the metal signature of the Zn-Pb(-Ag-Au-Ba-F) lenses and veins, and suggests deposition by relatively high-temperature (>300 °C) fluids in order to carry appreciable Cu and Bi in solution (cf. Lang and Baker, 2001). In addition, the Cu-rich deposits lack the associated aluminous alteration zones that typically surround the lenses and veins. Our preliminary model for the origin of the stratabound Cu-rich deposits involves high-temperature, pre- to syn-metamorphic mineralization that was focused within carbonate strata of the Mixed unit, prior to or during deformation of the host rocks. An alternative model involving a similar timing but linked to granite-derived hydrothermal fluids (see Lang and Baker, 2001) is also feasible.

Exploration Applications

Results of this study have important applications for assessment of mineral resources and mineral exploration programs. In particular, the recognition of a SEDEX origin for the stratabound sulfide lenses at Aurora Creek and Wheeler North suggests the likelihood of similar deposits occurring at or near the same stratigraphic level within the Calcareous metasiliceous unit (Fig. 3). This use of a stratigraphically focused target differs from that implied by a CRD model in which involvement of a hidden granite pluton is more mechanistically important than a specific lithologic unit or stratigraphic level. Especially relevant in resource assessment and exploration are the large sizes of the aluminous alteration zones that surround the Aurora Creek and Wheeler North deposits, extending for as much as 4 km and possibly more, along strike (Figs. 4 and 8). However, lack of outcrop and the penetrative nature of deformation associated with metamorphism make the size of the original alteration zones difficult to estimate. The areal distribution of these deformed alteration zones is much greater than that of the sulfide deposits, thus allowing the possibility that the causative hydrothermal systems were also large and not small as implied by the limited size of some deposits such as Wheeler North. On a regional scale, the stratabound Zn-Pb(-Ag-Au-Ba-F) deposits of the Nome Complex are broadly coeval with Late Devonian SEDEX deposits in the Selwyn Basin of Yukon Territory such as Tom, Jason, and Cirque (e.g., Goodfellow, 2007). If the host strata of the Nome Complex deposits are Mississippian, however, then the contained sulfide deposits may be temporally linked to SEDEX deposits of the Red Dog district in the western Brooks Range of Alaska (Kelley and Jennings, 2004).

Geologic mapping and geochronologic studies (Amato et al., 2009; Till et al., 2011; Till et al., this volume, Chapter 4) show that high-grade metamorphic rocks exposed in the Kigluaik, Bendeleben, and Darby Mountain ranges are higher metamorphic grade equivalents of the Nome Complex. Highly aluminous metasedimentary rocks have been recognized in all three mountain ranges (Till et al., 2011); at least some of these may be equivalents of the muscovite-chloritoid schists in the Calcareous metasiliceous unit.

CONCLUSIONS

Field and petrographic studies of Zn-Pb(-Ag-Au-Ba-F) deposits within Late Devonian to Mississippian(?) metasedimentary rocks of the Nome Complex, Seward Peninsula, Alaska, have delineated two pre-metamorphic types: stratabound and locally stratiform lenses, and deformed veins. The stratabound deposits show textural and paragenetic features that suggest formation on or near the paleoseafloor, as parts of sedimentary-exhalative (SEDEX) hydrothermal systems. The deformed veins, which have similar ore and gangue minerals and a similar metal signature, are interpreted as deep facies of SEDEX mineralizing systems. Both deposit types have spatially associated aluminous alteration zones that contain abundant muscovite and chloritoid, plus disseminated base-metal sulfide minerals; geochemical data for these aluminous altered rocks are consistent with a model involving pre-metamorphic hydrothermal alteration of precursor graywacke in which the aluminous mineralogy—and bulk composition—of the rocks was attained by major leaching of CaO and Na_2O by SEDEX-related hydrothermal fluids. The pre-metamorphic sulfide lenses and deformed veins within the Nome Complex likely formed on the margin of the North American continent, coeval with episodic rifting during Late Devonian to Mississippian(?) time.

ACKNOWLEDGMENTS

We thank Irene Anderson and Matt Ganley of Bering Straits Native Corporation for access to native lands and unpublished reports. Brigitte Dejou, formerly of Cominco-American, Inc. (now Teck Resources Ltd.), provided drill cores for sampling and maps of the Aurora Creek deposit for study. Discussions with USGS colleagues Robert Ayuso, Julie Dumoulin, and Joe Briskey are appreciated; Briskey also supplied unpublished field notes and geochemical analyses. John Jackson (USGS) provided XRD data. We also thank Bering Straits Native Corporation, Rio Tinto Minerals, Hawley Resource Group, and Teck Resources Ltd. for permission to cite field and analytical data in unpublished maps and reports. Appreciation is extended particularly to Karen Kelley (USGS) and Jan Peter (Geological

Downloaded from specialpapers.gsapubs.org on September 29, 2015

Survey of Canada) for thorough and constructive reviews of the manuscript, and to Julie Dumoulin (USGS) for careful editorial inspection, all of which greatly improved the final version.

REFERENCES CITED

Amato, J.M., Toro, J., Miller, E.L., Gehrels, G.E., Farmer, G.L., Gottlieb, E.S., and Till, A.B., 2009, Late Proterozoic–Paleozoic evolution of the Arctic Alaska–Chukotka terrane based on U-Pb igneous and detrital zircon ages: Implications for Neoproterozoic paleogeographic reconstructions: Geological Society of America Bulletin, v. 121, p. 1219–1235, doi:10.1130/B26510.1.

Apodoca, L.E., 1994, Genesis of lode gold deposits of the Rock Creek area, Nome mining district, Seward Peninsula, Alaska [Ph.D. thesis]: Boulder, University of Colorado, 208 p.

Armstrong, J.T., 1995, CITZAF: A package of correction programs for the quantitative electron microbeam X-ray analysis of thick polished materials, thin films, and particles: Microbeam Analysis, v. 4, p. 177–200.

Ayuso, R.A., and Till, A.B., 2014, this volume, Chapter 5, Geochemical and Nd-Sr-Pb isotopic evolution of metabasites from rifting of continental lithosphere, Seward Peninsula, Alaska, and implications for paleogeographic reconstruction, *in* Dumoulin, J.A., and Till, A.B., eds., Reconstruction of a Late Proterozoic to Devonian Continental Margin Sequence, Northern Alaska, Its Paleogeographic Significance, and Contained Base-Metal Sulfide Deposits: Geological Society of America Special Paper 506, doi:10.1130/2014.2506(05).

Ayuso, R.A., Kelley, K.D., Leach, D.L., Young, L.E., Slack, J.F., Wandless, G., Lyon, A.M., and Dillingham, J.L., 2004, Origin of the Red Dog Zn-Pb-Ag deposits, Brooks Range, Alaska: Evidence from regional Pb and Sr isotope sources: Economic Geology and the Bulletin of the Society of Economic Geologists, v. 99, p. 1533–1553, doi:10.2113/gsecongeo.99.7.1533.

Ayuso, R.A., Till, A.B., Slack, J.F., and Forni, F., 2014, this volume, Chapter 7, Pb isotope geochemistry of stratabound Zn-Pb(-Ag-Au-Ba-F) deposits and occurrences in the Nome Complex, Seward Peninsula, Alaska: Metal sources and regional comparisons, *in* Dumoulin, J.A., and Till, A.B., eds., Reconstruction of a Late Proterozoic to Devonian Continental Margin Sequence, Northern Alaska, Its Paleogeographic Significance, and Contained Base-Metal Sulfide Deposits: Geological Society of America Special Paper 506, doi:10.1130/2014.2506(07).

Bau, M., 1991, Rare-earth element mobility during hydrothermal and metamorphic fluid-rock interaction and the significance of the oxidation state of europium: Chemical Geology, v. 93, p. 219–230, doi:10.1016/0009-2541(91)90115-8.

Beeson, R., 1990, Broken Hill-type lead-zinc deposits—An overview of their occurrence and geological setting: Institution of Mining and Metallurgy Transactions, v. 99, sec. B, p. B163–B175.

Böttcher, M.E., Khim, B.-K., Suzuki, A., Gehre, M., Wortmann, U.G., and Brumsack, H.-J., 2004, Microbial sulfate reduction in deep sediments of the Southwest Pacific (ODP Leg 181, Sites 1119–1125): Evidence from stable sulfur isotope fractionation pore water modeling: Marine Geology, v. 205, p. 249–260, doi:10.1016/S0025-3227(04)00026-X.

Broadbent, G.C., Myers, R.E., and Wright, J.V., 1998, Geology and origin of shale-hosted Zn-Pb-Ag mineralization at the Century deposit, northwest Queensland, Australia: Economic Geology and the Bulletin of the Society of Economic Geologists, v. 93, p. 1264–1294, doi:10.2113/gsecongeo.93.8.1264.

Brobst, D.A., Pinckney, D.M., and Sainsbury, C.L., 1971, Geology and geochemistry of the Sinuk River barite deposit, Seward Peninsula, Alaska: U.S. Geological Survey Professional Paper, v. 750-D, p. D1–D8.

Brown, S.E., 1977, Annual report on Aurora Creek project, Nome quadrangle, Alaska: Spokane, Washington, unpublished report for Cominco American, Inc., 10 p.

Bundtzen, T.K., Reger, R.D., Laird, G.M., Pinney, D.S., Clautice, K.H., Liss, S.A., and Cruse, G.R., 1994, Progress report on the geology and mineral resources of the Nome mining district: Alaska Division of Geological and Geophysical Surveys, Public-Data File 94-39, 19 p.

Cathcart, S.H., 1922, Metalliferous lodes in southern Seward Peninsula: U.S. Geological Survey Bulletin 722-F, p. 163–261.

Chapman, L.H., 2004, Geology and mineralization styles of the George Fisher Zn-Pb-Ag deposit, Mount Isa, Australia: Economic Geology and the Bulletin of the Society of Economic Geologists, v. 99, p. 233–255, doi:10.2113/gsecongeo.99.2.233.

Chutas, N., and Robinson, J., 2010, 2010 Exploration summary of the Kugruk project, Seward Peninsula, Alaska [abs.]: Alaska Miners Association Annual Meeting, Anchorage, November 1–7, 2010, Abstracts, p. 20.

Coats, J.S., Smith, C.G., Fortey, N.J., Gallagher, M.J., May, F., and McCourt, W.J., 1980, Strata-bound barium-zinc mineralization in Dalradian schist near Aberfeldy, Scotland: Institution of Mining and Metallurgy Transactions, v. 89, sec. B, p. B110–B122.

Cox, S.F., Etheridge, M.A., and Wall, V.J., 1987, The role of fluids in syntectonic mass transport, and the localization of metamorphic vein-type ore deposits: Ore Geology Reviews, v. 2, p. 65–86, doi:10.1016/0169-1368(87)90024-2.

Davis, S.N., 1969, Porosity and permeability of natural materials, *in* DeWiest, R.J.M., ed., Flow through Porous Media: New York, Academic Press, p. 53–89.

Davis, W.J., Gall, Q., Jefferson, C.W., and Rainbird, R.H., 2011, Fluorapatite in the Paleoproterozoic Thelon basin: Structural-stratigraphic context, in situ ion microprobe U-Pb ages, and fluid-flow history: Geological Society of America Bulletin, v. 123, p. 1056–1073, doi:10.1130/B30163.1.

Deb, M., and Pal, T., 2004, Geology and genesis of the base metal sulphide deposits in the Dariba-Rajpura-Bethumni belt, Rajasthan, India, in the light of basin evolution, *in* Deb, M., and Goodfellow, W.D., eds., Sediment-Hosted Lead-Zinc Sulphide Deposits: New Delhi, Narosa Publishing, p. 304–327.

Dickinson, K.A., Cunningham, K.D., and Ager, T.A., 1987, Geology and origin of the Death Valley uranium deposit, Seward Peninsula, Alaska: Economic Geology and the Bulletin of the Society of Economic Geologists, v. 82, p. 1558–1574, doi:10.2113/gsecongeo.82.6.1558.

Dobson, D.C., 1982, Geology and alteration of the Lost River tin-tungsten-fluorine deposit, Alaska: Economic Geology and the Bulletin of the Society of Economic Geologists, v. 77, p. 1033–1052, doi:10.2113/gsecongeo.77.4.1033.

Dumoulin, J.A., Harris, A.G., Gagiev, M., Bradley, D.C., and Repetski, J.E., 2002, Lithostratigraphic, conodont, and other faunal links between lower Paleozoic strata in northern and central Alaska and northeastern Russia, *in* Miller, E.L., Grantz, A., and Klemperer, S.L., eds., Tectonic Evolution of the Bering Shelf-Chukchi Sea–Arctic Margin and Adjacent Landmasses: Geological Society of America Special Paper 360, p. 291–312.

Dumoulin, J.A., Slack, J.F., Whalen, M.T., and Harris, A.G., 2011, Depositional setting and geochemistry of phosphorites and metalliferous black shales in the Carboniferous–Permian Lisburne Group, northern Alaska: U.S. Geological Survey Professional Paper 1776-C, 64 p., available at http://pubs.usgs.gov/pp/1776/c/.

Dumoulin, J.A., Harris, A.G., and Repetski, J.E., this volume, 2014, Chapter 3, Carbonate rocks of the Seward Peninsula, Alaska: Their correlation and paleogeographic significance, *in* Dumoulin, J.A., and Till, A.B., eds., Reconstruction of a Late Proterozoic to Devonian Continental Margin Sequence, Northern Alaska, Its Paleogeographic Significance, and Contained Base-Metal Sulfide Deposits: Geological Society of America Special Paper 506, doi:10.1130/2014.2506(03).

Eakin, H.M., 1915, Iron-ore deposits near Nome: U.S. Geological Survey Bulletin 622-I, p. 361–365.

Emerson, S., and Hedges, J., 2003, Sediment diagenesis and benthic flux, *in* Mackenzie, F.T., ed., Sediments, Diagenesis, and Sedimentary Rocks, Treatise on Geochemistry: Amsterdam, Elsevier, v. 6, p. 293–319.

Emsbo, P., 2000, Gold in sedex deposits, *in* Hagemann, S.G., and Brown, P.E., eds., Gold in 2000: Reviews in Economic Geology, v. 13, p. 427–437.

Evans, B.W., and Patrick, B.E., 1987, Phengite-3T in high-pressure metamorphosed granitic orthogneisses, Seward Peninsula, Alaska: Canadian Mineralogist, v. 25, p. 141–158.

Ferla, P., and Omenetto, P., 2000, Metallogenic evolution of Peloritani Mountains (NE Sicily): A summary: Società Geologica Italiana Memorie, v. 55, p. 293–297.

Ford, R.C., 1993, Geology, geochemistry and age of gold lodes at Bluff and Mt. Distin, Seward Peninsula, Alaska [Ph.D. thesis]: Golden, Colorado, Colorado School of Mines, 302 p.

Ford, R.C., and Snee, L.W., 1996, $^{40}Ar/^{39}Ar$ thermochronology of white mica from the Nome district, Alaska: The first ages of lode sources to placer gold deposits in the Seward Peninsula: Economic Geology and the Bulletin of the Society of Economic Geologists, v. 91, p. 213–220, doi:10.2113/gsecongeo.91.1.213.

Downloaded from specialpapers.gsapubs.org on September 29, 2015

Franceschelli, M., Puxeddu, M., and Gattiglio, M., 2003, Geochemistry and origin of chloritoid schist from the Alpi Apuane, Italy: Evidence of a prevailing lateritic signature: European Journal of Mineralogy, v. 15, p. 575–588, doi:10.1127/0935-1221/2003/0015-0575.

Franklin, J.M., Kasarda, J., and Poulsen, K.H., 1975, Petrology and chemistry of the alteration zone of the Mattabi massive sulfide deposit: Economic Geology and the Bulletin of the Society of Economic Geologists, v. 70, p. 63–79, doi:10.2113/gsecongeo.70.1.63.

Full Metal Minerals Ltd., 2010, Boulder Creek uranium project, http://www.fullmetalminerals.com/s/bouldercreek.asp (accessed 25 August 2010).

Galley, A.G., 1993, Characteristics of semi-conformable alteration zones associated with volcanogenic massive sulphide districts: Journal of Geochemical Exploration, v. 48, p. 175–200, doi:10.1016/0375-6742(93)90004-6.

Goodfellow, W.D., 2007, Base metal metallogeny of the Selwyn Basin, Canada, *in* Goodfellow, W.D., ed., Mineral Deposits of Canada: A Synthesis of Major Deposit Types, District Metallogeny, the Evolution of Geological Provinces, and Exploration Methods: Geological Association of Canada, Mineral Deposits Division Special Publication No. 5, p. 553–579.

Goodfellow, W.D., and Lydon, J.W., 2007, Sedimentary exhalative (SEDEX) deposits, *in* Goodfellow, W.D., ed., Mineral Deposits of Canada: A Synthesis of Major Deposit Types, District Metallogeny, the Evolution of Geological Provinces, and Exploration Methods: Geological Association of Canada, Mineral Deposits Division Special Publication No. 5, p. 163–183.

Goodfellow, W.D., and Rhodes, D., 1990, Geological setting, geochemistry and origin of the Tom stratiform Zn-Pb-Ag-barite deposits, *in* Abbott, J.G., and Turner, R.J.W., eds., Mineral Deposits of the Northern Canadian Cordillera: Ottawa, International Association on the Genesis of Ore Deposits, Eighth Quadrennial Symposium, Field Trip 14 Guidebook, p. 177–244.

Goodfellow, W.D., Lydon, J.W., and Turner, R.J.W., 1993, Geology and genesis of stratiform sediment-hosted (SEDEX) zinc-lead-silver sulphide deposits, *in* Kirkham, R.V., Sinclair, W.D., Thorpe, R.I., and Duke, J.M., eds., Mineral Deposit Modeling: Geological Association of Canada Special Paper 40, p. 201–251.

Groves, D.A., 1984, Stratigraphy and alteration of the footwall volcanic rocks beneath the Archean Mattabi massive sulfide deposit, Sturgeon Lake, Ontario [M.S. thesis]: Duluth, Minnesota, University of Minnesota–Duluth, 132 p.

Guidotti, C.V., 1987, Micas in metamorphic rocks, *in* Bailey, S.W., ed., Micas: Reviews in Mineralogy, v. 13, p. 357–467.

Hawley, C.C., and Hudson, T.L., 2002, Nome quadrangle, Alaska Resources Data File: U.S. Geological Survey Open-File Report 02-113, 735 p., http://ardf.wr.usgs.gov/html/Nome.html.

Herreid, G., 1965, Geology of the Omilak-Otter Creek area, Bendeleben quadrangle, Seward Peninsula, Alaska: Alaska Division of Mines and Minerals, Geologic Report No. 11, 12 p.

Herreid, G., 1966a, Preliminary geology and geochemistry of the Sinuk River area, Seward Peninsula, Alaska: Alaska Division of Mines and Minerals, Geologic Report No. 24, 19 p.

Herreid, G., 1966b, The geology and geochemistry of the Inmachuk River map area, Seward Peninsula, Alaska: Alaska Division of Mines and Minerals, Geologic Report No. 23, 25 p.

Herreid, G., 1968, Progress report on the geology and geochemistry of the Sinuk area, Seward Peninsula, Alaska: Alaska Division of Mines and Geology, Geological Report 24, 19 p.

Herreid, G., 1970, Geology and geochemistry of the Sinuk area, Seward Peninsula, Alaska: Alaska Division of Mines and Geology, Geologic Report No. 36, 41 p., 4 appendices.

Hudson, T., 1998, Teller quadrangle, Alaska Resources Data File: U.S. Geological Survey Open-File Report 98-328, 236 p., http://ardf.wr.usgs.gov/html/Teller.html.

Hudson, T.L., and Arth, J.G., 1983, Tin granites of Seward Peninsula, Alaska: Geological Society of America Bulletin, v. 94, p. 768–790, doi:10.1130/0016-7606(1983)94<768:TGOSPA>2.0.CO;2.

Jennings, D.S., and Jilson, G.A., 1986, Geology and sulphide deposits of the Anvil Range, Yukon, *in* Morin, J., ed., Mineral Deposits of Northern Cordillera: Canadian Institute of Mining and Metallurgy, Special Volume 37, p. 319–361.

Jones, S., Gemmell, J.B., and Davidson, G.J., 2006, Petrographic, geochemical, and fluid inclusion evidence for the origin of siliceous cap rocks above volcanic-hosted massive sulfide deposits at Myra Falls, Vancouver Island, British Columbia, Canada: Economic Geology and the Bulletin of the Society of Economic Geologists, v. 101, p. 555–584, doi:10.2113/gsecongeo.101.3.555.

Kelley, K.D., and Jennings, S., eds., 2004, A special issue devoted to barite and Zn-Pb-Ag deposits in the Red Dog district, western Brooks Range, northern Alaska: Economic Geology and the Bulletin of the Society of Economic Geologists, v. 99, p. 1267–1280, doi:10.2113/gsecongeo.99.7.1267.

Kelley, K.D., Dumoulin, J.A., and Jennings, S., 2004a, The Anarraaq Zn-Pb-Ag and barite deposit, northern Alaska: Evidence for replacement of carbonate by barite and sulfides: Economic Geology and the Bulletin of the Society of Economic Geologists, v. 99, p. 1577–1591, doi:10.2113/gsecongeo.99.7.1577.

Kelley, K.D., Leach, D.L., Johnson, C.A., Clark, J.L., Fayek, M., Slack, J.F., Anderson, V.M., Ayuso, R.A., and Ridley, W.I., 2004b, Textural, compositional, and sulfur isotope variations of sulfide minerals in the Red Dog Zn-Pb-Ag deposits, Brooks Range, Alaska: Implications for ore formation: Economic Geology and the Bulletin of the Society of Economic Geologists, v. 99, p. 1509–1532, doi:10.2113/gsecongeo.99.7.1509.

Krauskopf, K.B., and Bird, D.K., 1995, Introduction to Geochemistry (third edition): New York, McGraw-Hill, Inc., 647 p.

Kříbek, B., Hladíková, J., Žák, K., Bendl, J., Pudilová, M., and Uhlík, Z., 1996, Barite-hyalophane sulfidic ores at Rozna, Bohemian massif, Czech Republic: Metamorphosed black shale-hosted submarine exhalative mineralization: Economic Geology and the Bulletin of the Society of Economic Geologists, v. 91, p. 14–35, doi:10.2113/gsecongeo.91.1.14.

Lang, J.R., and Baker, T., 2001, Intrusion-related gold systems: The present level of understanding: Mineralium Deposita, v. 36, p. 477–489, doi:10.1007/s001260100184.

Large, D., and Walcher, E., 1999, The Rammelsberg massive sulphide Cu-Zn-Pb-Ba-deposit, Germany: An example of sediment-hosted, massive sulphide mineralisation: Mineralium Deposita, v. 34, p. 522–538, doi:10.1007/s001260050218.

Large, R., Bodon, S., Davidson, G., and Cooke, D., 1996, The chemistry of BHT ore formation—One of the keys to understanding the differences between SEDEX and BHT deposits, *in* Pongratz, J., and Davidson, G.J., eds., New Developments in Broken Hill Type Deposits, CODES Special Publication 1: Hobart, Tasmania, Centre for Ore Deposit and Exploration Studies, p. 105–111.

Large, R.R., and McGoldrick, P.J., 1998, Lithogeochemical halos and geochemical vectors to stratiform sediment-hosted Zn-Pb-Ag deposits: 1. Lady Loretta deposit, Queensland: Journal of Geochemical Exploration, v. 63, p. 37–56, doi:10.1016/S0375-6742(98)00013-2.

Leach, D.L., Sangster, D.F., Kelley, K.D., Large, R.R., Garven, G., Allen, C.R., Gutzmer, J., and Walters, S., 2005, Sediment-hosted lead-zinc deposits: A Global Perspective, *in* Hedenquist, J.W., Thompson, J.F.H., Goldfarb, R.J., and Richards, J.P., eds., Economic Geology 100th Anniversary Volume 1905–2005: Littleton, Colorado, Society of Economic Geologists, Inc., p. 561–607.

Le Maitre, R.W., 1976, The chemical variability of some common igneous rocks: Journal of Petrology, v. 17, p. 589–598, doi:10.1093/petrology/17.4.589.

Levensaler, L.A., and Anderson, E., 1944, Kogruk galena mine and associated properties, Seward Peninsula, Alaska (Independence mine): Alaska Territorial Department of Mines, Report MR-44-3, 12 p.

Lockwood, M.B., Franklin, J.M., and Moore, J.M., 1985, Grant 221. The significance and genesis of chloritoid alteration in volcanic rocks of the Michipicoten belt, Ontario: Ontario Geological Survey Miscellaneous Paper 127, p. 175–185.

Lottermoser, B.G., 1992, Rare earth elements and hydrothermal ore formation processes: Ore Geology Reviews, v. 7, p. 25–41, doi:10.1016/0169-1368(92)90017-F.

Ma, G.-L., Beaudoin, G., Zhong, S.-J., Li, Y., and Zeng, Z.-G., 2007, Geology and geochemistry of the Dengjiashan Zn-Pb SEDEX deposit, Qinling belt, China: Canadian Journal of Earth Sciences, v. 44, p. 479–492, doi:10.1139/e06-093.

MacLean, W.H., and Barrett, T.J., 1993, Lithogeochemical techniques using immobile elements: Journal of Geochemical Exploration, v. 48, p. 109–133, doi:10.1016/0375-6742(93)90002-4.

Mako, D.A., and Shanks, W.C., III, 1984, Stratiform sulfide and barite-fluorite mineralization of the Vulcan prospect, Northwest Territories: Exhalation of basinal brines along a faulted continental margin: Canadian Journal of Earth Sciences, v. 21, p. 78–91, doi:10.1139/e84-009.

Downloaded from specialpapers.gsapubs.org on September 29, 2015

Megaw, P.K.M., Ruiz, J., and Titley, S.R., 1988, High-temperature, carbonate-hosted Ag-Pb-Zn(Cu) deposits of northern Mexico: Economic Geology and the Bulletin of the Society of Economic Geologists, v. 83, p. 1856–1885, doi:10.2113/gsecongeo.83.8.1856.

Meister, P., Liu, B., Ferdelman, T.G., Jørgensen, B.B., and Khalili, A., 2013, Control of sulphate and methane distributions in marine sediments by organic matter reactivity: Geochimica et Cosmochimica Acta, v. 104, p. 183–193, doi:10.1016/j.gca.2012.11.011.

Mertie, J.B., Jr., 1918, Lode mining and prospecting on Seward Peninsula: U.S. Geological Survey Bulletin, v. 662, p. 425–449.

Millrock Resources, Inc., 2010, Bluff project, http://www.millrockresources.com/projects/bluff/ (accessed 18 October 2010).

Moro, M.C., Cembranos, M.L., and Fernandez, A., 2001, Celsian, (Ba,K)-feldspar and cymrite from SEDEX barite deposits of Zamora, Spain: Canadian Mineralogist, v. 39, p. 1039–1051, doi:10.2113/gscanmin.39.4.1039.

Mulligan, J.J., 1962, Lead-silver deposits in the Omilak area, Seward Peninsula, Alaska: U.S. Bureau of Mines Report of Investigations 6018, 44 p.

Mulligan, J.J., 1965, Examination of Hannum lead prospect, Fairhaven district, Seward Peninsula, Alaska: U.S. Bureau of Mines Open-File Report 6-65, 16 p.

Mulligan, J.J., and Hess, H.D., 1965, Examination of the Sinuk iron deposits, Seward Peninsula, Alaska: U.S. Bureau of Mines Open-File Report, 34 p.

Newberry, R.J., Crafford, T.C., Newkirk, S.R., Young, L.E., Nelson, S.W., and Duke, N.A., 1997, Volcanogenic massive sulfide deposits of Alaska, *in* Goldfarb, R.J., and Miller, L.D., eds., Mineral Deposits of Alaska, Economic Geology Monograph 9: Littleton, Colorado, The Economic Geology Publishing Company, p. 120–150.

NovaGold Resources, Inc., 2012, NovaGold announces divestiture of Rock Creek, http://www.novagold.com/section.asp?pageid=21740 (accessed 5 March 2013).

Otto, B.R., Piekenbrock, J., and Odden, J., 2009, Structural evolution of the Rock Creek gold deposit, Seward Peninsula, Alaska: Economic Geology and the Bulletin of the Society of Economic Geologists, v. 104, p. 945–960, doi:10.2113/econgeo.104.7.945.

Partey, F., Lev, S., Casey, R., Widom, E., Lueth, V.W., and Rakovan, J., 2009, Source of fluorine and petrogenesis of Rio Grande rift-type barite-fluorite-galena deposits: Economic Geology and the Bulletin of the Society of Economic Geologists, v. 104, p. 505–520, doi:10.2113/gsecongeo.104.4.505.

Pesquera, A., and Velasco, F., 1989, The Arditurri Pb-Zn-F-Ba deposit (Cinco Villas massif, Basque Pyrenees): A deformed and metamorphosed stratiform deposit: Mineralium Deposita, v. 24, p. 199–209, doi:10.1007/BF00206443.

Pettijohn, F.J., 1963, Chemical composition of sandstones, excluding carbonate and volcanic sands: U.S. Geological Survey Professional Paper 440-S, 19 p.

Pink, C.L., and Rodgers, D.W., 2010, Structural controls on gold mineralization at the Rock Creek deposit, Nome, Alaska: Implications for Middle Cretaceous lode emplacement on the southwest Seward Peninsula: Geological Society of America Abstracts with Programs, v. 42, no. 5, p. 476.

Plimer, I.R., 1984, The role of fluorine in submarine exhalative systems with special reference to Broken Hill, Australia: Mineralium Deposita, v. 19, p. 19–25, doi:10.1007/BF00206593.

Plumlee, G.S., Goldhaber, M.B., and Rowan, E.L., 1995, The potential role of magmatic gases in the genesis of Illinois-Kentucky fluorspar deposits: Implications from chemical reaction path modeling: Economic Geology and the Bulletin of the Society of Economic Geologists, v. 90, p. 999–1011, doi:10.2113/gsecongeo.90.5.999.

Porterfield, B., Franklin, R., and Enos, N., 1996, Aurora Lease 1995 Summary Report: Spokane, Washington, unpublished report for Kennecott Exploration, 57 p., 9 appendices.

Puchner, C.C., 1986, Geology, alteration, and mineralization of the Kougarok Sn deposit, Seward Peninsula, Alaska: Economic Geology and the Bulletin of the Society of Economic Geologists, v. 81, p. 1775–1794, doi:10.2113/gsecongeo.81.7.1775.

Read, J.J., and Meinert, L.D., 1986, Gold-bearing quartz vein mineralization at the Big Hurrah mine, Seward Peninsula, Alaska: Economic Geology and the Bulletin of the Society of Economic Geologists, v. 81, p. 1760–1774, doi:10.2113/gsecongeo.81.7.1760.

Renock, D., and Becker, U., 2011, A first principles study of coupled substitution in galena: Ore Geology Reviews, v. 42, p. 71–83, doi:10.1016/j.oregeorev.2011.04.001.

Rimstidt, J.D., 1997, Gangue mineral transport and deposition, *in* Barnes, H.L., ed., Geochemistry of Hydrothermal Ore Deposits (third edition): New York, John Wiley and Sons, Inc., p. 487–515.

Rossetti, P., and Ferrero, S., 2008, The Zn-Pb deposits of Casario (Ligurian Alps, NW Italy): Late Paleozoic sedimentary-exhalative bodies affected by the Alpine metamorphism: Geodinamica Acta, v. 21, no. 3, p. 117–137, doi:10.3166/ga.21.117-137.

Sainsbury, C.L., 1975, Geology, ore deposits, and mineral potential of the Seward Peninsula, Alaska: U.S. Bureau of Mines Open File Report 73-75, 108 p.

Sanford, R.F., Pierson, C.T., and Crovelli, R.A., 1993, An objective replacement method for censored geochemical data: Mathematical Geology, v. 25, p. 59–80, doi:10.1007/BF00890676.

Shanks, W.C.P., III, Slack, J.F., Till, A.B., Thurston, R., and Gemery-Hill, P., 2014, this volume, Chapter 8, Sulfur and oxygen isotopic study of Paleozoic sediment-hosted Zn-Pb(-Ag-Au-Ba-F) deposits and associated aluminous alteration zones in the Nome Complex, Seward Peninsula, Alaska, *in* Dumoulin, J.A., and Till, A.B., eds., Reconstruction of a Late Proterozoic to Devonian Continental Margin Sequence, Northern Alaska, Its Paleogeographic Significance, and Contained Base-Metal Sulfide Deposits: Geological Society of America Special Paper 506, doi:10.1130/2014.2506(08).

Sharp, T.G., and Buseck, P.R., 1993, The distribution of Ag and Sb in galena: Inclusions versus solid solution: The American Mineralogist, v. 78, p. 85–95.

Sharpe, R., and Gemmell, J.B., 2001, Alteration characteristics of the Archean Golden Grove Formation at the Gossan Hill deposit, Western Australia: Induration as a focusing mechanism for mineralizing hydrothermal fluids: Economic Geology and the Bulletin of the Society of Economic Geologists, v. 96, p. 1239–1262, doi:10.2113/gsecongeo.96.5.1239.

Slack, J.F., Meier, A.L., Malcolm, M.J., Fey, D.L., Doughten, M.W., and Wandless, G.A., 2000, Trace element and rare earth element geochemistry of bedded and massive sulphides from the Sullivan Pb-Zn-Ag deposit, British Columbia—A reconnaissance study, *in* Lydon, J.W., Höy, T., Slack, J.F., and Knapp, M.E., eds., Geological Environment of the Sullivan Deposit, British Columbia: Geological Association of Canada, Mineral Deposits Division Special Volume No. 1, p. 720–735.

Slack, J.F., Dumoulin, J.A., Schmidt, J.M., Young, L.E., and Rombach, C.S., 2004a, Paleozoic sedimentary rocks in the Red Dog Zn-Pb-Ag district and vicinity, western Brooks Range, Alaska: Provenance, deposition, and metallogenic significance: Economic Geology and the Bulletin of the Society of Economic Geologists, v. 99, p. 1385–1414, doi:10.2113/gsecongeo.99.7.1385.

Slack, J.F., Kelley, K.D., Anderson, V.M., Clark, J.L., and Ayuso, R.A., 2004b, Multistage hydrothermal silicification and Fe-Tl-As-Sb-Ge-REE enrichment in the Red Dog Zn-Pb-Ag district, northern Alaska: Geochemistry, origin, and exploration applications: Economic Geology and the Bulletin of the Society of Economic Geologists, v. 99, p. 1481–1508, doi:10.2113/gsecongeo.99.7.1481.

Slack, J.F., Till, A.B., Shanks, W.C., III, and Belkin, H.E., 2013, Aluminous alteration zones related to stratabound Zn-Pb(-Ag-Au-Ba-F) deposits in Devonian–Carboniferous(?) metasedimentary rocks, northwestern Alaska, USA, *in* Jonsson, E., et al., eds., Mineral Deposit Research for a High-Tech World: Uppsala, Sweden, Geological Survey of Sweden, Proceedings of the 12th Biennial Society for Geology Applied to Mineral Deposits Meeting, August 12–15, 2013, v. 2, p. 683–686.

Smith, P.S., 1908, Investigations of the mineral deposits of Seward Peninsula: U.S. Geological Survey Bulletin, v. 345, p. 206–250.

Smith, P.S., 1910, Geology and mineral resources of the Solomon and Casadepaga quadrangles, Seward Peninsula, Alaska: U.S. Geological Survey Bulletin 433, 234 p.

Spear, F.S., 1993, Metamorphic Phase Equilibria and Pressure-Temperature-Time Paths: Washington, D.C., Mineralogical Society of America, 799 p.

Stolz, J., and Large, R.R., 1992, Evaluation of the source-rock control on precious metal grades in volcanic-hosted massive sulfide deposits from western Tasmania: Economic Geology and the Bulletin of the Society of Economic Geologists, v. 87, p. 720–738, doi:10.2113/gsecongeo.87.3.720.

Sutton, S.J., and Land, L.S., 1996, Postdepositional chemical alteration of Ouachita shales: Geological Society of America Bulletin, v. 108, p. 978–991, doi:10.1130/0016-7606(1996)108<0978:PCAOOS>2.3.CO;2.

Taylor, S.R., and McLennan, S.M., 1985, The Continental Crust: Its Composition and Evolution: Oxford, UK, Blackwell Scientific Publications, 312 p.

Downloaded from specialpapers.gsapubs.org on September 29, 2015

Thompson, T.B., and Beaty, D.W., 1990, Geology and origin of ore deposits in the Leadville district, Colorado: Part II. Oxygen, hydrogen, carbon, sulfur, and lead isotope data and development of a genetic model, *in* Beaty, D.W., Landis, G.P., and Thompson, T.B., eds., Carbonate-Hosted Sulfide Deposits of the Central Colorado Mineral Belt, Economic Geology Monograph 5: Littleton, Colorado, The Economic Geology Publishing Company, p. 156–179.

Till, A.B., Dumoulin, J.A., Werdon, M.B., and Bleick, H.A., 2011, Bedrock geologic map of the Seward Peninsula, Alaska, and accompanying conodont data: U.S. Geological Survey Scientific Investigations Map 3131, 2 sheets, scale 1:500,000, 75 p., http://pubs.usgs.gov/sim/3131/.

Till, A.B., Amato, J.M., Aleinikoff, J.N., and Bleick, H.A., 2014, this volume, Chapter 4, U-Pb detrital zircon geochronology as evidence for the origin of the Nome Complex, northern Alaska, and implications for regional and trans-Arctic correlations, *in* Dumoulin, J.A., and Till, A.B., eds., Reconstruction of a Late Proterozoic to Devonian Continental Margin Sequence, Northern Alaska, Its Paleogeographic Significance, and Contained Base-Metal Sulfide Deposits: Geological Society of America Special Paper 506, doi:10.1130/2014.2506(04).

Till, A.B., Dumoulin, J.A., Ayuso, R.A., Aleinikoff, J.N., Amato, J.M., Slack, J.F., and Shanks, W.C.P., III, 2014, this volume, Chapter 1, Reconstruction of an early Paleozoic continental margin based on the nature of protoliths in the Nome Complex, Seward Peninsula, Alaska, *in* Dumoulin, J.A., and Till, A.B., eds., Reconstruction of a Late Proterozoic to Devonian Continental Margin Sequence, Northern Alaska, Its Paleogeographic Significance, and Contained Base-Metal Sulfide Deposits: Geological Society of America Special Paper 506, doi:10.1130/2014.2506(01).

TintinaGold Resources, Inc., 2010a, Kugruk prospect, http://www.mantramining.com/Kugruk_Prospect_hy_Page.aspx?m_id=2712 (accessed 25 August 2010).

TintinaGold Resources, Inc., 2010b, Omilak property, http://www.tintinagold.com/Omilak_Project_hy_Page.aspx?m_id=2732 (accessed 25 August 2010).

Turner, R.J.W., 1990, Jason stratiform Zn-Pb-barite deposit, Selwyn Basin, Canada (NTS 105-O-1): Geological setting, hydrothermal facies and genesis, *in* Abbott, J.G., and Turner, R.J.W., eds., Mineral Deposits of the Northern Canadian Cordillera: Ottawa, Geological Survey of Canada, International Association on the Genesis of Ore Deposits, Eighth Quadrennial Symposium, Field Trip 14 Guidebook, p. 137–175.

Verlaguet, A., Goffé, B., Brunet, F., Poinssot, C., Vidal, O., Findling, N., and Menut, D., 2011, Metamorphic veining and mass transfer in a chemically closed system: A case study in Alpine metabauxites (western Vanoise): Journal of Metamorphic Geology, v. 29, p. 275–300, doi:10.1111/j.1525-1314.2010.00918.x.

Walters, S., Skrzecynski, B., Whiting, T., Bunting, F., and Arnold, G., 2002, Discovery and geology of the Cannington Ag-Pb-Zn deposit, Mount Isa eastern succession, Australia: Development and application of an exploration model for Broken Hill-type deposits, *in* Goldfarb, R.J., and Nielsen, R.L., eds., Integrated Methods for Discovery: Global Exploration in the 21st Century, Special Publication No. 9: Littleton, Colorado, Society of Economic Geologists, Inc., p. 93–116.

Werdon, M.B., 1996, Drenchwater, Alaska: Zn-Pb-Ag mineralization in a mixed black shale-volcanic environment, *in* Coyner, A.R., and Fahey, P.L., eds., Geology and Ore Deposits of the American Cordillera: Reno, Geological Society of Nevada Symposium, Proceedings, v. 3, p. 1341–1354.

Werdon, M.B., 2000, Geologic setting of Mississippian vein-breccias at the Kady Zn-Pb-Cu-Ag prospect: Plumbing system for a failed sedex deposit?: U.S. Geological Survey Professional Paper, v. 1614, p. 5–34.

Werdon, M.B., Layer, P.W., and Newberry, R.J., 2004, $^{40}Ar/^{39}Ar$ dating of Zn-Pb-Ag mineralization in the northern Brooks Range, Alaska: Economic Geology and the Bulletin of the Society of Economic Geologists, v. 99, p. 1323–1343, doi:10.2113/gsecongeo.99.7.1323.

Wimmler, N.L., 1926, Lode deposits in Seward Peninsula: Alaska Territorial Department of Mines Miscellaneous Report 192-01, 10 p.

Young, L.E., 2004, A geologic framework for mineralization in the western Brooks Range, Alaska: Economic Geology and the Bulletin of the Society of Economic Geologists, v. 99, p. 1281–1306, doi:10.2113/gsecongeo.99.7.1281.

Manuscript Accepted by the Society 10 February 2014

Downloaded from specialpapers.gsapubs.org on September 29, 2015

Geological Society of America Special Papers

Late Devonian–Mississippian(?) Zn-Pb(-Ag-Au-Ba-F) deposits and related aluminous alteration zones in the Nome Complex, Seward Peninsula, Alaska

John F. Slack, Alison B. Till, Harvey E. Belkin, et al.

Geological Society of America Special Papers 2014;506; 173-212 , originally published onlineJune 30, 2014
doi:10.1130/2014.2506(06)

E-mail alerting services click www.gsapubs.org/cgi/alerts to receive free e-mail alerts when new articles cite this article

Subscribe click www.gsapubs.org/subscriptions to subscribe to Geological Society of America Special Papers

Permission request click www.geosociety.org/pubs/copyrt.htm#gsa to contact GSA.

Copyright not claimed on content prepared wholly by U.S. government employees within scope of their employment. Individual scientists are hereby granted permission, without fees or further requests to GSA, to use a single figure, a single table, and/or a brief paragraph of text in subsequent works and to make unlimited copies of items in GSA's journals for noncommercial use in classrooms to further education and science. This file may not be posted to any Web site, but authors may post the abstracts only of their articles on their own or their organization's Web site providing the posting includes a reference to the article's full citation. GSA provides this and other forums for the presentation of diverse opinions and positions by scientists worldwide, regardless of their race, citizenship, gender, religion, or political viewpoint. Opinions presented in this publication do not reflect official positions of the Society.

Notes

© 2014 Geological Society of America



THE
GEOLOGICAL
SOCIETY
OF AMERICA